UNIVERSITY OF GÄVLE

FACULTY OF ENGINEERING AND SUSTAINABLE DEVELOPMENT

Department of Building, Energy and Environmental Engineering

Application of the hot-box technique to test the insulation effect of low-emissivity film on old windows

Albert Vergés Gil

2018

Student thesis, Master degree (one year), 15 HE

Energy Systems

Master Programme in Energy Systems

2017-2018

Supervisor: Dr. Magnus Mattsson

Examiner: Dr. Abolfazl Hayati

Abstract

Nowadays humanity is electric depended. The increasing consumption of electricity negatively affects the environment due to the way it is obtained. Furthermore, the energy usage in residential buildings accounts for 27.1% of the worlds' total consumption, where governments have started to settle their boundaries.

Windows account for a total of energy leakage in a buildings of around 40%, which makes them one of the biggest contributor of energy leakage. Due to this reason, the first objective is to improve the efficiency of the overall building in the designated area. However, there are buildings that cannot be modified, as they are historical and, in consequence, protected by law. In those cases, it is needed to find other ways of upgrading them.

Most of the available test methods for calculating the thermal transmittance [U-Value] of a window are performed in specialized facilities, where a sample is needed in order to perform the test. As obtaining a sample for performing a laboratory test is not possible, an onsite methodology based on the hot box test method was designed and constructed in one of the rooms in Gävle Rådhuset, the main building of the city council of Gävle.

The proposed solution was built using insulation materials and thermocouples type T, reducing the cost needed for special facilities and not requiring any destructive method. Furthermore, low emissivity films were installed and tested for calculating the best installation position and to quantify the reduction of the U value. Three different scenarios were compared, two of which were made using the same type of film, though installed in a different position.

It was found a U-value for the overall 2-pane window (incl. frames) of $2.19 W/K \cdot m^2$ (for a scenario without film, where the outdoor of the window was used as outdoor environment). Additionally, a reduction of 33% of the U-value was obtained, when a low emissivity film is applied between the two glazing surfaces of the window. On the other hand, when installed in the region recommended by the manufacturer – the innermost glass – the reduction of 22% has been achieved, which is slightly lower than the value given by the manufacturer of 26%. The feasibility of the adaptations of the method used for this study seems to be properly made, despite that a more complex calculations for the U-values and testing with known U-value materials is needed to be able to assure the correct and trustable operation of the apparatus. Furthermore, with the results obtained, the option for outdoor environment for calculating the U-value that seems more correctly is choosing the external window surface temperature.

Keywords: low-emissivity film, U-value, hot-box technique, in-situ experiment, humidity dependence, energy efficiency

Preface

This thesis would not have been possible without the support of many people that have supported and guided me through all the process from the beginning to the end of this project.

Firstly, I am indebted with Prof. Jan Akander, Mikael Sundeberg, Elisabet Linden, Hossein Khosravi Bakhtiari, Arman Ameen, Ola Jeppsson among other staff from the Department of Building, Energy and Environmental Engineering. Without their contribution this project would have not been performed as well as for sharing their knowledge and experience regarding the topics treated, that helped me to grow as an engineer.

Furthermore, I am especially grateful to Dr. Magnus Mattsson, whose guidance, support, motivation and knowledge have made the completion of this project possible.

At least but not last, I want to thank my family and friends for the support and motivation given during the development of this project, without which it would not have been concluded.

Nomenclature

Acronym	Description
HFM	Heat flow meter method
CHB	Calibrated hot box method
GHB	Guard hot box method
SHB-HFM	Simple hot box-heat flow method
PID	Proportional–integral–derivative controller
CFD	Computational fluid dynamics
AC	Alternating current
DC	Direct Current

Symbol	Description	Unit
q	Heat flux	[W/m²]
A	Area	[m²]
d	Thickness	[m]
λ	Thermal conductivity	[W/(K·m)]
ΔT	Temperature difference	[K]
U	Thermal transmittance	[W/K·m²]
Pvs	Saturated vapour pressure	[Pa]
W	Absolute humidity	[g water /kg of air]
RH	Relative humidity	[%]

Table of contents

Contents

1 Introduction

1.1 Background

Windows are one of the most important areas in buildings, as windows allow the sunlight to illuminate indoor facilities. They enable the occupants of a house to enjoy the views of the neighbourhood or locality, and they serve to keep the house ventilated and providing light to the interior of the building, apart from many other functionalities. Therefore, they constitute an essential entity of residential buildings. Furthermore, buildings are one of the most energy users as residential buildings consumes 27.1%[1] of the world energy

Recent Swedish building regulation codes [2], strengthen the legislation when it comes to cautious renovation and prohibition of distortion of historic buildings aiming to maintain cultural capital in the building stock. In this context, windows are a key element in regard to both a buildings expression and its role in the vicinity's environment. Furthermore, it has been seen that windows-to-wall connections appear to be specially important and can contribute up to 40% [3] of the total heat losses caused by thermal bridges in thermal envelope.

Even though national investigations, following outdated judgements in which the addition of an external wall insulation was omitted, have taken place, nothing has been mentioned regarding windows.

Improving buildings windows is expected to increase the efficiency of the overall building and consequently reduce the energy demand, thus reducing the cost of energy consumption.

However, in most of the cases, buildings are already constructed, modifications in its layout are necessary in order to decrease the thermal bridges between the buildings envelope and windows. Facade changes, such as those targeting efficiency improvements, which should not be performed in historical buildings, immobile witnesses of our history, which should be inherited by future generations as they were designed without compromising the environment, should be implemented by applying the minimum changes to a building's construction.

Starting from the point that old functional windows should not be replaced by new ones and that, at the same time, old windows should be upgraded to give better thermal performance, energy-saving and comfort improvement measures minimizing the modifications of the old functional windows should be considered.

New technical products, have been developed in the late years obtaining good performance with a minimal modification on the building, being a good solutions for issues as the previously commented.

This project complements the research project “Field study of two methods for improved energy performance of old windows” a project supervised by Dr.Eng. Magnus Mattsson together with Dr.Eng. Jan Akander and Prof. Björn O. Karlsson as co-supervisors, a project that is being carried out in Högskolan i Gävle supported by the Swedish Energy Agency and the Municipality of Gävle.

1.2 Literature Review

Windows are one of the weakest points from the energy efficiency of a building, leaking about the 40% of the total energy of the building [3],in which solar radiation is the factor that has most impact and, therefore, making it the first choice for optimizing the energy impact of a window [4].

In order to reduce those losses, the most common is to replace them for new models or to optimize them by the use of new materials as aerogel, that can decrease the heat loses up to 30% depending on the thickness [5], but other possibilities are available [6].

In the case of historical buildings, in most of the countries is forbidden by law to apply modifications and other alternatives have to be applied.

One possibility that can have a lower impact on the building is the installation of low emissivity films, which filters the radiation from the sun, reducing the heat radiation that enter the building maintaining the incoming light. However, the most efficient are installed directly to the glass during the fabrication process and consequently are mostly applied to new buildings [7].

Regarding low emissivity films, the two main groups that are currently coping the market are opaque, most suitable for attics, and clear, although some distortion with the incoming light is made. One suitable candidate for historical buildings are self-adhesive films, as are low cost and easy to install, despite the manufacturer recommends that the installation should be done by a professional, as the performance is directly related to the presence of air bubbles. Using this type of film, that are a combination of different layers, values shown that the reduction in heat losses can be from 18% up to 47% per square meter [6][8][9].

However, those films have to be installed in the inside surface of the glass as they are not able to handle the climate conditions. Furthermore, it has not been found information about the performance through aging as the times goes by, it is expected to decrease due to the presence of particles and dirt. Additionally, it has been found that rarely the value given by the manufacturer is related to the real one, as the conditions where it has been measured are ideals and not realistic, being in most of the cases lower than the given one [7].

For calculating, the U-value reduction associated to these reductions, in most of the cases a completely hot box facility has been constructed, being able to control all the parameters that would affect the test. Generally, hot-box method is used, calculating only one material each time and pondering it lately. Those constructions had shown that PID controllers are reliable for maintaining the temperature even [8][4][10][11].

Those methodologies cannot be considered in situ, as it is mandatory to have a test material for the calculation, being impractical if the building is protected by law. However IR measurements complemented by heat flux meters had been use for in situ measurements, but the accuracy found can be between 3% and 30% depending on the experience managing the equipment, as well as some environmental variables had not been taken account as humidity.

Additionally, a Simple Hot box-heat flow meter method has been used for obtaining the thermal transmittance of a wall obtaining a maximum system error of 7.5%. Unfortunately, the temperature difference needed for that experiment was between 20-60º C having a huge dependence of the climate where the measurements had been done [10].

Technological advances towards windows have reduced the thermal transmittance on the windows in late years, improving from a U-value of 5.5 W/k·m² on a single clear glass window with metal frame to a lower value than 1 W/K·m² for a vacuum or quadruple glazed that is currently under development[1].

However, the type that had been more used among Europe is the double clear glass window with wood frame with a value of 2.8 W/ W/K·m²[12] despite several European countries are improving their building requirements being more strict with values around 1.1 W/K·m².

For obtaining this literature review, the focus was set on searching information regarding building energy performance, hot-box test method and low emissivity film among others. Furthermore, the selected databases used for searching the information had been ScienceDirect and Scopus by Elsevier, trustable sources of scientific data.

As previously seen, there is no specific adaptation of the u value calculation method that is really applied to in situ measurements being difficult to improve the performance of already built buildings without modifications, being the main aim for performing the present study.

1.3 Aims

This thesis is focused on the study of the application of the hot-box method test to an old window located in Gävle city hall and the subsequent study of its performance. This kind of tests are mainly performed in technical facilities with a huge economical cost and focused only on one material, therefore not allowing to carry on further tests on buildings previously built. Conjointly, one of the main goals of this project is the adaptation and construction of an on-site test instrument for this type of tests.

Additionally, low emissivity film will be tested and compared to the window performance, besides the investigation of the optimal position for its installation.

1.4 Approach

To minimize modifications in old functional windows, the hot-box test method has been selected. Its aim is to create an environment inside a window close to an indoors climate, and so be able to maintain a constant temperature inside the building. By doing this, the room's heat losses are aimed to be reduced, as the volume in contact with the window is diminished.

First of all, a hot-box was designed and constructed in the laboratory. In addition, the instrumentation selected and used was previously calibrated in a controlled environment in order to test its performance.

Once the model was finished and the apparatus calibrated, it was installed in the study scenario to obtain real results, which would afterwards be contrasted to the theoretical ones.

After the data was obtained and the analysis performed, a film was installed in the windows to test its impact on heat loses. Additionally, the film was installed in two other different surfaces of the glazing to verify if there were variations due to the selected surface.

2 Theory

2.1 Hot-box test method

Nowadays it is of high importance to minimize energy losses, which is reflected directly on the composition bill, being transcendental to continue investigating and performing tests on new materials looking to decrease its thermal resistance, which would improve the thermal insulation and prevents heat transfer with the environment, improving building efficiency.

However, the complex calculations in order to obtain the thermal transmittance of the material lead to a need for different methodologies and performed in laboratory facilities, including the hot-box test method.

The hot-box measures the general heat transfer of the material sample and it is based on maintaining a specific temperature difference on both sides of the specimen, allowing a constant heat flow transfer. The power through the sample is derived by properly correcting the power measured in the hot chamber, being necessary a control system in order to perform this step. Moreover, the overall box has a good insulation towards the heat in order to decrease the heat transfer with the environment, isolating the sample from the surroundings.

After the test has been done, indirectly from the power needed for maintaining those temperatures, the thermal transmittance of the sample can be obtained.

During a test, there are two main stages for the determination of the thermal transmittance, according to ISO 12567-1[13]:

"Firstly, measurements are made on two or more calibration panels with accurately known thermal properties, from which the surface coefficient of the heat transfer (radiative and convective components) on both sides of the calibration panel with surface emissivity's on average similar to those of the specimen to be tested and the thermal resistance of the surround panel are determined.

Secondly, measurements are made with the window or door specimens in the aperture and the hot-box apparatus is used with the same fan settings on the cold side as during the calibration procedure."

There are two methods for performing this test: Calibrated Hot Box Method [CHB] and the guard hot box method [GHB] with some advantages and disadvantages.

One of the main differences between both methods is found in the measurement box, and the location of a heat source for generating the thermal flow to the specimen. Furthermore, another main difference between both methods is that while the GHB can only operate in steady state conditions, CHB can also make dynamic measurements.

Regarding dimensions, the CHB measurement box has to be equal to or greater in dimensions than the study subject, as it covers the entire section of the hot side.

Meanwhile, for the GHB measurement box is smaller than the dimensions of the construction element, being installed on the hot side as the CHB.

The mentioned differences can be observed in Figure 1.

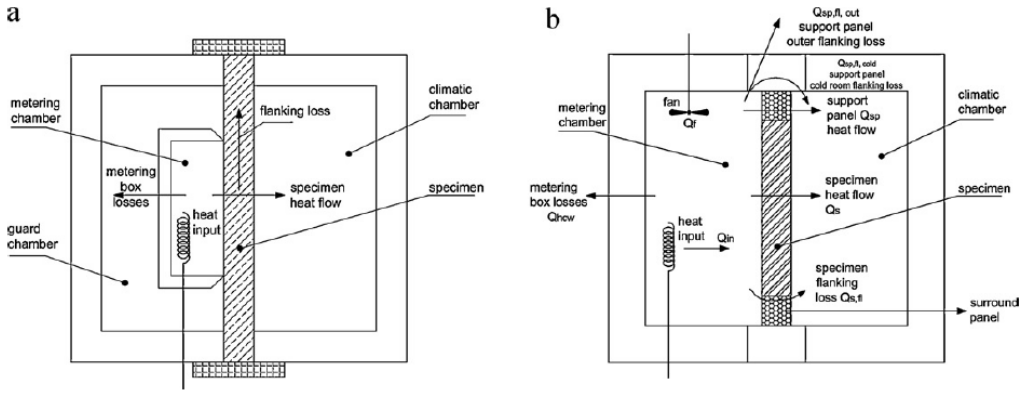

Figure 1: Scheme of the guarded hot box (a) and the calibrated hot box (b) [14].

The guarded hot-box method has a greater accuracy in the data acquisition, minimizing the direct heat exchange from the measuring box to the environment. Furthermore, as the heat source can be directly directed towards the specimen, the lateral heat flow suffered from the specimen decreases. However, the cost is higher than for the calibrated box, being necessary a more complex control system for the system, as well as more equipment located in the hot zone is affected by the temperature fluctuations.

Regarding the calibrated hot-box method, it is faster to assembly for each test performed as it only needs to be separated and mounted again, with a simpler heating systems being necessary a less complex control system. Furthermore, for the way it is constructed, there is less equipment inside the hot box that will be affected by the heat flow changes.

However, with this method, as the heat power cannot be directed, the heat flow is non-unidirectional towards the specimen having a greater lateral heat loss as well as a loss of heat from the measuring box to the external environment.

Besides this, Methods have been widely tested and are widely used in laboratories, on the other hand, due to the complexity of calibrating the heat losses for the surroundings [14], they are not usually used on the field.

Another test widely used is the Heat Flow Meter [HFM], which operates as the previous mentioned.

The specimen to be studied is placed between two metal surfaces that can vary its temperature, generating a known heat flux. A heat flux meter sensor located in the apparatus, measures the real heat flow through the sample. As the output and the real values are calculated, the thermal conductivity of the specimen is found. However, this method is limited as for the dimensions of the sample, that usually is smaller than the previous mentioned, as well as for the temperature difference, having a great dependence on seasons, and forced cooling and heating [15].

A schematic image of the experimental procedure can be seen in Figure 2.

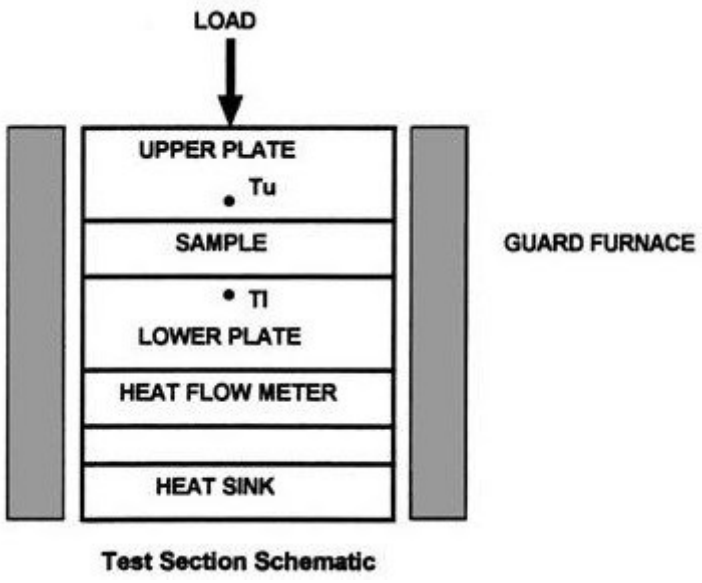

Figure 2: Schematic figure of the hfm test [16].

2.2 Low emissivity film

Low Emissive films (Low-ε films) are a product whose main quality is to improve the energy efficiency of windows. This way the heat losses in buildings are lower, by reflecting part of the energy emitted by heating appliances and by returning it to the interior environment. At the same time, they have a minimal effect on the transition of natural light, being well balanced between heat energy saving and the usage of light (Figure 3).

The low emissive film acts as a barrier, decreasing a percentage of the radiation that goes to the opposite environment, maintaining the heat surplus in winter from going to the environment as well as preventing the heat exchange during the summer period, where the building temperature tends to be lower.

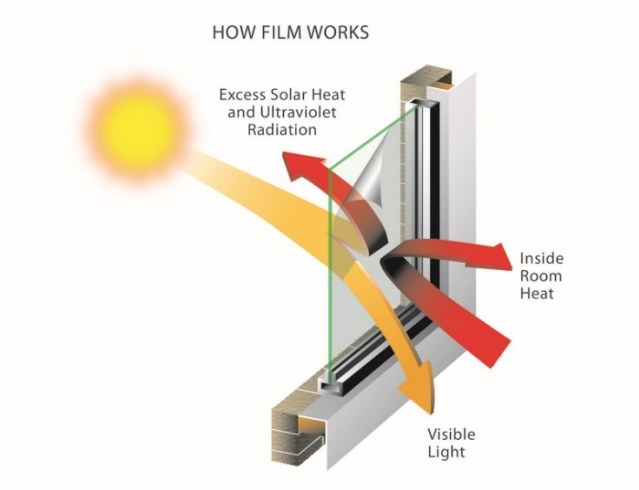

Figure 3: Simplification scheme of how a low emission works [17].

Low emissivity films, can be opaque or transparent, depending on the purpose. This kind of films is commonly used in attic storage where this space do not need to have a need for sunlight. There are two main ways for the application of this films; while fabricating the glasses, and installed in the factory or self-adhesives that can be applied in existing windows. However, some of them can only be applied once and are impossible to remove once installed.

The construction of the film is based on the refractivity of the materials that have been made with, as some material reflect specific radiation wavelengths, by using different coatings, as the example seen in Figure 4, for its composition, the final efficiency is reached.

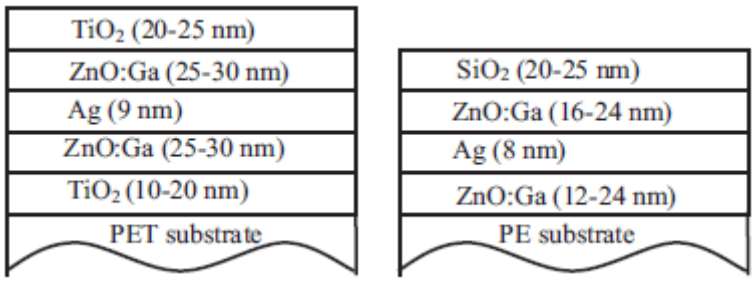

Figure 4: Example of the coating components of two different low emissivity films [9].

Usually, a polymeric material is used as subtract lately applying different metallic coatings of different thickness than can vary from 4-20 nm. Each manufacturer has its own coatings, thus reaching different performances; improving its behaviour in the field of insulation.

3 Method

Prior to developing the project, a literature research took place to sort out methods, among which, the following were selected to carry out the study. The followed methodology was selected from a variety of models currently used in the laboratory.

Nowadays, the most used methods are the heat flow meter method (HFM), the calibrated hot box method (CHB) and the guard hot box method (GHB). However, as these methods are intended to be operated in a controlled environment, thus, all of them turned to have limitations when it came to temperature gradients or seasonality.

For this reason, the selected and followed methodology is a variant of the Simple hot box-heat flow method (SHB-HFM) [15], in which both, the materials and the measurement equipment were optimized.

For a more comprehensive description of the methodology, it has been dissected in four sections, one for each main part of the project.

3.1 Project Definition.

3.1.1 Study location.

The project was developed in Gävle Rådhuset, where two rooms, 210 and 226, were designated for the study, each of them with a different orientation Figure 5.

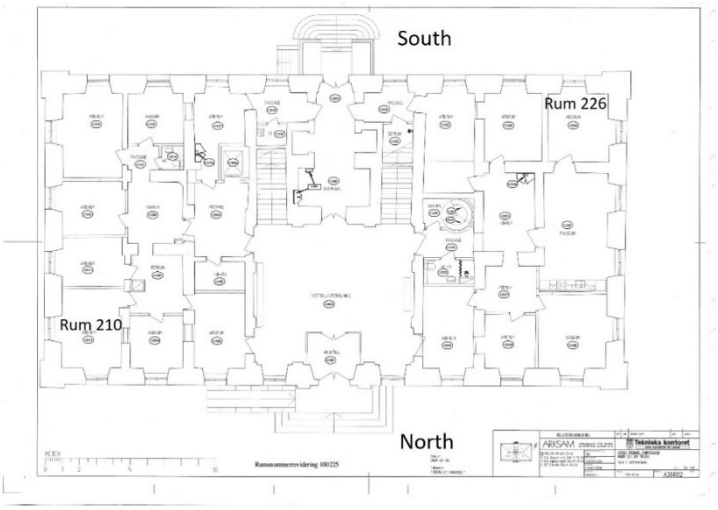

Figure 5: Location of the studied rooms in Rådhuset Blueprint [4].

3.1.2 Window measurements and creation of 3D models.

Once the study location was confirmed, measurements of all the available windows were taken to create blueprints and 3D models, which were further used in posterior steps of the study.

The measurements were taken using a Laser distance measurer, Leica DISTO A6, with an accuracy of ± 1.5 mm for the range of use [18] . For small measurements, a Tape Measure of 5 meters with an accuracy of ±1mm was used (Figure 6).

Figure 6: Measurement tools used for acquiring the measurements of the windows.

Once all the measurements had taken place in both rooms, a model of all the windows was created with the software SOLIDWORKS Student Edition 2016-2017 [19], that will be used for all the 3d models and blueprints.

Figure 7, displays a picture of the studied windows, form room 210 and 226, as well as their corresponding measurements. Moreover, the detailed blueprints for each window can be found in Appendix A.A. The cavities were the windows are installed are slightly different with a deviation of less than one centimeter considered as irrelevant when constructing the hot box.

Figure 7: a) Picture and blueprints of windows from room 226. On the left the one facing the south and on the right the one facing west. b) Picture and blueprints of windows from room 210. On the left the one facing the north and on the right the one facing east.

3.1.3 Methodology of study

For the calculation of the thermal transmittance associated to each window, an uncertainty regarding which to use as outdoor measurement was found leading to the calculation of two different values, which will be further discussed in the following chapters.

It was stated that the box temperature as well as the room temperature would remain constant with a temperature estimated to be around 22ºC. To ascertain this purpose, the borders of the cavity in the wall surrounding the window were isolated aiming to neglect the heat transfer between the walls and the window itself as it could be a source of uncertainty.

Furthermore, to measure and estimate the temperature profile inside the hot-box, temperature data was acquired using thermocouples, due to their high reliability and low cost. As the surface of study was vast, to reduce the number of thermocouples needed for the study, a symmetry premise was assumed, focusing then the study in one side and verifying the symmetry using checkpoints in the opposite other side.

Additionally, to validate the calculated values, nine heat flux sensors were installed in different surfaces of the box.

3.1.4 Modular Hot-box proposal.

The main focus after the first set ups of the experimental location was to characterize the Hot-Box for its subsequent construction.

The hot-box had to possess certain features to accomplish its expected goals, such characteristics were: being constructed with insulation materials, in order to reduce heat losses towards the surrounding environment; to have a design which allowed the removal of the box's cover, more concretely the part facing the room, for sensor installation purposes; and the possibility to install the necessary sensors.

Following these requests and in order to have the possibility of using the hot-box in other scenarios, a modular pre-design was constructed by creating a 3d model of the hot box that had all the aforementioned features; see Figure 8. By using this proposed model, the tool could suit different study scenarios by adapting the surrounding insulation, decreasing the budged needed for further study cases.

The detailed measurements associated to this preliminary design can be found in Appendix A.B.

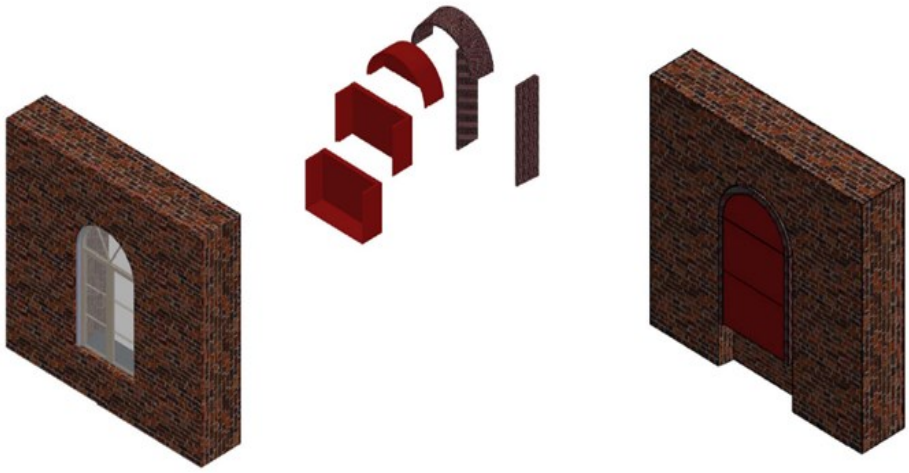

Figure 8: Exploded view (left) and installed view (right) of a modular proposal for the hot-box construction, divided in three parts for covering the overall surface and with surrounding insulation for adaptation to different cases.

3.1.5 Definition of study cases.

Once the hot box was built, the study cases carried out were settled as a part of the calculation of the window's thermal resistance value. One company was interested in validate their products. Therefore, firstly, a study of the window without addition of products was carried out in order to validate the correct functioning of the hot box, as well as to obtain the reference value of the thermal resistance of the overall window.

Lately, low emissivity films manufactured by the company Sunstop were installed in different surfaces of the window glasses to measure the impact on the overall thermal resistance value.

3.2 Project design

3.2.1 Final site decision

Due to bureaucratic issues found during the development of the project, unfortunately the only room available for the performance the study turned to be room 226. Additionally, because of some misunderstandings with the suppliers, the window studied was facing south. It was the one where the hot box was installed.

3.2.2 Initial check-up and preparation

Previous to start performing the experimental plan in the facility, characteristics of the room had to be sorted out, as the temperature of the room had to remain constant prior to consider the room as a controlled environment. Accordingly, a research of energy and air leakage was performed on site.

A simplified adaptation of the Blower door test method was performed by sealing the intake of air while maintaining the inlet system on; therefore creating a slight over pressure that would emphasize the leakages for a posterior search with an infrared camera.

For the performance of this test, an infrared camera, FLIR C2 Educational Kit, with an accuracy of ±2ºC [20] was used being enabling the detection of leakages around the framework of the window as well as some cracks in the window's cavity, (Figure 9), where the leakages induced lower temperatures.

Once the leakages were found, the weather stripes previously installed on the window were replaced with new ones, as the old ones where rotten and not working. Furthermore, the visible cracks were filled using mastic obtaining a better performance of the window as can be seen in Figure 9, were both images were taken having approximately the same amount of overpressure.

Figure 9: Thermal image of south window of room 226 where air leakages can be seen in a darker colour (left) and the same window where the leakages had been corrected.

3.2.3 Material Selection

Once the study environment was adapted, the hot box model design took place, starting with material selection. The hot box material choice was important, as limitations of certain materials could lead to major changes in the design.

To do so, the software CES EduPack 2017 Educational version was used. Prior to the application of constrains, the data base's third level was chosen, as it includes technical material as well as specific alloys.

By following the guidelines provided from the manufacturer, Granta Design [21] three main steps were followed in order to select the material:

- First Stage: Selection of the properties that were to be studied, having the possibility to choose from materials to shaping processes. As what was going to be select was the material, the material catalogue was selected, not including any constrain to have the major variety of possible candidates.

Second stage: In this stage, some requirements were set to refine the candidate search. In the study case, the selected constrains concerned to mechanical and thermal properties and durability. The selected curbs can be seen in detail in Table 1.

Table 1: Constrains used for selecting the materials with the software CES Edupack that would be used to construct the hotbox.

Category	Restriction	Max/Min.	Value	Justification
Process universe	Shaping Form		Machining	Tools in Workshop
Durability	UV radiation (sunlight)	Good/ Excellent		Hot box will face the sun
Durability	Flammability	Self-extinguishing		Safety
Thermal properties	Thermal Conductivity	Max.	0,1 W/ m·ºC	[22]
Mechanical properties	Elongation	Min.	5%	Stiffness [23]
Mechanical properties	Bulk Modulus	Max.	2GPa	Stiffness [23]

The restriction previously mentioned, lead to 3968 possible materials. To narrow down the candidate materials, a third stage was applied.

- Third stage: despite the importance of mechanical properties and durability, the most critical property was the thermal conductivity, as the material's main purpose was to serve as a good insulator. Consequently, a plot of thermal conductivity versus price per unit of volume was selected.

  The reason for choosing that plot was, that some specific materials that accomplish the selected criteria, are expensive, being the difference with another not technical regarding thermal conductivity negligible.

Once both properties were plotted, as shown in Figure 10, the materials with the lowest thermal conductivity possible were selected.

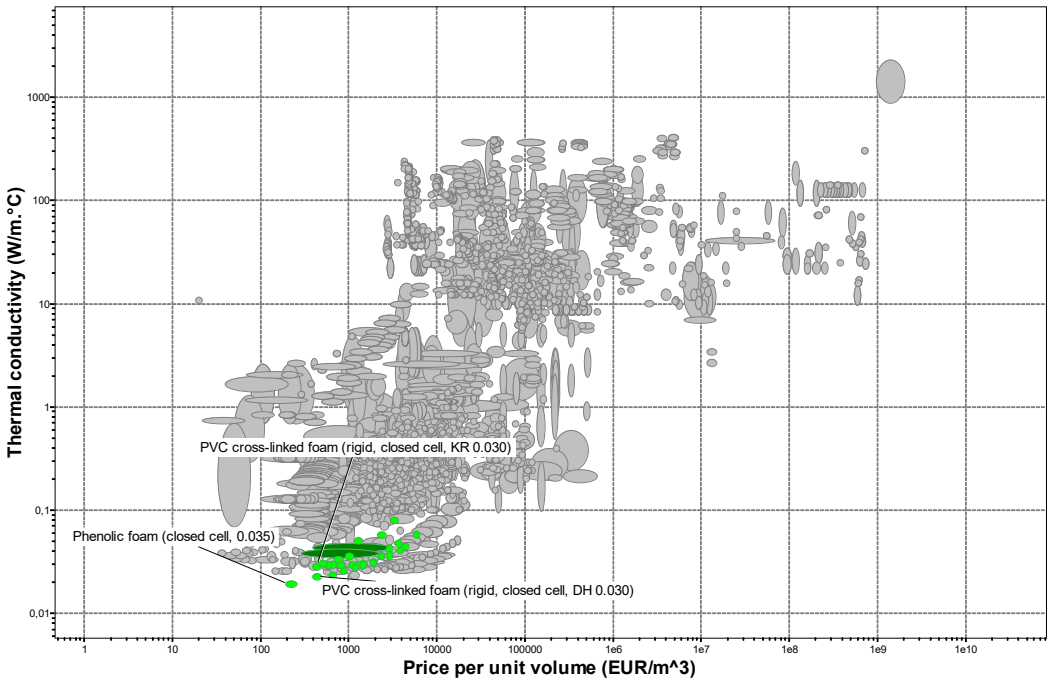

Figure 10: Plot of thermal conductivity vs price per unit of volume. The coloured one represents the most suitable candidate.

Following this criteria, the most suitable materials can be found in Figure 11, selecting as final candidates the PVC cross-linked foam (rigid, closed cell, DH 0.030) and Phenolic foam (closed cell, 0.035).

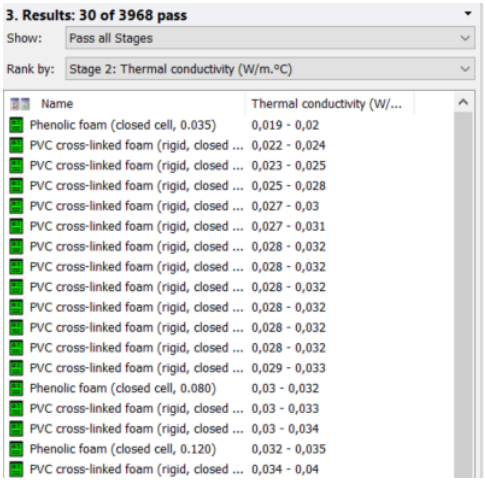

Figure 11: Rank of materials selected minimizing the thermal conductivity as well as the price.

Even though both suggested materials would have been suitable for the construction, the Phenolic foam was chosen, as it had a lower price than the PVC as well as a lower water absorbance per day. Datasheets correspondent to both materials can be found in Appendix B. The data sheet provided tradenames of the suggested selected material, being the one for phenolic foam KOOLPHEN K, CELLOBOND. However, some other materials were recommended by experts in the area which were Kingspan IS phenolic foam, with a thermal conductivity of 0.022 W/ K·m for the sides [24] and Armaflex AF-25 for the arc, with a thermal conductivity value of 0.038W/K·m [25]. The other materials were way stiffer than Armaflex.

A comparison of the new suggested materials and the one narrowed down by the software minimum differences between the materials. Due an out of the project's scope delivery time for the software's suggested material, the materials suggested by the project's supervisor were selected.

3.2.4 Final 3D model

After the materials were selected, some changes in the preliminary design of the hot box took place, as some tolerance and thickness values were unachievable, due to the limitations on the available size offered by the manufacturer.

Changes in the hot box entailed a thickness of 50 mm for the surfaces, except for 100 mm for the backside. Thicknesses were selected to assure a minimum heat exchange between the box and the surrounding environment.

For the final design, workers of the workshop of the Energy research group were requested for suggestions, as their experience working with those kinds of materials was something to bear in mind.

With all the information acquired and taking into account the limitations of the board sizes provided by the manufacturers, the model was designed in a modular way, to enable the removal of the cover for sensor installation.

The final modular layout can be seen in Figure 12, where the pieces involved in final construction can be seen. Additionally, the detailed blueprints for each part can be found in Appendix A.C

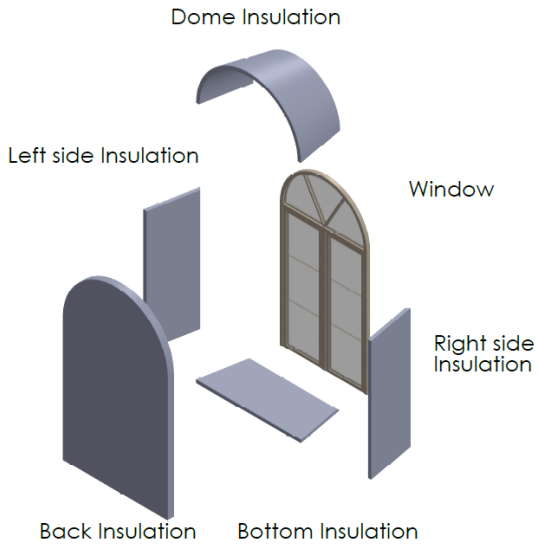

Figure 12: Final Hot box design including all the parts that are involved in the construction.

3.2.5 Sensors selection

As the final model was defined, the instruments used for data acquisition were defined.

To estimate where the sensors should be installed and which temperatures should be expected, lecturer Arman Ameen at University of Gävle performed a CFD simulation of the hot box in 2D, Figure 13, where the target temperature was 20ºC.

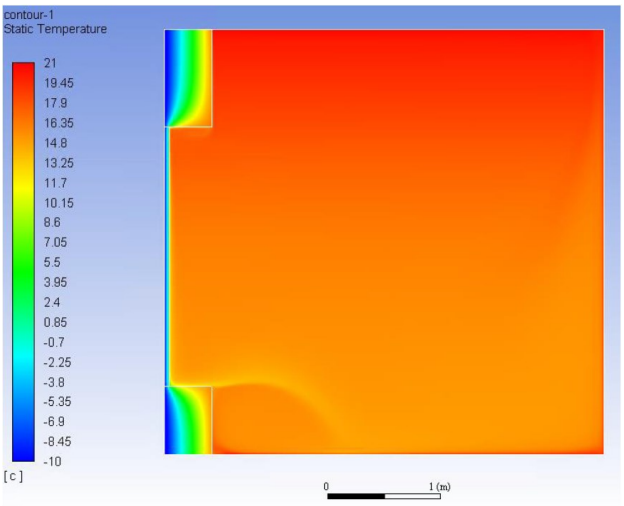

Figure 13: CFD simulation of the hot box, performed by lecturer Arman Ameen, where the window is located at the left, acquiring the lowest temperature. In this case the target temperature was of 20ºC.

With the available information, the selection of the thermocouple took into account the range on which the hot box was expected to work, being the T-Type the most suitable for that range as well as, for the expected scenario it has the most linear lability regarding the Seebeck coefficient as shown in Figure 14. The Seebeck coefficient is the measure of the inducted thermoelectric voltage due corresponded to a temperature difference across the thermocouple junction, [26] .

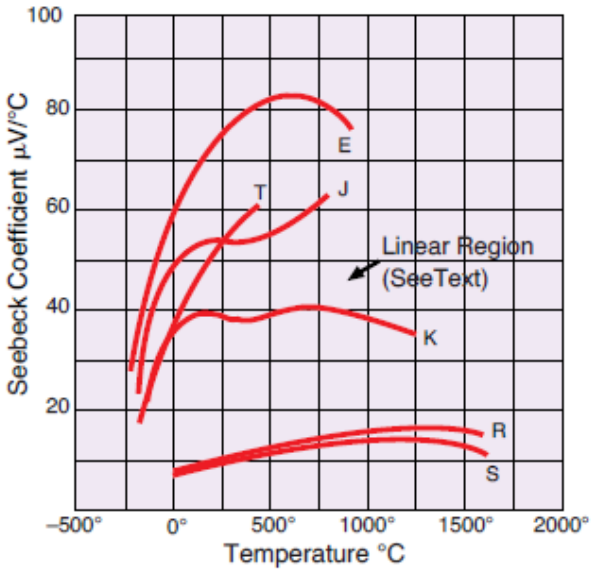

Figure 14: Seebeck coefficient vs Temperature for each thermocouple type [12].

Taking advantage of the symmetry present in the final model, the sensors were focused in one side, whereas in the other side, only stalling checkpoints to verify that symmetry were taken. The reason for this was to optimize the number of sensors used without scarifying the acquired data, as too much data would have required more instruments as well as more powerful computers for data analysis, increasing the project's budget. With the performed optimization, costs were avoided without sacrificing data. A provisional layout can be seen in Figure 15.

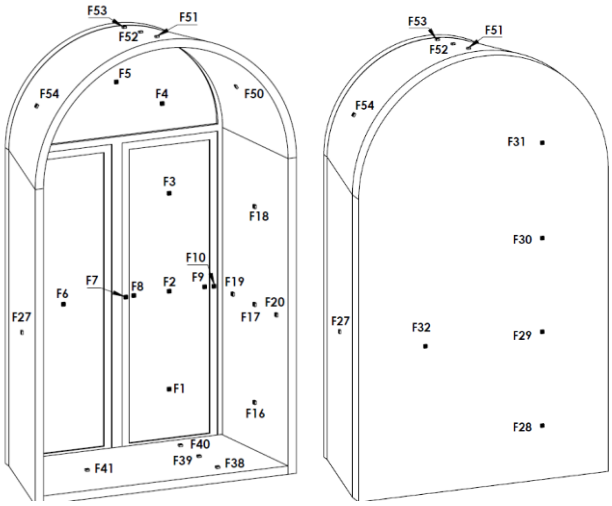

Figure 15: Temperature sensor layout for the hot box. Each sensor on the left side has another sensor in the opposite surface at the same position.

3.3 Execution

3.3.1 Hot-Box construction

The hot box was constructed by the workshop of the department of energy buildings, adding a 45º angle in the edge facing the window, to let the whole window construction (with frames) constitute the tested object.

As previously mentioned, the board sizes provided by the manufacturer were not enough to build the back insulation in one piece. Due to this fact, it was divided in three different parts, assembled in the construction area. The divisions done can be found in Figure 16. However, from now on, in blueprints, it will appear as only one part for simplifications.

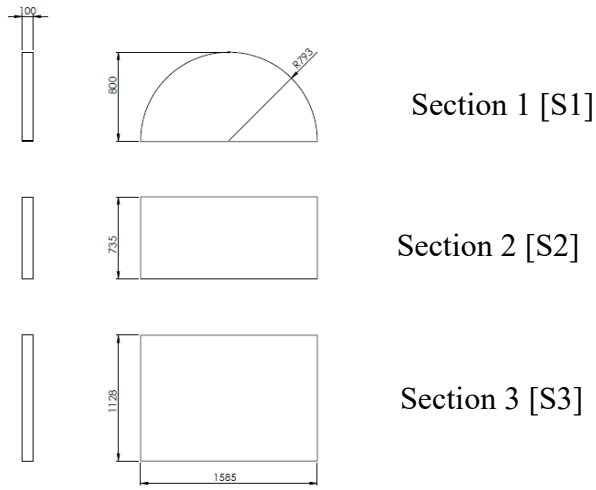

Figure 16: Divisions for construction of the back part insulation with the name of the reference section.

3.3.2 Heating installation

As one of the factors that was aimed to remain constant was the temperature of the hot box, the installation of power-controlled heating devices was necessary.

For that task, heating films that will be attached to the back plate were used, added to a heating rod for covering the heat leakages of energy inside the hot box. The power necessary for balancing those loses, less the heat flow that goes through the insulation, was assumed, as the power that is leaking through the window.

For a constant temperature maintenance, device capable of regulating the temperature inside the hot box plus the room was needed, being designed and constructed by the Electronic lab at the university. This device was named “Adaptable temperature regulator”, which can be seen in Figure 17. It has two electric outputs, one in DC at 60V and another in AC at 220V. Built inside the instrument, PID controllers, in charge of temperature maintenance were implemented. Consequently, for its task performance, it needed temperature input, so four thermocouples were used; three measuring back plate surface temperatures and one measuring air temperature in middle of the hotbox. The overall of the inaccuracy involving the whole instrument was set by the electronic lab around ±2%.

Figure 17: Adaptable temperature regulator used for maintaining the temperature even. The DC and the AC outputs can be seen as well as the thermocouple inputs.

Moreover, as some voltage loses were expected due to the length of the cables, an extra sensor measuring the voltage that arrives to the heating device was needed to reduce them.

Furthermore, the selected model used for this task was an underfloor heating for caravans manufacturer by Ebeco with a power of 80W/m^2 [27]. However, as this model was intended for caravans that runs at 48V and the DC output for this is 60V, the power expected for each film was of 100W/m^2.

As shown in picture Figure 18, not all the surface of the heating foils were heating surfaces, having channels between the heating surfaces for an easier installation.

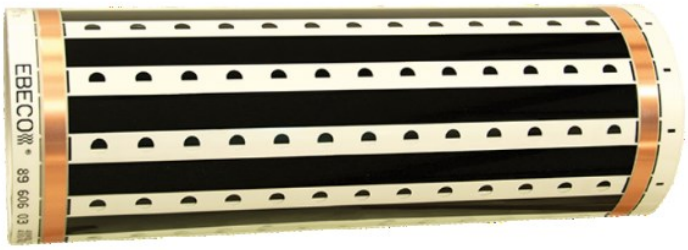

Figure 18: Picture of the heating foils used where only the black lines are the ones that produces heating [13].

Consequently, as an even heating was desired, a 1 mm aluminum plate painted in black, was installed above the heating foils for a uniform heating distribution, which was verified by an IR camera as shown in Figure 19.

Figure 19: IR image of section 3, where can be seen the heating foils installed as well as hoy heat distributes among the 1mm aluminium plate.

Those films were settled to cover as much area as possible, taking in account that the maximum electric current that the Adaptable temperature regulator could handle was 15A. As can be seen in Table 2, the maximum intensity used by all the heating devices is 13.03A, far from the maximum one. These check-up measurements were performed with a digital multimeter manufactured by Keysight Technologies whose accuracy was of ±0.025% + 5 cents for DC voltage and ± 0.05% +5 cents for DC current [28].

Table 2: Summary of the maximum current, voltage and power used by the heating foils of each section as well as the heating rods.

Section	Voltage [V]	Max. Current [A]	Power [W]
Heating foil S1	60	1.230	73.8
Heating foil S2	60	2.155	129.3
Heating foil S3	60	2.685	161.1
Heating Rods	60	6.960	417.6
TOTAL		13.03	781.8

In reference to the heating rods, which were completely manufactured by the electronic lab, which is why there not many details could be provided, which were placed on the bottom plate at a distance of 50mm from the backplate and protecting the surfaces of the hot box from its emissivity using aluminium shields as can be seen in Figure 20.

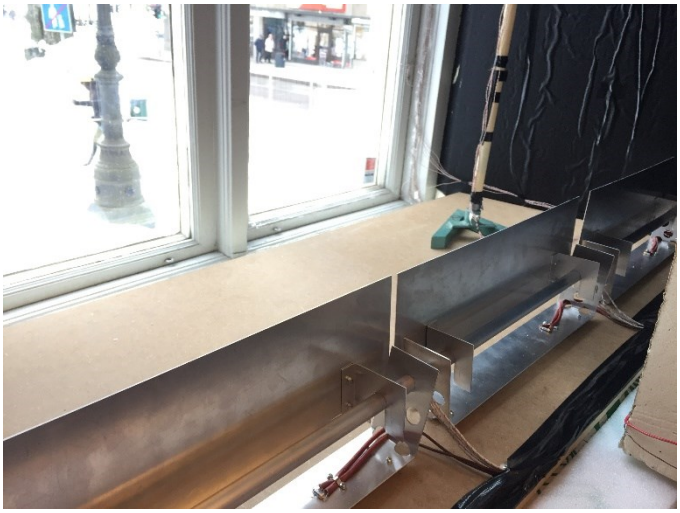

Figure 20: Heating rods installed on the Hot Box at a distance of 5cm with a barrier aluminum plates for radiation towards the box.

With the purpose of maintaining a constant temperature inside the room, a 2000W [29] heating radiator was used, without the fan, as nor was more air mixing necessary. Its power was controlled by another Adaptable temperature regulator.

3.3.3 Sensor placement

Once the hot box was constructed, it was necessary to decide the layout of the sensors in order to collect the necessary data properly, and so optimizing its number. For the decision of the layout, the standards SS-EN ISO 12567-1:2010 [13] and ISO 8990-1994 [30] were followed, adapting its regulation to the project's needs. As there were not enough sensors for following them blindly, it was decided, as stated before, to focus on one side of the hot box and assuming a symmetry inside it, that was verified by the usage of checkpoints.

Once the layout was decided, a sensor layout was performed by using the 3D model previously build and the approximate length of each sensor was calculated positioning them in the 3D model.

As de dimensions of the thermocouples used for measured in comparison with the hot box is negligible, for representing them it was used a cube of 20x20x10mm, that was taken into account during the length calculation.

Nevertheless, due to the difference between the 3D model and the reality, some issues were found, being necessary, in some cases, an extension for some of the sensors. Those issues were primarily because the lengths were calculated as straight lines, being necessary in some cases to curb those cables, incrementing the length needed.

In the design phase, 69 sensors were stated to be installed, labelled as F1-F69 from the Swedish word “fönster”. All of them were manufactured from the same thermocouple roll with a diameter of 0.3mm, that followed the colour code IEC 60584.3 [31], minimizing the possible variability due to the inhomogeneity of the material. Furthermore, for the connections, IEC miniature Thermocouple connectors were used, not considering possible loses on the connection as they were manufactured from the same thermocouple alloys than the cables [32] as said in ASTM E220-13 [33].

The sensors were calibrated by following the standard ASTM E220-13 [33] despite the fact that the apparatus used for comparison test was one manufactured by the university instead of one manufactured by a company. However, the apparatus used fulfilled the requirements stated by the standard for the temperature interval studied as well as it had been previously used for that main task. Once tested, the variation obtained between sensors stayed within ± 0.005ºC, typical temperature levels of the tests (at worst, ±0.017ºC at a low temperature of 5 ºC), being able to consider those measurements as accurate[26].

Other issues found in the sensor’s layout were the change of reference, as in some cases for building purposes, it was necessary to change the reference from one point to another, lengthening the cables needed. As the previous cables were calibrated, following ASTM E220-13 [33], it was not needed to calibrate them again.

Furthermore, extra sensors were required to build on site for measurements purpose, as for example sensor F70, or for data validation, i.e. sensors F71-F75, that were installed at the beginning of the second case to validate some calculations.

Due to the fragility of the thermocouples and the requirements of mounting and dismounting the back part of the insulation, three thermocouples were broken, being imperative to build them on site. The sensors built in Rådhuset were tested following ASTM E220-13 by the utilization of a calibrated thermometer [34], consequently, those values could be considerate accurate as well.

In Figure 21, an overall view off all the thermocouples installed in the hot box can be seen including its most important dimensions.

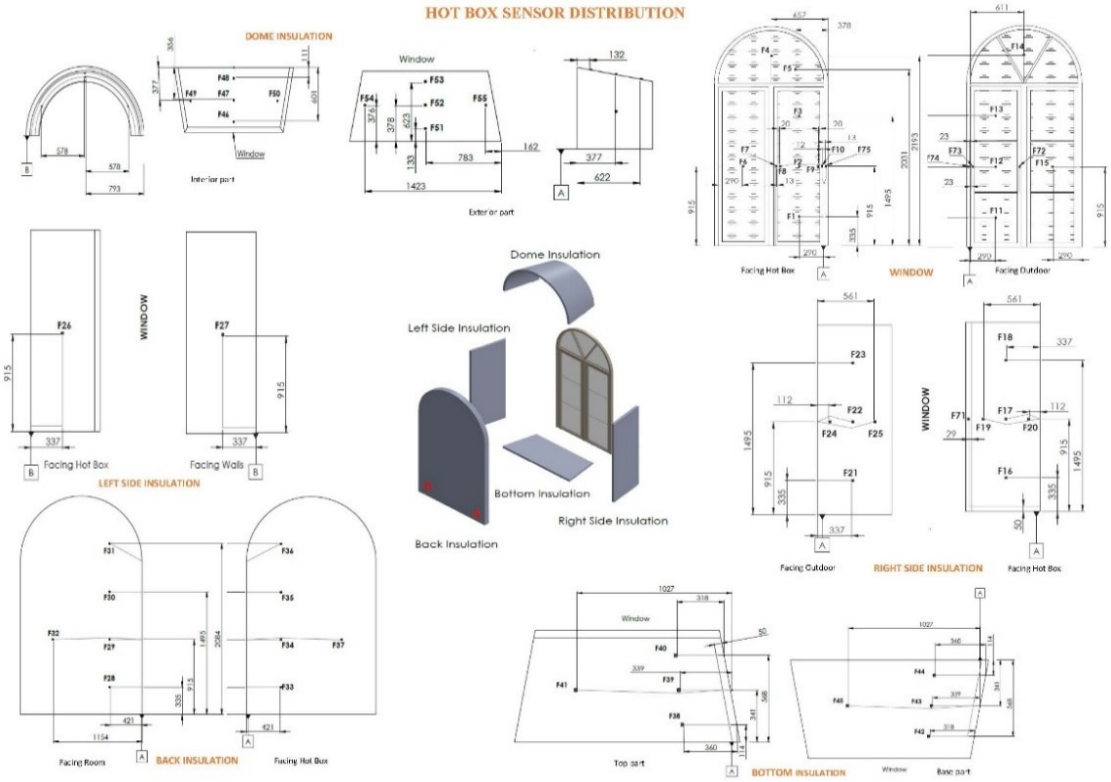

Figure 21: Hot box Thermocouple layout for each surface including reference connection point and its most important measurements.

In addition to the Hot box surfaces, other sensors were used, measuring the air temperature inside the hot box, the room temperature and the temperature of the walls on both sides, whose layout is shown in Figure 22.

All the sensors related to the surfaces, were installed directly in contact with its correspondent surface, using transparent tape for fixing the sensors placed on both windows surfaces, and black electric tape for the ones related to the surfaces of the hot box to assure that the sensors will not move. Regarding the sensors that are intended to measure air temperature, all of them where installed at least at 3 cm from the rod used for installing them in different vertical position, estimating that the heat transfer method that they will suffer will be convection, ergo the air temperature.

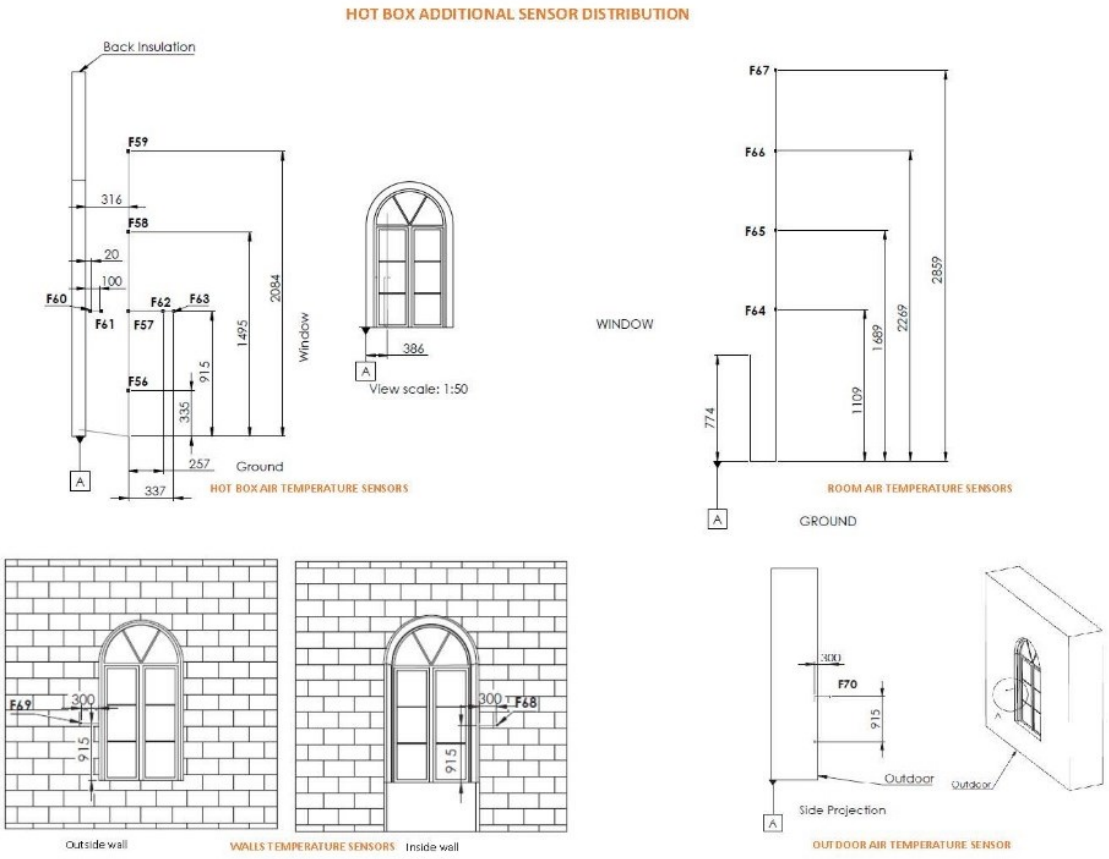

Figure 22: Additionally layout of the thermocouple sensors used during the project as well as its most important measurements.

After the construction of the sensors, the data provided by the sensors had to be logged as well as converted from the electrical signal output of the thermocouple into a digital signal that could understood from a computer.

For the performance of such task, an Agilent 20 channel Multiplexer Module was used as connection to an Agilent Data Logger Switch Unit, connected to a computer were a code designed by the electronic lab in Labview 2015 was executed.

Although the sensors could have been connected directly to the multiplexer, the standard cold junction accuracy, of 0.8ºC [35], was considered too high for the expected gradients in temperature. In view of that, from the Electronic lab, an improved cold junction was designed and manufactured, where the cables were connected directly to a stainless steel fragment that would keep the offset constant for all the sensors connected. Furthermore, one of the 20 channels available, were used to obtain that reference point improving the accuracy of the measurements.

The aspect of those new cold junction boxes is shown in Figure 23 during the calibration process. The white cable that came from it is the connector that went directly to the multiplexer.

Figure 23: Cold junctions used for calibrating the sensors can be seen on the left in three different colours, with sensors calibrated and the loggers used for acquiring the data.

As previously mentioned, the loggers were connected to a computer where a Labview program was running. The program was implemented for plotting the eight possible multiplexers connected to the loggers, used likewise for capturing the data in a text file for its later analysis. In order to obtain the same reference, all the loggers used the same clock reference embed inside the software.

The software was programed for to sample every twenty seconds for every sensor available, throughout a minute. Once elapsed, the mean value obtained for that interval was plotted and written in a text file.

3.3.4 Humidity measurements

Humidity measurements were taken inside the box, inside the room and in a building near the study location, at an approximate height of 4m with an accuracy of ±0.3ºC for temperature and ±0.3% for relative humidity [36].

3.3.5 Hot Box insulation

Lastly, when all the insulations, sensors and other parts were correctly placed, that the seal between the plates was not perfect, allowing leakages between the hot box and the room. Those leakages would affect negatively the study, as the control volume studied would be converted into an open volume, not allowing to discern if the heat went through the window or to the room.

As a result of this statement, weather stripes were installed in the entrance door to the room, acquiring a slight overpressure on the room, which would be beneficial for the study. Additionally, a wooden structure was installed in surrounding the hot box to apply mechanical pressure by introducing wooden wedges between the hot box and the structure was included, forcing the backplate insulation towards the hotbox side insulations, thus improving its tightening. Such structure can be seen in Figure 24, where can also be seen in the close position the wedges used for closing the hot box.

Figure 24: Final layout of the Hot box construction. On the left it can be seen in the open position whereas in the right it is completely closed.

3.4 Following and control

3.4.1 Data obtainment and hot box revision.

As the hot box was settled, data acquisition began. For the first days, the data was acquired without any film installation in order to have a reference case that would be lately compared to the film installation.

While this data acquirement was performed, a problem was found as the sun radiation made that the temperature reached by some surface was close to 90ºC. As a result, some pieces of the tape used for keeping the sensors in place felt, despite electrical tape was used.

For this reason, an eyesight revision of the layout was necessary prior to run every test.

3.4.2 Film installation

After 10 days, data acquisition for the reference case, that will be further be referred as "Base Case", the company SunStop, the official authorized dealer of 3M in Sweden, came to install the film, model 3M Thinsulate Climate Control 75 in all of the glasses of the window. The installation was requested to be done by them in order to reduce possible errors while the installation process.

Moreover, according to the manufacturer it was expected a reduction of 26% on heat losses [37], that would be verified when compared with the base case.

The first installation was performed on the surface 3 of Figure 25, which will be further referred to as "Film Middle window case". That installation was maintained during 6 days while data acquisition.

After this period, the film was removed and a new one was installed on Surface 4 of Figure 25. The reason for this change was that the installation on surface 4 was the one recommended by the manufacturer and it aimed to see the impact of the surface chosen for the installation. This case will be further referred to as “Film inner window case”.

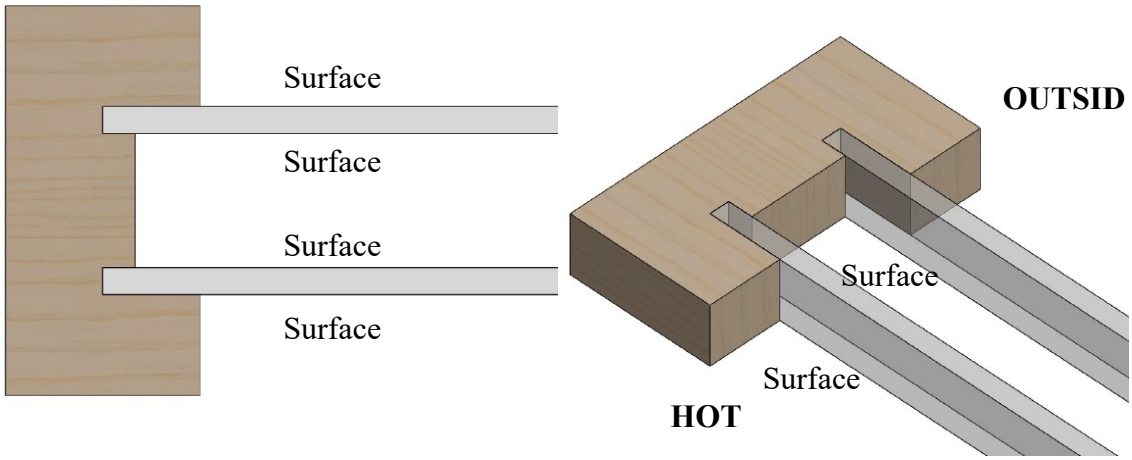

Figure 25: Rendering of the double clear glass window studied during the project.

3.5 Calculations

After obtaining the data, calculations were done for obtaining the different values that were interested for the project.

As previously mentioned, the data was written in a text file consisting on the date, the sampling time, the values for all the thermocouples and the output power from the heating devices.

3.5.1 Calculation thermal flux losses

Firstly, the losses through the insulation was calculated as by knowing how much energy was lost by the insulation and the total amount of power given to the heating power, the heating loss through the window can be obtained.

For this estimation, every surface was divided in different parts taking into account the number of sensors available. For example, for the right and left surfaces, the number of division done was nine, five correspondent to the installed sensors and four more where a symmetry was used for calculating the temperature correspondent to that surface as shown in Figure 26.

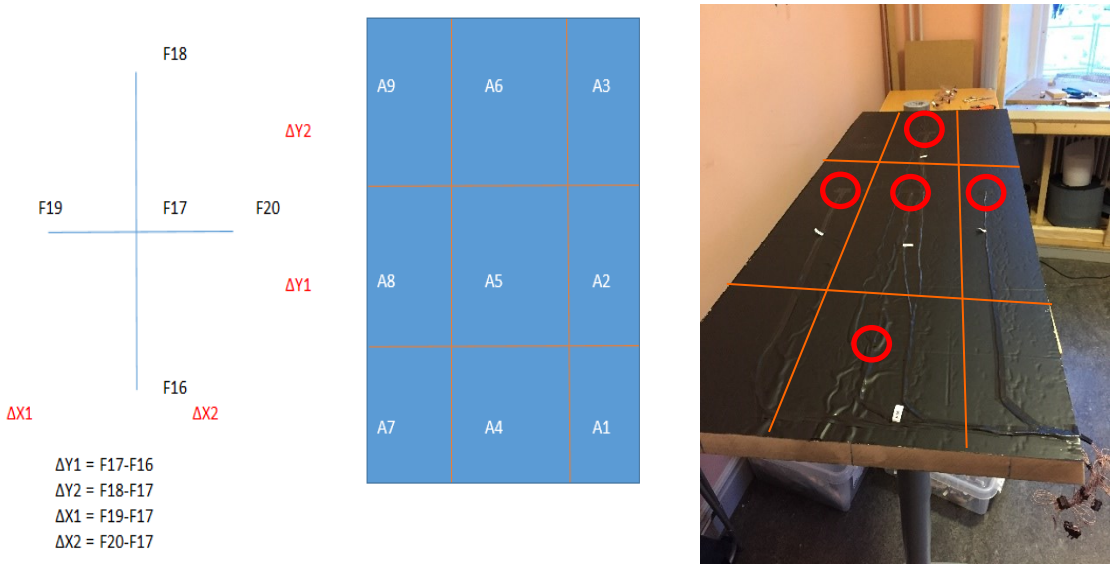

Figure 26: (LEFT) Schematic of the subdivisions done to side insulation to calculate the heat flux associated to each pair of sensors. (RIGHT) Picture of the subdivisions performed and the sensors in red circles

The calculation was performed by using the sensors on both sides of the insulation and the surfaces obtained by the 3D model. Lately, using equation number *(1)* the thermal flux trough the surface was obtained.

$$\boldsymbol{q = A \cdot \frac{\lambda}{d} \cdot \Delta T}$$

$$q = Heat\ Flux\ [W]$$

$$A = area\ [m^2] \qquad (1)$$

$$\lambda = Thermal\ Conductivity\ \left[\frac{W}{m \cdot K}\right]$$

$$d = thickness\ of\ the\ layer\ of\ insulation\ [\mathrm{m}]$$

$$\Delta T = Temperature\ difference\ [K]$$

The same methodology was replicated for every insulation surface; whose result gave the total thermal flux loses through the insulation.

3.5.2 Calculation of the indoor temperature

A tessitura was faced arriving at this point, as currently the thermocouple mainly is affected by convection and the influence of radiation is not taken into account.

To solve this deal, it was decided to assume that the air temperature as well as the radiation would have the same weight in the estimation of the indoor temperature.

For the calculating the air temperature, the vertical sensors F56-F59 were used, dividing the total volume of the hot-box in four sections, where each sensor was situated in the centroid of the volume. An image of the subdivisions can be seen in Figure 27. Each temperature was weighted by its correspondent surface versus the total for obtaining the temperature related to the air.

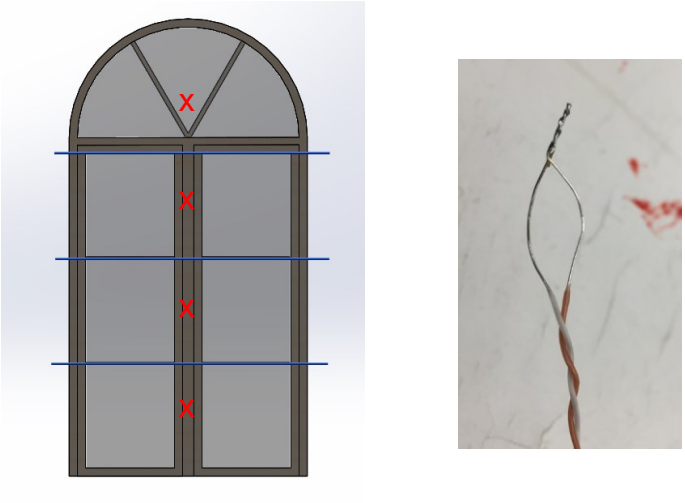

Figure 27: (LEFT) Subdivision for weighting the air temperature, each one related to one vertical air temperature sensor represented with a red x. (RIGHT) Thermocouple T-Type of 0,3mm used for presumably calculate air temperature

3.5.3 Calculation of the surface temperature

Regarding the mean radiant temperature associated to the surface it was calculated by weighting the temperature associated to each surface by its view factor referring the window.

In order to calculate the view factor, some simplifications were performed in order to simplify the calculations. Those simplifications consisted in the conversion of the geometry of the hot box to a cubic objects seen in Figure 28.

In order to minimize the errors due to this simplification, the average of the surfaces was performed. Furthermore, for calculating the associated temperature to that surface, a weighting by the real surface and the used for the calculated was taken into account and multiplied by temperature referred to that surface.

The motivation of those simplifications was to be able to use simplified equations for the view factors, assuming that every surface was or perpendicular or parallel to the window.

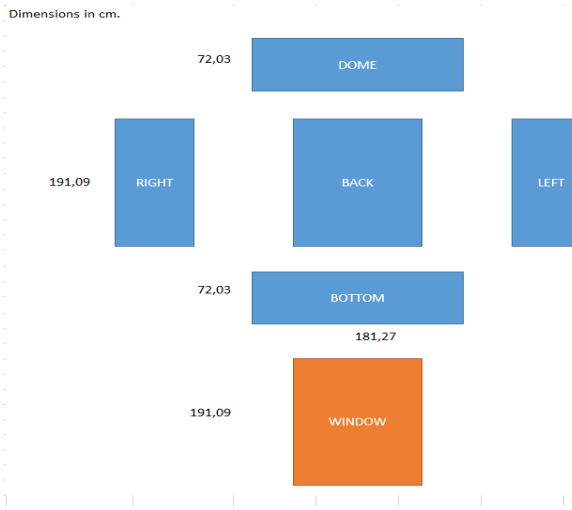

Figure 28: Extrapolation of the surfaces of the hot box to a cubic shape.

Consequently, with those simplifications, it was possible to calculate the view factor with the formulas shown in Figure 29. Furthermore, to verify the correct calculation of them, a verification that the sum of all of the view factors was equal to one was performed.

Geometry	Relation
Aligned Parallel Rectangles (Figure 13.4) 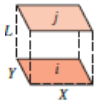	$\overline{X} = X/L, \overline{Y} = Y/L$ $F_{ij} = \frac{2}{\pi \overline{X}\,\overline{Y}} \left\{ \ln \left[\frac{(1+\overline{X}^2)(1+\overline{Y}^2)}{1+\overline{X}^2+\overline{Y}^2} \right]^{1/2} + \overline{X}(1+\overline{Y}^2)^{1/2} \tan^{-1} \frac{\overline{X}}{(1+\overline{Y}^2)^{1/2}} + \overline{Y}(1+\overline{X}^2)^{1/2} \tan^{-1} \frac{\overline{Y}}{(1+\overline{X}^2)^{1/2}} - \overline{X} \tan^{-1} \overline{X} - \overline{Y} \tan^{-1} \overline{Y} \right\}$
Coaxial Parallel Disks (Figure 13.5) 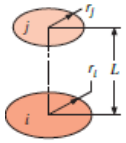	$R_i = r_i/L, R_j = r_j/L$ $S = 1 + \frac{1+R_j^2}{R_i^2}$ $F_{ij} = \frac{1}{2}\{S - [S^2 - 4(r_j/r_i)^2]^{1/2}\}$
Perpendicular Rectangles with a Common Edge (Figure 13.6) 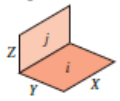	$H = Z/X, W = Y/X$ $F_{ij} = \frac{1}{\pi W} \left(W \tan^{-1} \frac{1}{W} + H \tan^{-1} \frac{1}{H} - (H^2+W^2)^{1/2} \tan^{-1} \frac{1}{(H^2+W^2)^{1/2}} + \frac{1}{4} \ln \left\{ \frac{(1+W^2)(1+H^2)}{1+W^2+H^2} \left[\frac{W^2(1+W^2+H^2)}{(1+W^2)(W^2+H^2)} \right]^{W^2} \times \left[\frac{H^2(1+H^2+W^2)}{(1+H^2)(H^2+W^2)} \right]^{H^2} \right\} \right)$

Figure 29: Equations used for the estimation of the view factor [38].

3.5.4 Calculation of the U-value and selection of the steady state interval.

The International Organization for Standardization defines U-Value "the thermal transmittance of the element, environment to environment and is given by equation *(2)* [39].

$$U = \frac{q}{(T_i - T_e)} \qquad (2)$$

In the present case of study, there was an incertitude regarding which outdoor environment to use, the outdoor window or the outdoor natural environment.

The ISO standard for buildings defines environment as "*natural, man-made or induced external and internal conditions that may influence performance (3.1.78.1)(3.1.78.2) and use of a building"* [40], being both choices correct for the calculations.

For that reason, both U values were calculated, and studied, as there is no certainty of which one has used the manufacturer of the low emission film.

As the thermal flux has been calculated using the area, the equation used for the calculations would be equation *(3)*. Moreover, as two cases were studied at the same time, for the case that outdoor window was considered as outdoor environment, named T_w, equation *(4)* was used for calculating the temperature difference, whereas for the outside air as outdoor environment equation *(*5) was used.

$$U = \frac{q_{TOT}}{A \cdot \Delta T} \quad (3)$$

$$\Delta Tw = Tin - T\_F12 \quad (4)$$

$$\Delta Ta = Tin - T\_F70 \quad (5)$$

T_F12 = Temperature sensor on outside of external window [K]

T_F70 = Temperature sensor for outdoor air temperature [K] representative sensor temperature for the external environment [K]

ΔTw = Temperature difference between the inside of the Hot Box and the external window. [K]

ΔTa = Temperature difference between the inside of the Hot Box and external environment. [K]

U-value was calculated for every data available of the day studied, obtaining a plot time dependant, where it was seen that the interval from 4:00 to 5:30 was the most stable, with a standard error of 0,01207, equation *(8)*, as will be seen in the following chapter, being the reason why the mentioned interval was used for all the calculations done.

Furthermore, the mentioned calculation was adapted from ISO 8990 [30], where simplifications had been applied.

However, this method of calculation is a rough approximation and therefore, the obtained values would not be so accurate. For properly calculating those values, a standard as EN 673 must have been followed.

3.5.5 Conversion of humidity

For calculations regarding humidity, equations (6) and (7) had been used to convert relative humidity and temperature to absolute humidity [41].

$$p_{vs} = \frac{e^{77{,}345+0{,}0057T-\frac{7235}{T}}}{T^{8{,}2}} \quad (6)$$

$$w = \frac{0.622 \cdot \left(\frac{RH}{100}\right) \cdot Pvs}{\left(101325 - \left(\left(\frac{RH}{100}\right) \cdot Pvs\right)\right) \cdot 1000} \quad (7)$$

$$p_{vs} = Saturated\ vapour\ pressure\ [Pa]$$

$$RH = Relative\ Humidity\ [\%]$$

$$w = absolute\ humidity\ \frac{g\ water}{kg\ air}$$

4 Results

4.1 Statistical Results

As previously mentioned, a statistical analysis of the data obtained was performed for selecting the interval of study.

In Figure 30, the evolution of the U-value obtained for a data set as exemplification can be seen, showing the fluctuations between the values during the period of study. It was found that when the sun rises, the temperature reached by the hot box was up to 90ºC not being worthy to acquire data.

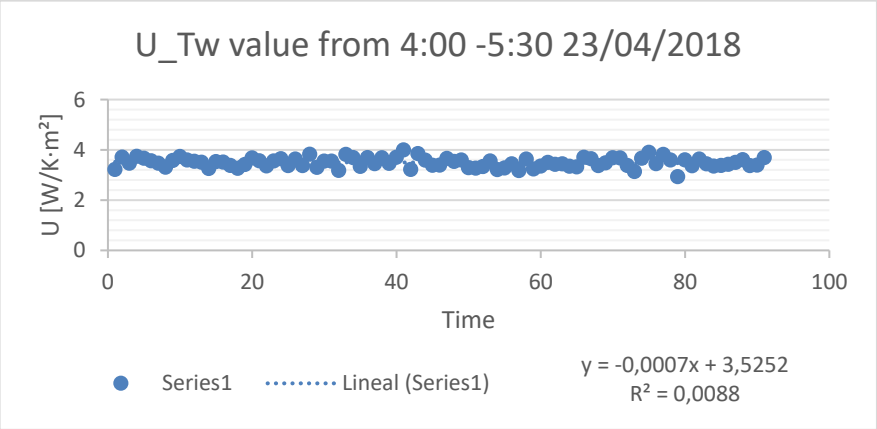

Figure 30: Variation of U-value during the studied period between 4:00 and 5:30 as a steady state conditions.

In order to be confident about the selected interval, the standard deviation (S) has been calculated with the software MINITAB 18, obtaining a value of 0,190745, Figure 31.

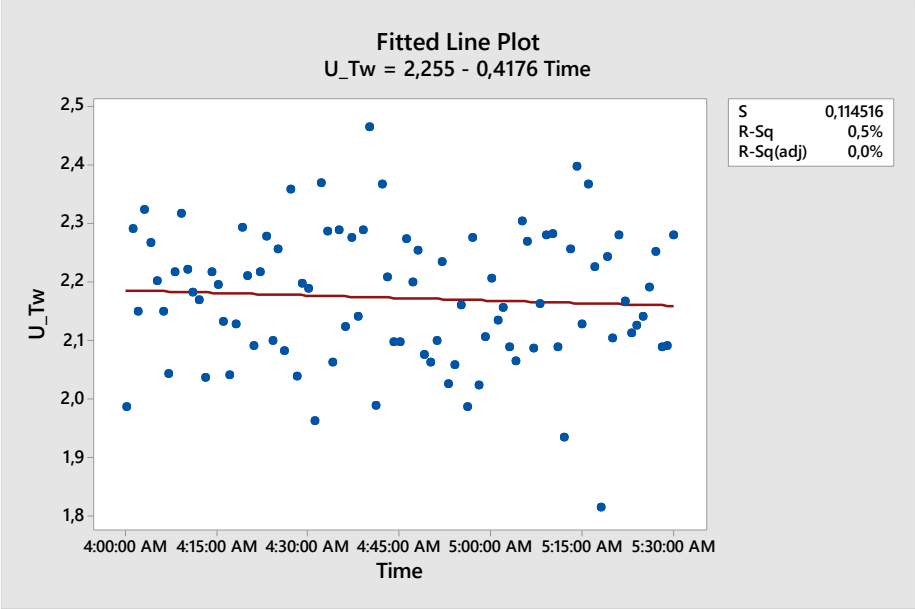

Figure 31: Statistical analysis of the data obtained from 4:00 to 5:30, obtaining a standard deviation of 0.190747

In order to estimate the standard error, equation *(8)* was used with the values correspondent to that exemplification obtaining a standard value of 0,01207.

$$U_A = \frac{S}{\sqrt{n}} \rightarrow \frac{0{,}114516}{\sqrt{90}} = 0{,}01207 \quad (8)$$

Ua = standard error

S = standard deviation

n = number of samples

As this value was lower than the 10% of the mean value, it was trustable for further calculations[42].

4.2 U-value results.

The values found for each case can be seen in Table 3 and a comparison between them in Table 4

Table 3: Summary of the mean values obtained for each case, divided by the source used as outdoor temperature

	U_ΔTw [W/ (K·m²)]	U_ΔTa [W/ (K·m²)]
Base Case	2,19	1,77
Film Middle Window	1,48	1,30
Film Inner Window	1,72	1,46

Table 4: Reduction values referring the base case found for each case.

	Base Case U_ΔTw	Base Case U_ΔTa
Film Middle Window	-33%	-27%
Film Inner Window	-22%	-18%

Additionally, in order to see if there was a correlation between the outdoor humidity and the temperature used for calculating T_a, they were plotted together as can be seen in Figure 32.

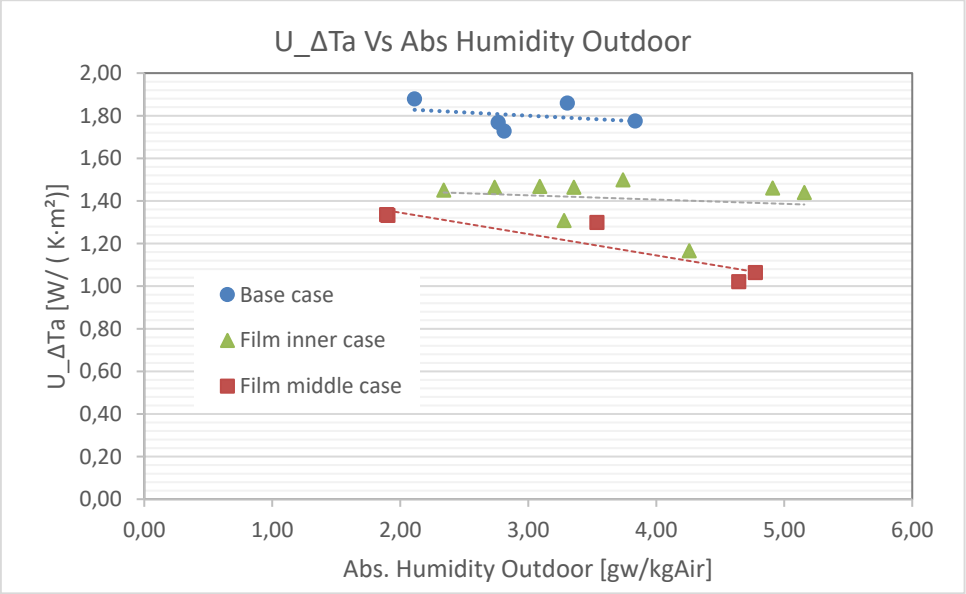

Figure 32: Plot showing the relationship between the u value using T_a and the absolute humidity of the outdoor environment for each case.

Furthermore, a plot (Figure 33) including the differences used for calculating the U-value as well as the indoor temperature and humidity was done in order to look for a correlation between them.

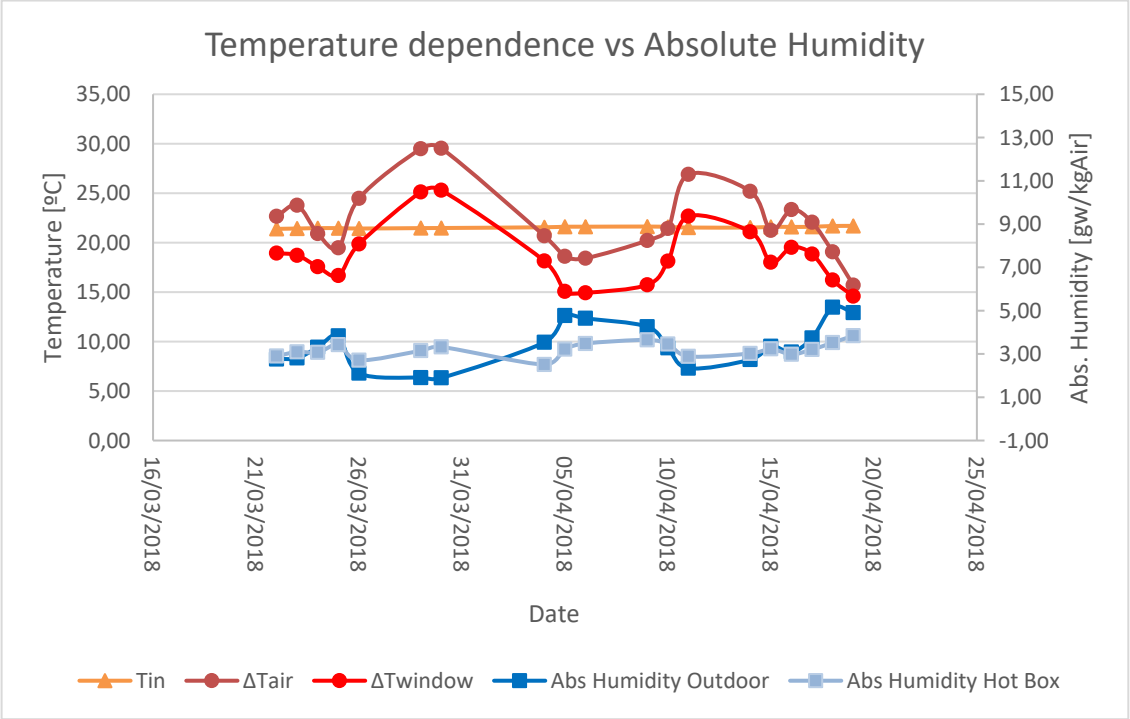

Figure 33: Plot showing the different differences used for calculating the U-value and the absolute humidity for the outdoor environment and inside the hot box.

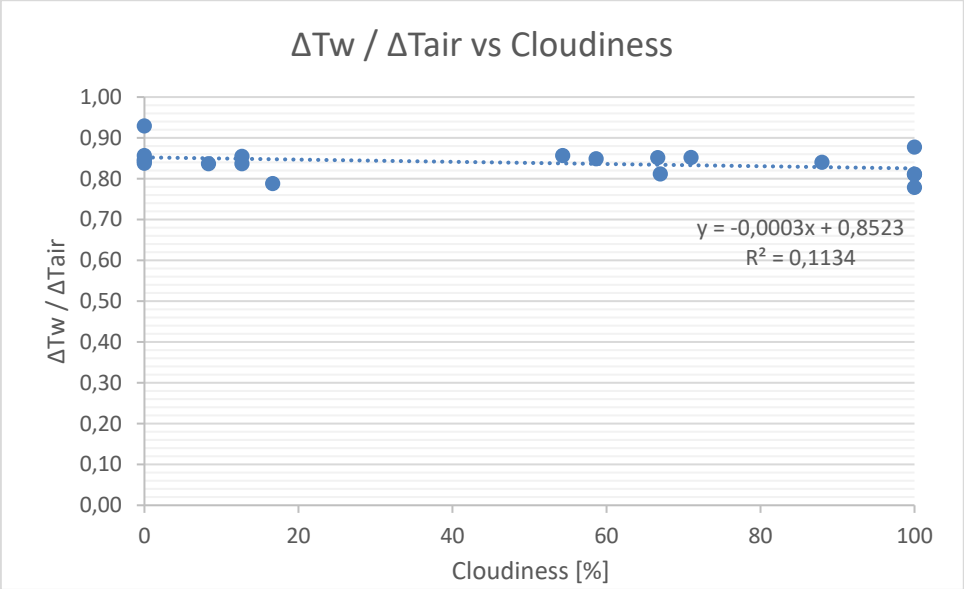

Figure 34: Plot of the relationship between the temperatures used for calculations versus cloudiness.

Related to the comparison between U-value and the absolute humidity, shown in Figure 35 and Figure 36, the trend equation has been extracted and used for calculating the U Value associated at that absolute humidity. Both values and its differences are shown in Table 5.

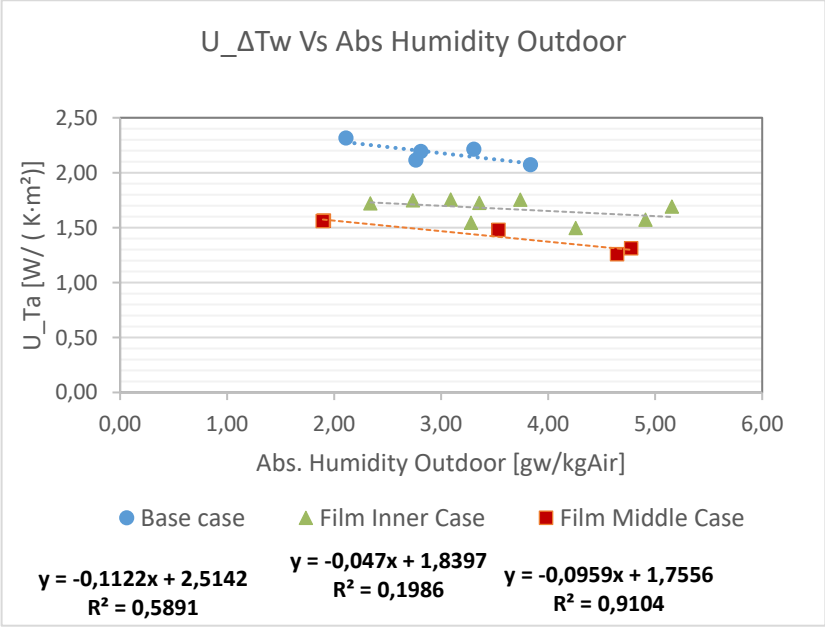

Figure 35: Plot of U value obtained for ΔTw with the correspondent trend equations used for calculating the U values referred to the absolute humidity.

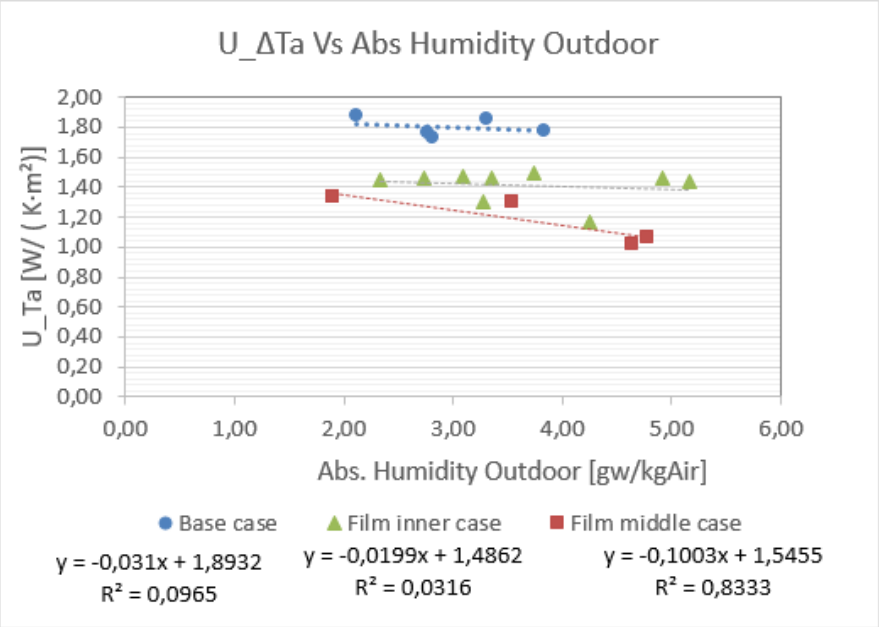

Figure 36: Plot of U value obtained for ΔTa with the correspondent trend equations used for calculating the U values referred to the absolute humidity

Table 5: Comparison between the values obtained from the hot box towards the ones obtained from the equations of humidity as well a comparison between the obtained values. Units in [W/(K·m²)]

U-Values calculated by Hot Box [HB] and Absolute humidity [w] [W/(K·m²)]				
	U_ΔTa_w	**U_ΔTw_w**	**U_ΔTa_HB**	**U_ΔTw_HB**
Base Case	1,79	2,14	1,77	2,19
Film Middle Glass Case	1,21	1,66	1,30	1,48
Film Inner Glass Case	1,42	1,68	1,46	1,72

Differences values obtained Hot Box [HB] vs Absolute humidity [w]		
	U_ΔTa_HB-w	**U_ΔTw_HB-w**
Base Case	2%	-1%
Film Middle Glass Case	-12%	6%
Film Inner Glass Case	2%	3%

Differences values obtained Hot Box [HB] vs Absolute humidity [w] vs Base Case				
	Base Case ΔTa_w	**Base Case ΔTw_w**	**Base Case ΔTa_HB**	**Base Case ΔTw_HB**
Film Middle Glass Case	32%	23%	27%	33%
Film Inner Glass Case	21%	21%	18%	22%

Regarding the effect of dependence between relative humidity and its dynamics, a comparison between outdoor, the hot box and the room has been done for three different cases varying the cloudiness as shown in Figure 37, Figure 38 and Figure 39. Showing a dependency between the relative humidity of the hot box and the outdoor.

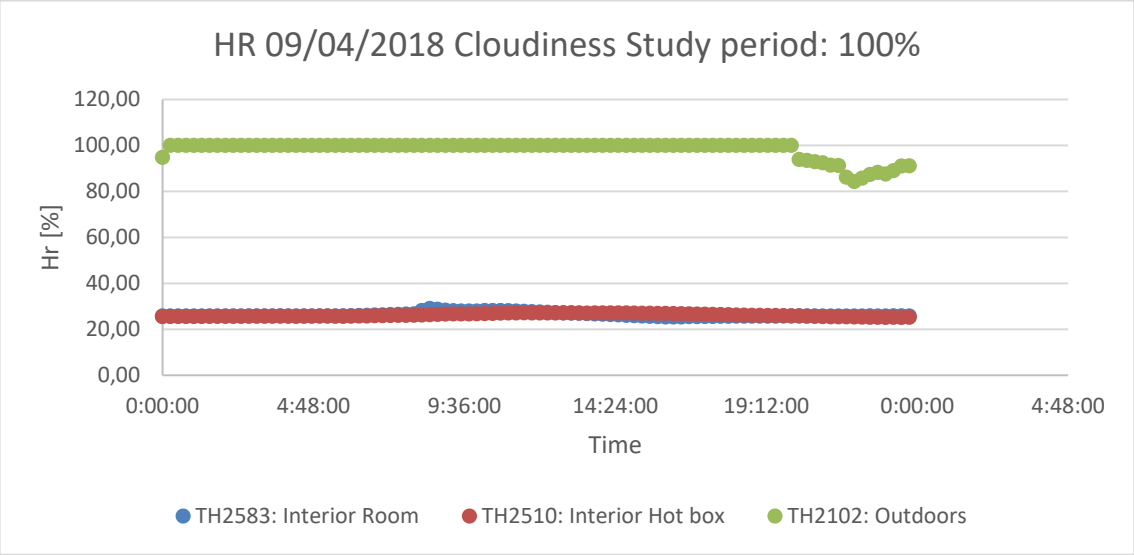

Figure 37: Comparison of relative humidity between spaces for a cloudy day.

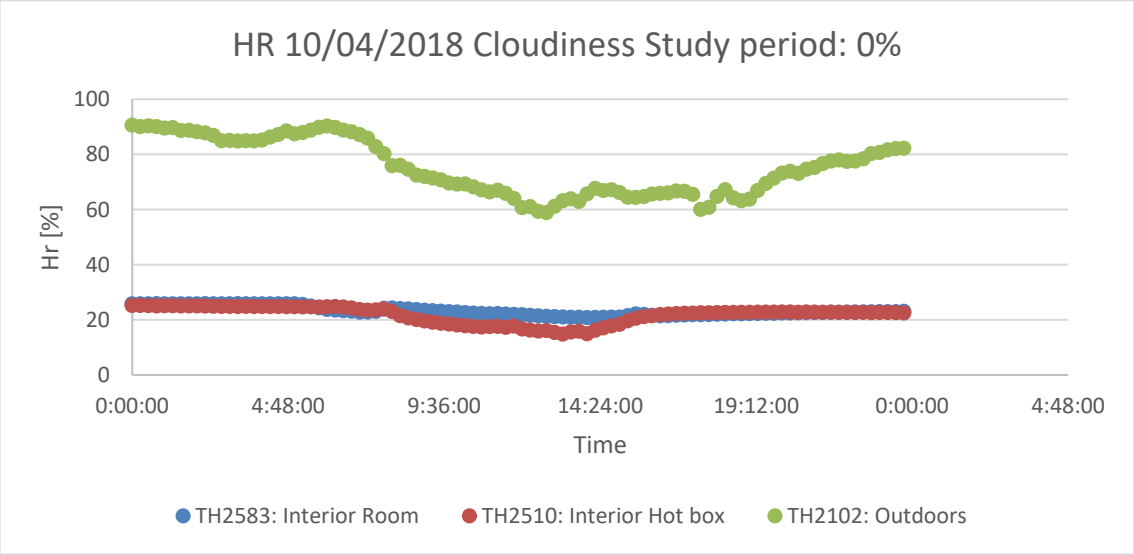

Figure 38: Comparison of relative humidity between spaces for a sunny day.

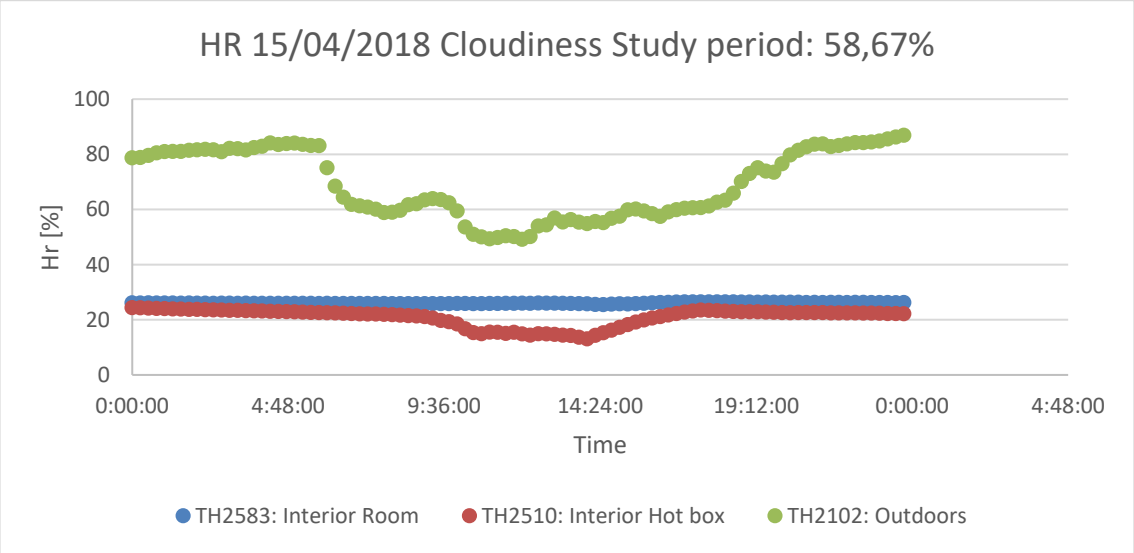

Figure 39: Comparison of relative humidity between spaces for a day both cloudy and sunny.

The relationship between U value and absolute humidity has been corroborated with a stadistical ANOVA analysis using Minitab 18 as illuatrated in Figure 40.

Analysis of Variance

Source	DF	Adj SS	Adj MS	F-Value	P-Value
Abs. Humidity Outdoor [gw/kgAir	1	0,05845	0,058453	5,99	0,027
Scenarios	2	0,80252	0,401258	41,13	0,000
Error	15	0,14635	0,009757		
Total	18	1,12033			

Model Summary

Figure 40: Results of the ANOVA study for the relationship between U value and absolute humidity showing a p lower than 0,05 verifying its dependence

4.3 Film installation issues

Despite being installed by the company, some bubbles of air between the glass and the film were formed that could reduce the performance of the film, as shown in Figure 41.

Furthermore, when the installation company was contacted regarding this issue, they informed that some issues were found with the used film batch and with the newer batches and being a bit more careful regarding possible human errors, such bubbles should nor occur.

Figure 41: Bubble between low emissivity and the window can be seen as water drops.

4.4 Energy Reduction by applying films in the world.

If the film studied was installed in the overall world, the reduction will be important as reducing the losses will mean, if keeping all the other related interaction with consumption as constant, a lower energy generated need,

$$Reduction = E_B \cdot L_{W-B} \cdot R_F$$

$E_B = Total\ final\ energy\ use\ by\ residential\ and\ commercial\ sectors\ [Mtoes]$

$L_{W-B} = Losses\ in\ a\ building\ due\ to\ windows\ [\%]$ *(9)*

$R_F = Reduction\ of\ the\ losses\ in\ a\ window\ due\ to\ Low-E\ Film\ installation\ [\%]$

The value for E_B is equal to 2589Mtoes including both types [22], and the losses of energy true the window can be assumed as 10% [1]. Consequently, assuming that those values as well the reduction found previously for the low emissivity film between the glazing the total reduction will be of 85.44 Mtoes.

5 Discussion

As stated before, one of the problems found during the development of the project was to discern about what temperature to use regarding the outdoor environment temperature. The international standards (ISO) do not specify which temperature should be used, leading to performing calculations towards the two possibilities; the temperature difference between indoor and the external window [ΔTw] and between indoor-outdoor air temperature [ΔTa].

The values obtained for the base scenario, where no low emissivity films were installed, were 2.19 W/K·m² for ΔTw and 1.77 W/K·m² for ΔTa. These values were expected to be higher as the building was constructed in 1870's and the value obtained for current double glazed windows with wooden frames is approximately 2.8 W/K·m², not being very trustable as technology has improved the quality of the windows and improved its efficiency.

However, nowadays windows have a ratio of 15% frame 85% glass whereas the old window studied has a relationship of 30% frame and 70% glass, taking into account the values obtained from the 3D model representing the window. Furthermore, as wood is a better insulator as glass and the proportion is nearly the double, this can be the cause of being a lower value than the expected.

In regards to the calculations results obtained considering the surrounding environment as the outdoors, they indicate that the original window would present a better efficiency than the double low emission glasses and vinyl frame window. This result, however, makes no sense, since the outdoor window itself is one of the considered choices as outdoor environment.

All in relation to ΔTa, for which the outdoor thermocouple is much less sensitive to sky radiation. This fact leads to ΔTw to be selected instead of ΔTa, as ΔTw can be considered more representative of the outdoor temperature of the window than Ta, which would be more related to the outdoor air temperature. This statement is supported as ΔTa uses the sensors T_F70 for outdoor temperature despite being practically only measuring the outside air temperature related to convection hence missing the radiation impact especially from clear night skies. On the other hand, ΔTw, that uses T_F12 has de advantage of taking both outdoor air and radiation temperature into account, despite having the disadvantage of missing the heat flow between the outdoor window and the external environment (he-value).

Furthermore, neither the correlation nor the relationship seen is not solid, making the selection of ΔTw also not solid, being necessary further measurements related to this topic in order to be able to state which one is more representative.

In reference to the impact from radiation over the U-value, in Figure 34 can be seen that there is a tendency towards the expected direction – i.e. less cloudiness (clearer sky) – making window temperature lower, presumably due to radiation heat loss to sky, and, thus obtaining a higher ΔTw.

The absolute humidity seen in the relation between Figure 33, indicates that there is a tendency for higher humidity, especially outdoor, to reduce the U-value. Besides being a small difference between the three cases Figure 35 and Figure 36, it was not possible to find a good explanation after a thorough data analysis, being necessary further studies regarding relative humidity and its dynamics.

The study regarding relative humidity dynamics, Figure 37, Figure 38 and Figure 39, seems to show a trend that relative humidity inside the hot box, however, the fact that RH decreases both outdoor and in box when the sun rises is probably due to the simultaneous rise of air temperature. However, the fact that RH stays approximately even in all environments during the studied interval indicates that no considerable changes between vapour interactions with material happens during this time.

One way to handle the dependence on absolute humidity is to compare the U-values with it, using the mean value of humidity for all cases as a central point. Once represented, using the equations given by the trend lines and calculating the mean of the attained U-values from the individual test. The values obtained differ only 1% in the base case against 6% in the Film inner window, verifying the correlation between absolute humidity and the U-value, verified by the ANOVA test performed shown in Figure 40.

In reference to the installation of the films, it has been obtained a reduction of 33% with the film installed in the middle glazing of the window whereas the reduction for the installation on the innermost glass was 22%.

As found in the literature review, the value obtained is lower than the one given by the manufacturer, as can be expected. Moreover, this can also be due to the installation performed by the company, as has been shown in Figure 41, bubbles were formed during the installation and did not disappear, lowering the performance of the film as expected.

The manufacturer informed us that an issue was found with the batch used in the studied windows and informed that the installation would be done again as soon as possible. Additionally, some human errors could have been made during the installation us the worker was used to do it on his own, and by having people asking around him could have put him out of his comfort zone, consequently with higher changes of making mistakes during the installation process.

Furthermore, it has been found that the best position for the film it is the middle position, but it is not installed there as their life cycle decreases, due to the climate conditions.

Overall, it can be said that the performance of the hot box has been addressed, validating the assumptions made in the project and regarding the specialized facilities can be verified. However, a detailed test should be performed with a material whose thermal transmittance is known, in order to calibrate the apparatus, avoiding this way inaccuracy in the overall measurements.

Furthermore, despite that the method indicates the relative improvement regarding U-values of the films pretty well, in order to more accurate values regarding thermal conductance, a more complex method of calculation shall be applied, i.e. ISO EN 10077-1-2017 or SS-EN 673 among others.

6 Conclusions

6.1 Study results

For a scenario without film, where the outdoor of the window was used as outdoor environment, the study has shown the feasibility of the employed method obtaining a value of 2.19W/K·m². Furthermore, a reduction of 33% of the U-value was obtained, when a low emissivity film is applied between the two glasses of the window whereas for the recommended glazing from the manufacturer the reduction has been of 22%, lower than the value given by the manufacturer of 26% using the methodology of calculation explained previously.

6.2 Outlook

Future development to an apparatus for taking in situ measurements is recommended, as it would be able to perform no-destructible analysis, leading to optimize building that were out of scope. However, the methodology and apparatus studied during this project needs further experimentation, and should be tested with known samples for validating the results found as well as using a better model for calculating U-value in order to be able to make direct comparison or verifications of U-values obtained.

In reference to the low emissivity film, as has been found, the actual installation of the films is not the optimal, as manufacturers have prioritize the life of the products towards the efficiency of them. This information shall be given to the user to let them have the choice where to install them, as economically talking, the reduction of the losses would be of greater importance than the cost of having to replace more often the films.

Further studies towards the ageing of low emissivity films is still required as new technology development to improve its efficiency.

6.3 Perspectives

As have been previously seen, the installation of the self-adhesive low emissivity film in the middle window would be beneficial in energy efficiency terms increasing the efficiency of the window as well as the overall window with a low impact cost, despite having a lower life cycle. If this solution would be only applied to the commercial and residential buildings along the world, assuming that the efficiency of the Low-e films along with the leakages through the window remains, according to the statistics of energy balance for 204-2005 by IEA[1], it would correspond to a reduction of the world energy usage of 85.44 Mtoe (Million Tons of oil equivalent), as calculated with equation *(9)*. This reduction would mean that fewer energy would be needed to be produced by contaminant methods, having a beneficial impact to the environment as well as to society.

References

[1] IEA, *Transition to Sustainable Buildings - Strategies and opportunities to 2050*. 2013.

[2] Boverket, *Planning and Building Act (2010:900) Planning and Building Ordinance (2011:338)*. 2016.

[3] C. Misiopecki, M. Bouquin, A. Gustavsen, and B. P. Jelle, "Thermal modeling and investigation of the most energy-efficient window position," *Energy Build.*, vol. 158, pp. 1079–1086, 2018.

[4] G. Ficco, F. Iannetta, E. Ianniello, F. R. D'Ambrosio Alfano, and M. Dell'Isola, "U-value in situ measurement for energy diagnosis of existing buildings," *Energy Build.*, vol. 104, pp. 108–121, 2015.

[5] M. Ibrahim, L. Bianco, O. Ibrahim, and E. Wurtz, "Low-emissivity coating coupled with aerogel-based plaster for walls' internal surface application in buildings: Energy saving potential based on thermal comfort assessment," *J. Build. Eng.*, vol. 18, no. April, pp. 454–466, 2018.

[6] G. Baldinelli *et al.*, "Energy and environmental performance optimization of a wooden window: A holistic approach," *Energy Build.*, vol. 79, pp. 114–131, 2014.

[7] B. P. Jelle, S. E. Kalnæs, and T. Gao, "Low-emissivity materials for building applications: A state-of-the-art review and future research perspectives," *Energy Build.*, vol. 96, no. 7491, pp. 329–356, 2015.

[8] G. Baldinelli, "A methodology for experimental evaluations of low-e barriers thermal properties: Field tests and comparison with theoretical models," *Build. Environ.*, vol. 45, no. 4, pp. 1016–1024, 2010.

[9] A. A. Solovyev, S. V. Rabotkin, and N. F. Kovsharov, "Polymer films with multilayer low-E coatings," *Mater. Sci. Semicond. Process.*, vol. 38, pp. 373–380, 2015.

[10] X. Meng, T. Luo, Y. Gao, L. Zhang, Q. Shen, and E. Long, "A new simple method to measure wall thermal transmittance in situ and its adaptability analysis," *Appl. Therm. Eng.*, vol. 122, pp. 747–757, 2017.

[11] G. Desogus, S. Mura, and R. Ricciu, "Comparing different approaches to in situ measurement of building components thermal resistance," *Energy Build.*, vol. 43, no. 10, pp. 2613–2620, 2011.

[12] C. A. Brebbia and H. H. Al-Kayiem, *Energy and sustainability V*. .

[13] Swedish Standards Institute, "SS-EN ISO 12567-1:2010 Thermal performance of windows and doors – Determination of thermal transmittance by hot-box method – Part 1: Complete windows and doors (ISO 12567-1:2010)," 2010.

[14] F. Asdrubali and G. Baldinelli, "Thermal transmittance measurements with the hot box method : Calibration , experimental procedures , and uncertainty analyses of three different approaches," *Energy Build. Build.*, vol. 43, no. 7, pp. 1618–1626, 2011.

[15] X. Meng, Y. Gao, Y. Wang, B. Yan, W. Zhang, and E. Long, "Feasibility experiment on the simple hot box-heat flow meter method and the optimization based on simulation reproduction," *Appl. Therm. Eng.*, vol. 83, pp. 48–56, 2015.

[16] Azo Materials, "Measuring Thermal Conductivity According to the ASTM E1530 Guarded Heat Flow Meter Method." [Online]. Available: https://www.azom.com/article.aspx?ArticleID=11518. [Accessed: 23-Mar-2018].

[17] Apex Window Films, "Low-Emissivity (Low-E)." [Online]. Available:

http://www.apexfilms.ca/low-emissivity/. [Accessed: 18-Apr-2018].
[18] Leica Geosystems AG, “Leica DISTO ™ A6 User Manual,” 2007.
[19] Dassault Systèmes, “SOLIDWORKS Student Design Kit 2016-2017.” 2016.
[20] I. FLIR Systems, “FLIR C2-EDU Compact Thermal Imager Educational Kit Datasheet.” p. 2.
[21] Granta Design Limited, “CES EduPack TM 2014 CES EduPack User Manual and Getting Started Guide,” no. April, 2014.
[22] IEA and OECD, “Sweden National Building Regulations (2010),” 2018. [Online]. Available: https://www.iea.org/beep/sweden/codes/building-regulations-2010.html. [Accessed: 04-Dec-2017].
[23] B. Moore, T. Jaglinski, D. S. Stone, and R. S. Lakes, “On the Bulk Modulus of Open Cell Foams,” vol. 26, no. 1, pp. 1–10, 2007.
[24] Kingspan Insulation Ltd., “Thermapitch TP10 Product Brochure.” 2017.
[25] Armacell LLC, “AP/Armaflez Sheet & Roll Insulation Datasheet.” p. 2, 2016.
[26] ASTM, *Manual on the Use of Thermocouples in Temperature Measurement*. 1993.
[27] EBECO AB, “Underfloor heating for caravans - on a roll.” pp. 1–2.
[28] Keysight Technologies, “Keysight Technologies U1250 Series Handheld Digital Multimeters Data Sheet.”
[29] Clas Ohlson AB, “Convector Heater Art. nº 18-1314.”
[30] International Organization for Standardization, “ISO 8990:1994 (E) Thermal insulation - Determination of steady-state thermal transmission properties,” vol. 1993, no. 121535, 1994.
[31] TC Ltd., “Thermocouple Cable - PFA Insulated from TC.” [Online]. Available: http://www.tc.co.uk/thermocouple/B10_thermocouple_cable.html. [Accessed: 28-Apr-2018].
[32] RS PRO, “Datasheet IEC Miniature Thermocouple Connector Quick Wire plugs.”
[33] ASTM, “Standard Test Method for Calibration of Thermocouples By Comparison Techniques 1,” pp. 1–16, 2016.
[34] L. LUTRON ELECTRONIC ENTERPRISE CO., “4 channels THERMOMETER Model : TM-947SD,” *Memory*, pp. 100–101.
[35] Keysight Technologies Inc., “Keysight 34970A Data Acquisition / Switch Unit Family technical Overview,” 2018.
[36] Mitec Satellite, “Mitec SatelLite data loggers.”
[37] 3M TM, “3M Thinsulate Climate Control Family Card,” 2018.
[38] F. P. Incropera, D. P. DeWitt, T. L. Bergman, and A. S. Lavine, *Fundamentals of Heat and Mass Transfer*. 2007.
[39] International Organization for Standardization, “ISO 9869:1994 (E) Thermal insulation - In-situ measurement of thermal resistance and thermal transmittance.”
[40] International Organization for Standardization, “ISO/TR 15686-11 Buildings and constructed assets — Service life planning,” vol. 2014, 2014.
[41] M. Hautala, T. Jokiniemi, and J. JA Ahokas, *MAATILAKUIVURIT - Energia Akatemia*. .
[42] J. Tellinghuisen, “Can you trust the parametric standard errors in nonlinear least squares? Yes, with provisos,” *Biochim. Biophys. Acta - Gen. Subj.*, vol. 1862, no. 4, pp. 886–894, 2018.

Appendix A

A. Detailed measurements of studied windows.

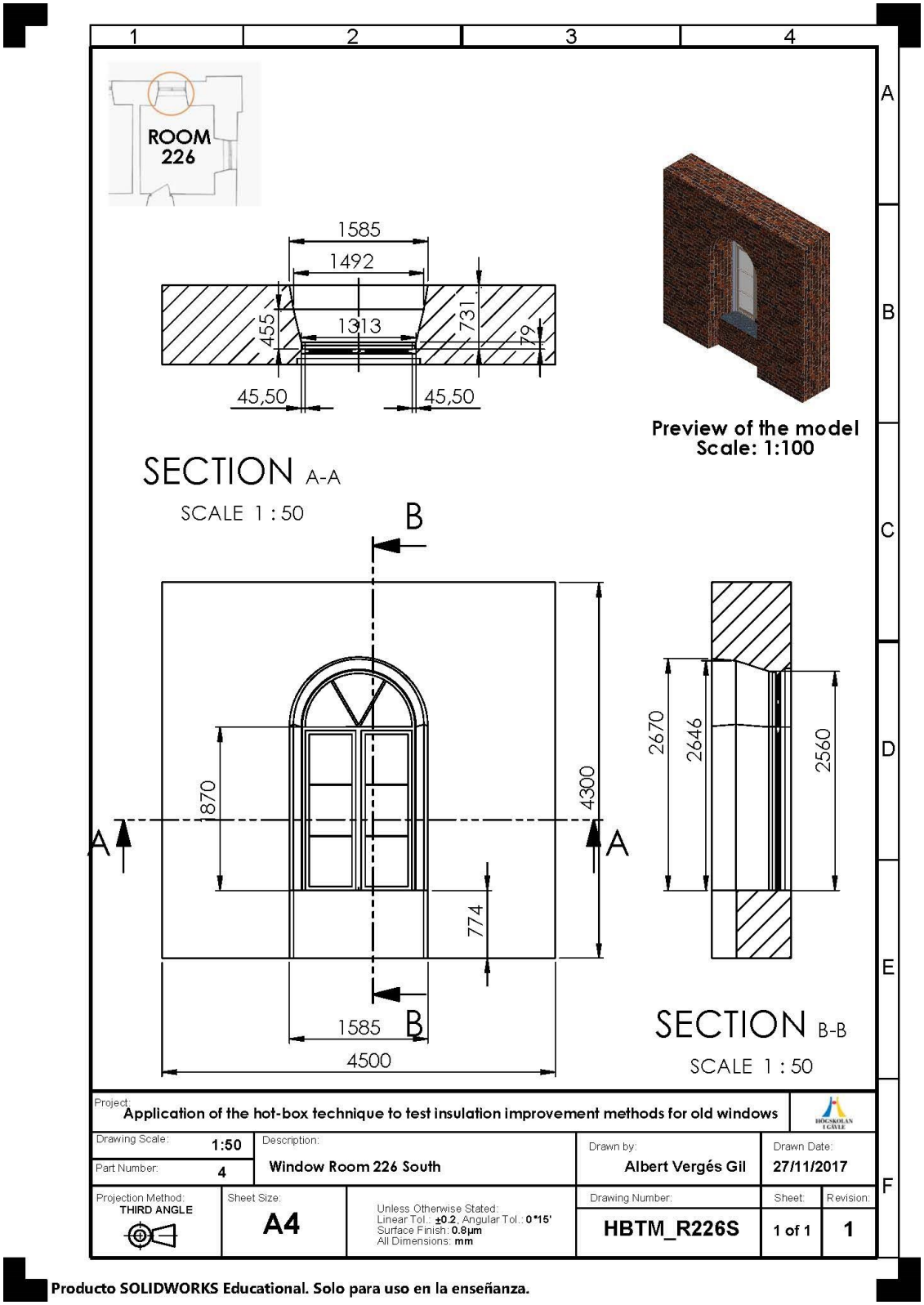

Appendix A.1: detailed measurements of window facing south of room 226.

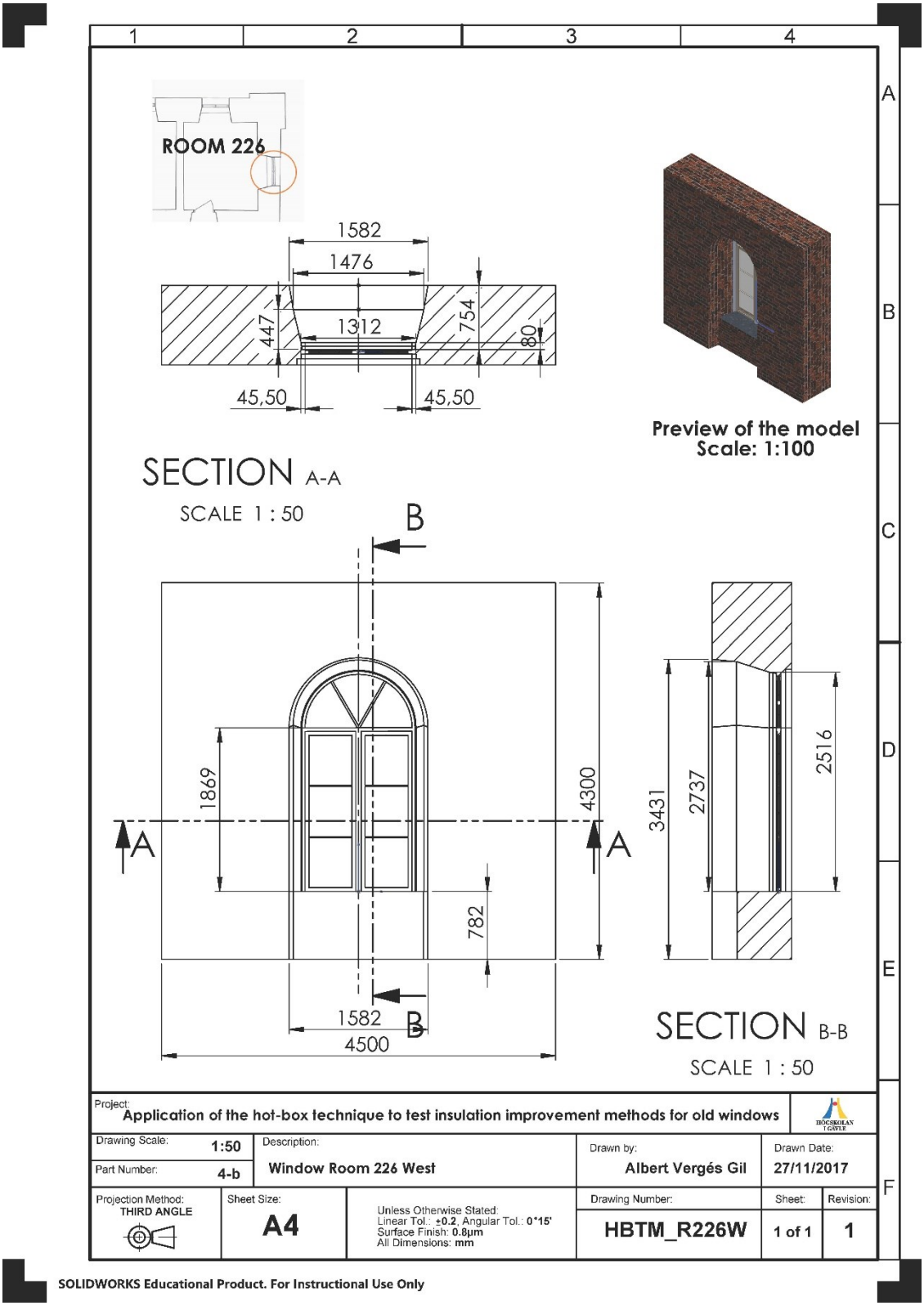

Appendix A.2: detailed measurements of window facing west of room 226.

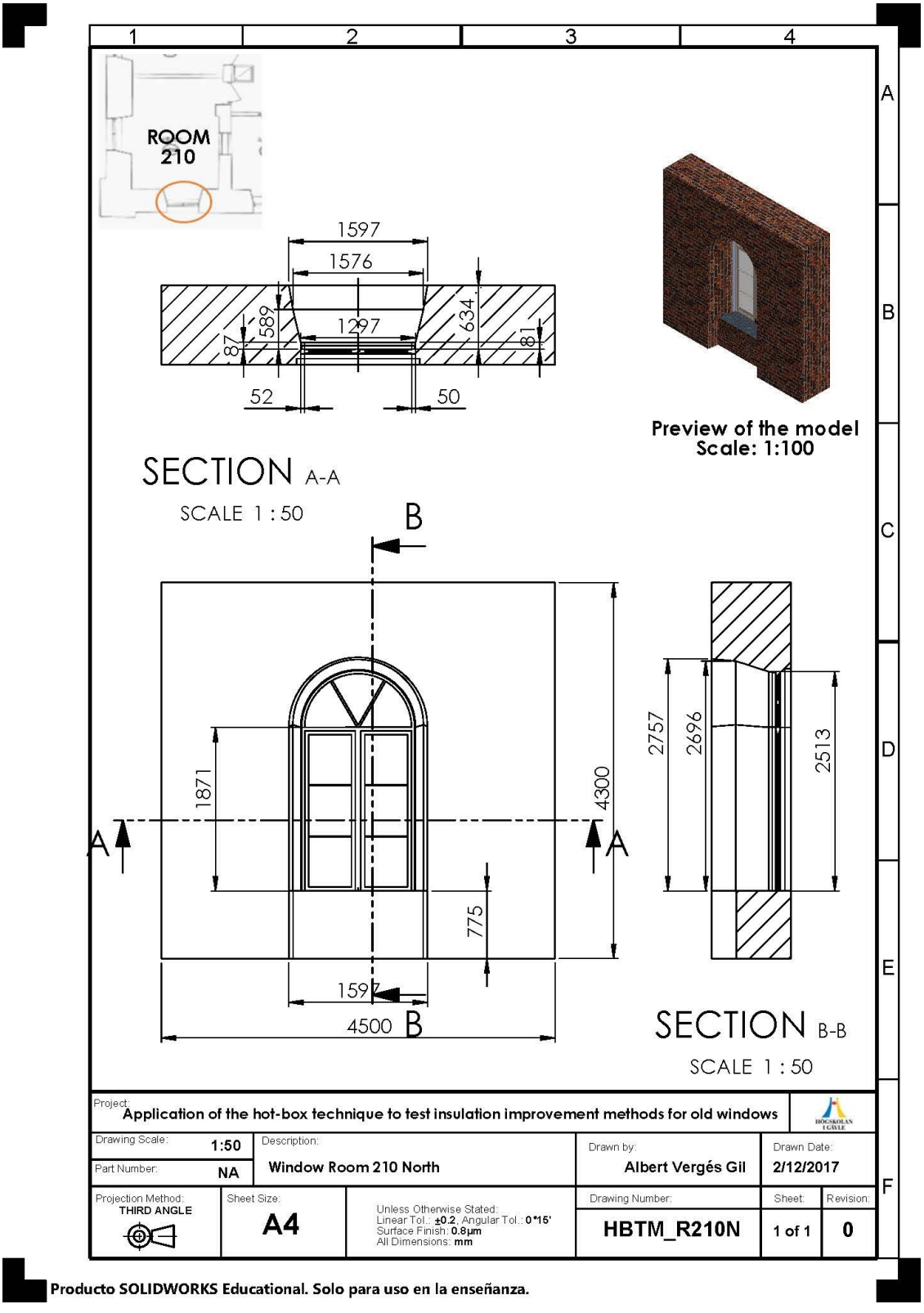

Appendix A.3: detailed measurements of window facing north of room 210.

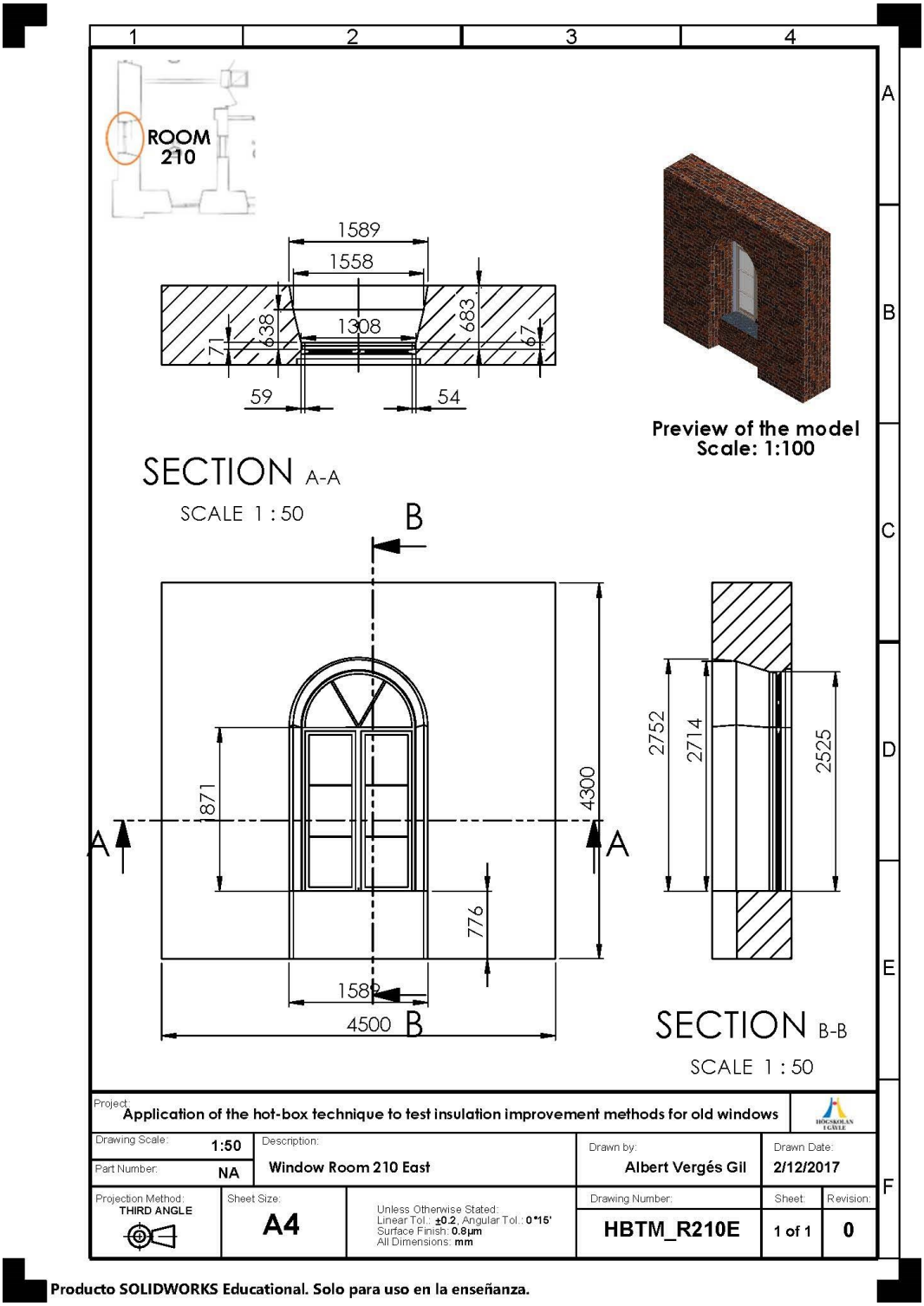

Appendix A.4: detailed measurements of window facing east of room 210.

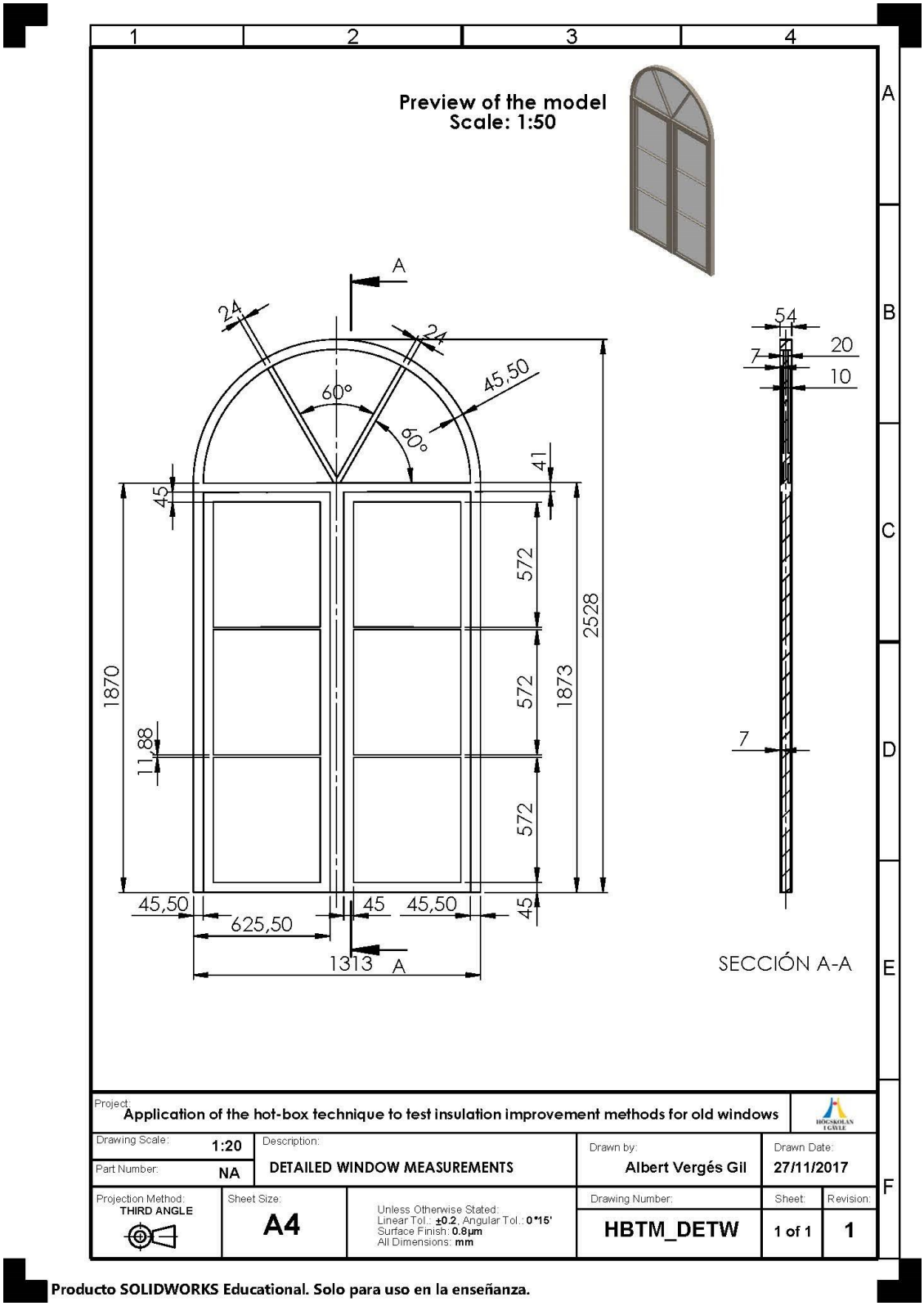

Appendix A.5: Detailed measurements of the window and frameworks.

B. Blueprints of the modular preliminary proposal for the construction of the hot box.

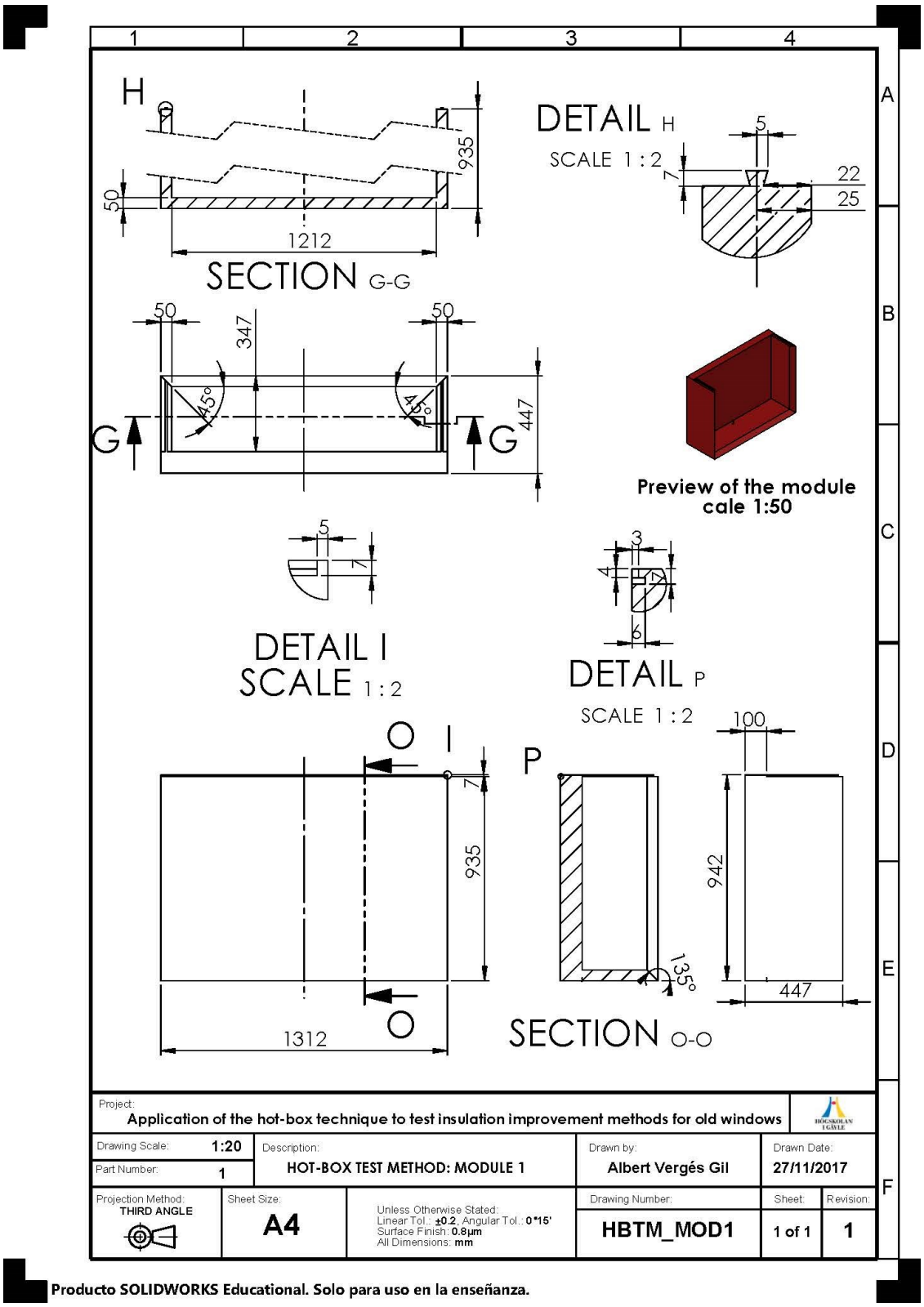

Appendix A 6: Detailed measurements of module 1 from the preliminary proposal.

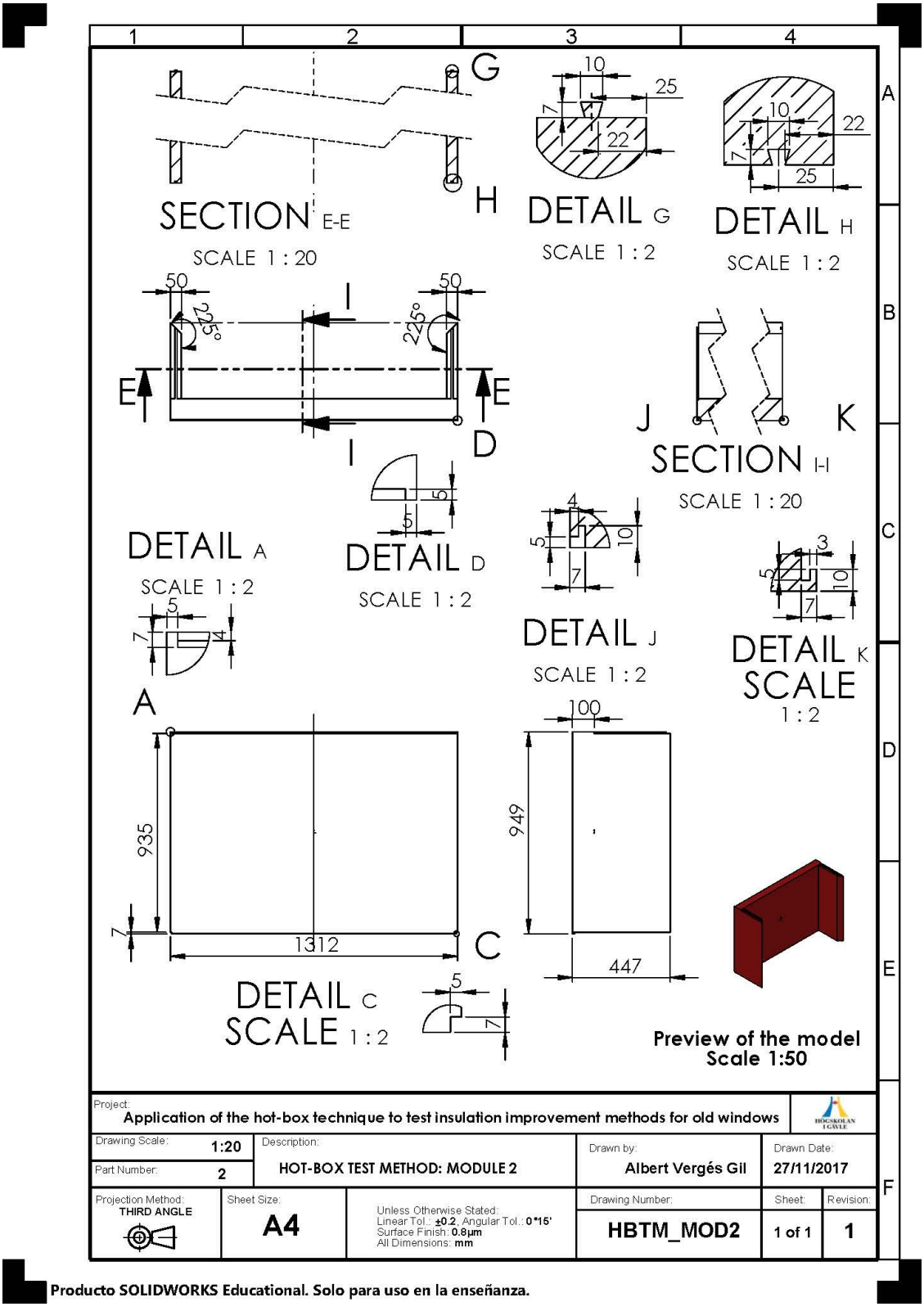

Appendix A 7: Detailed measurements of module 2 from the preliminary proposal.

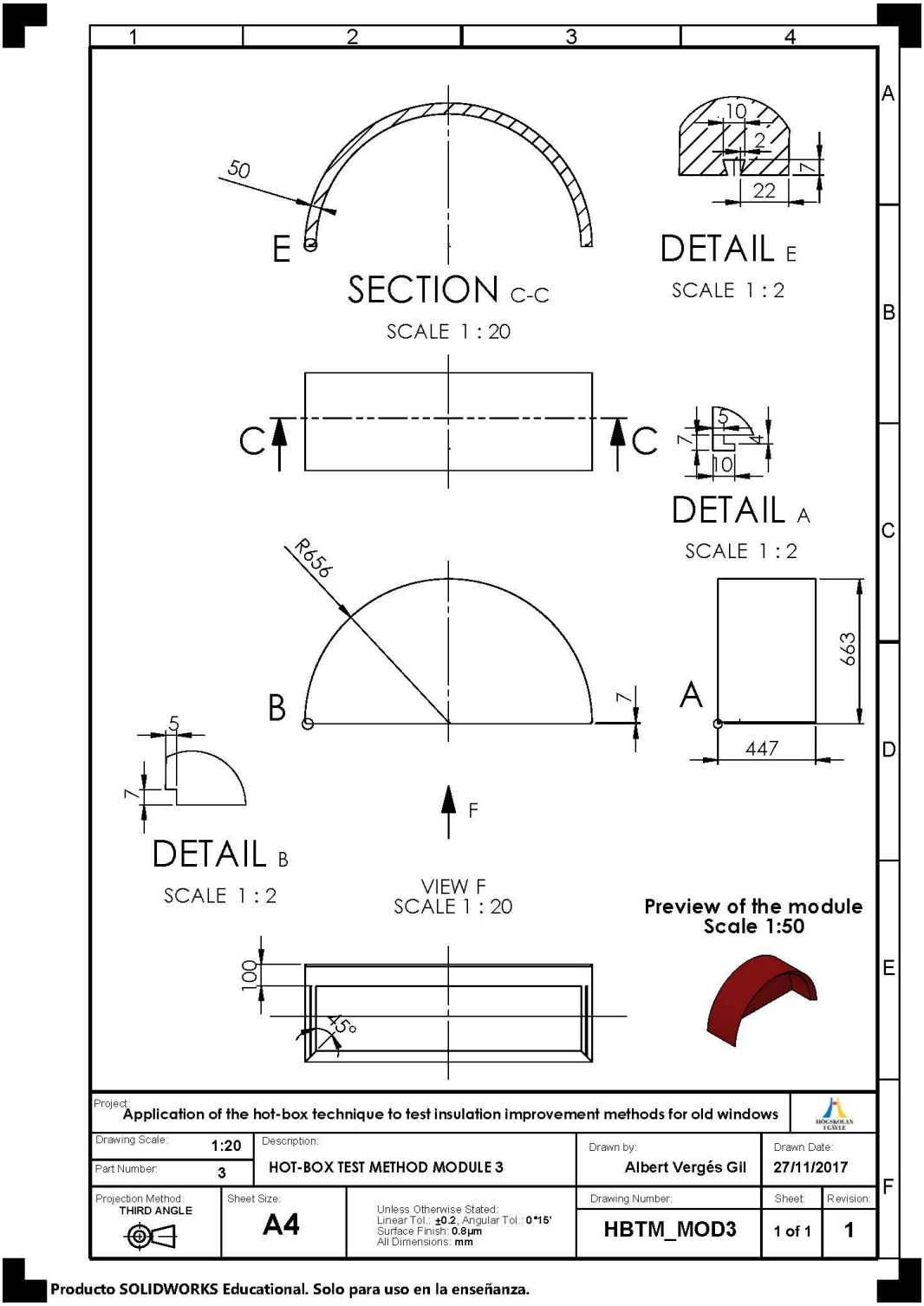

Appendix A 8: Detailed measurements of module 3 from the preliminary proposal.

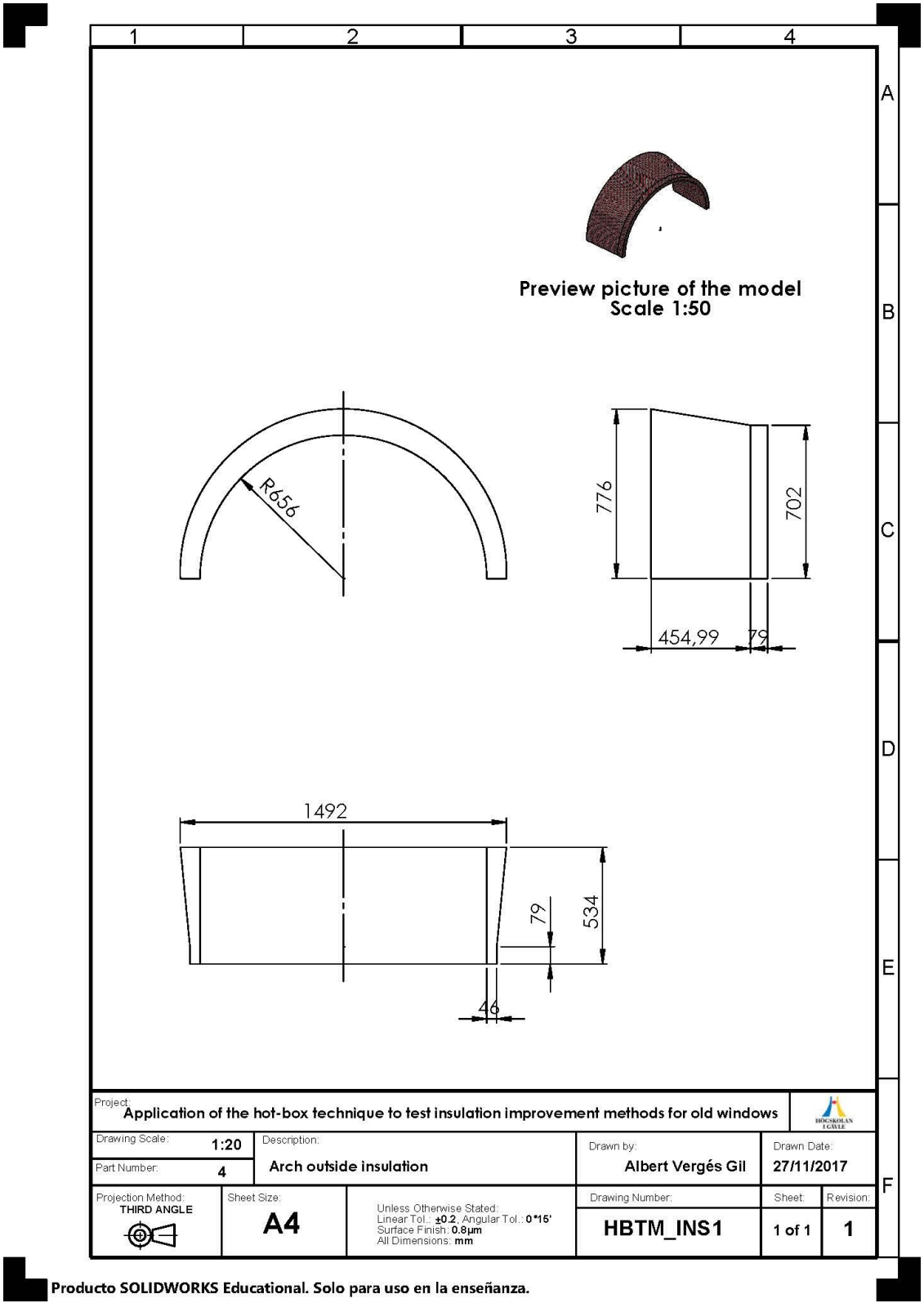

Appendix A 9: Detailed measurements of the outside insulation for the arch from the preliminary proposal.

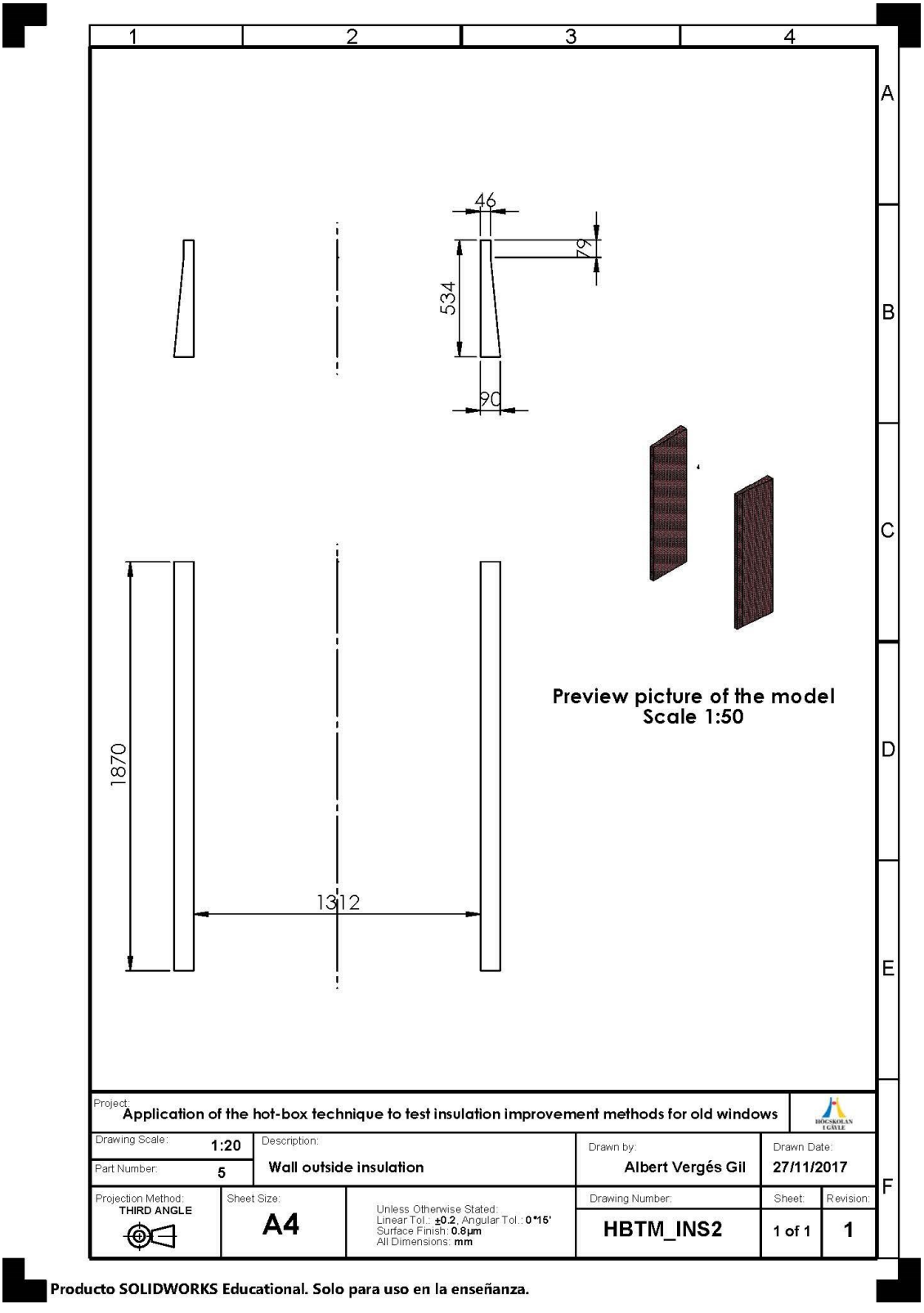

Appendix A 10: Detailed measurements of the outside wall insulation from the preliminary proposal.

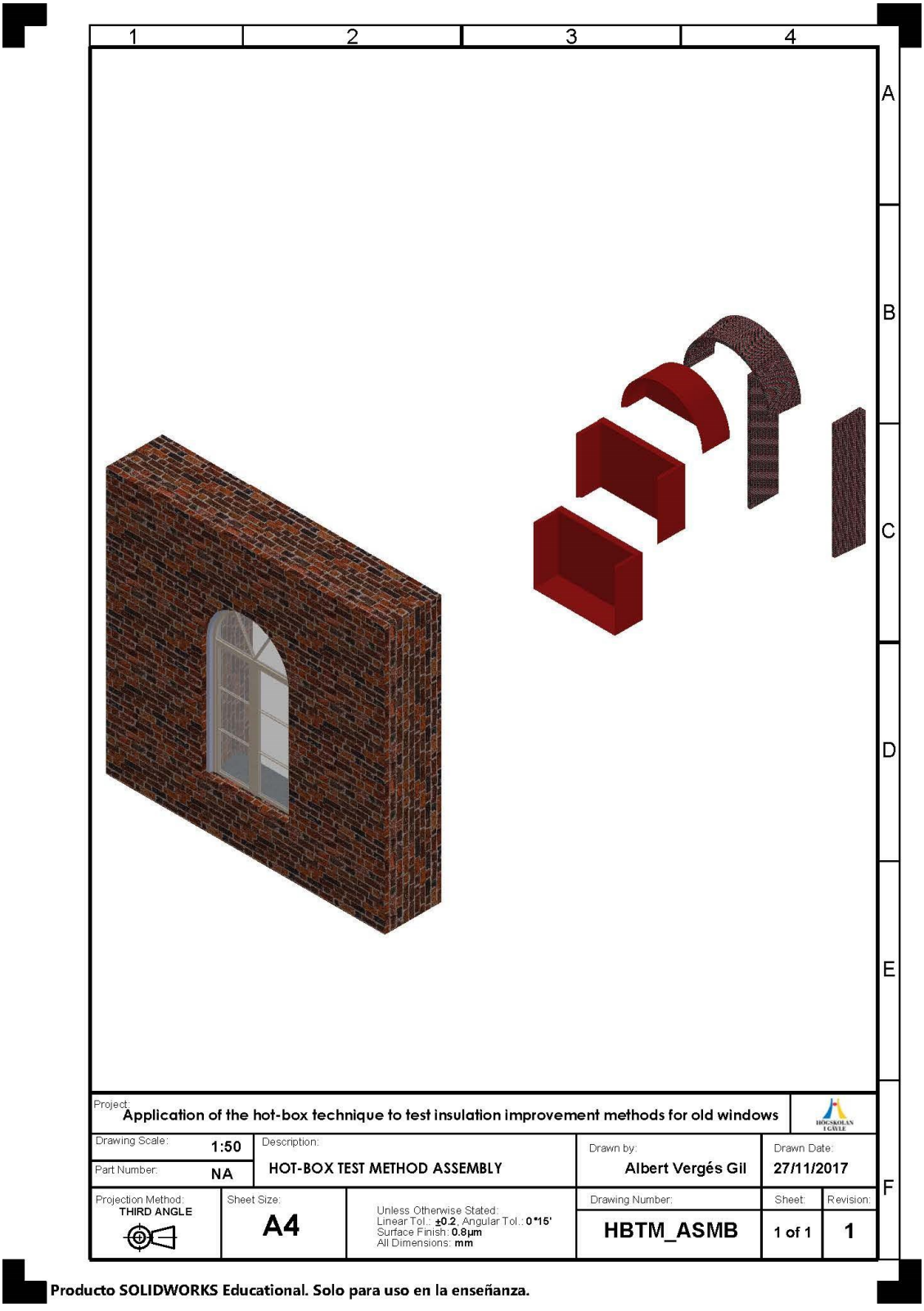

Appendix A 11:Exploited view of the preliminary proposal.

C. Blueprints of the final model for the construction of the hot box.

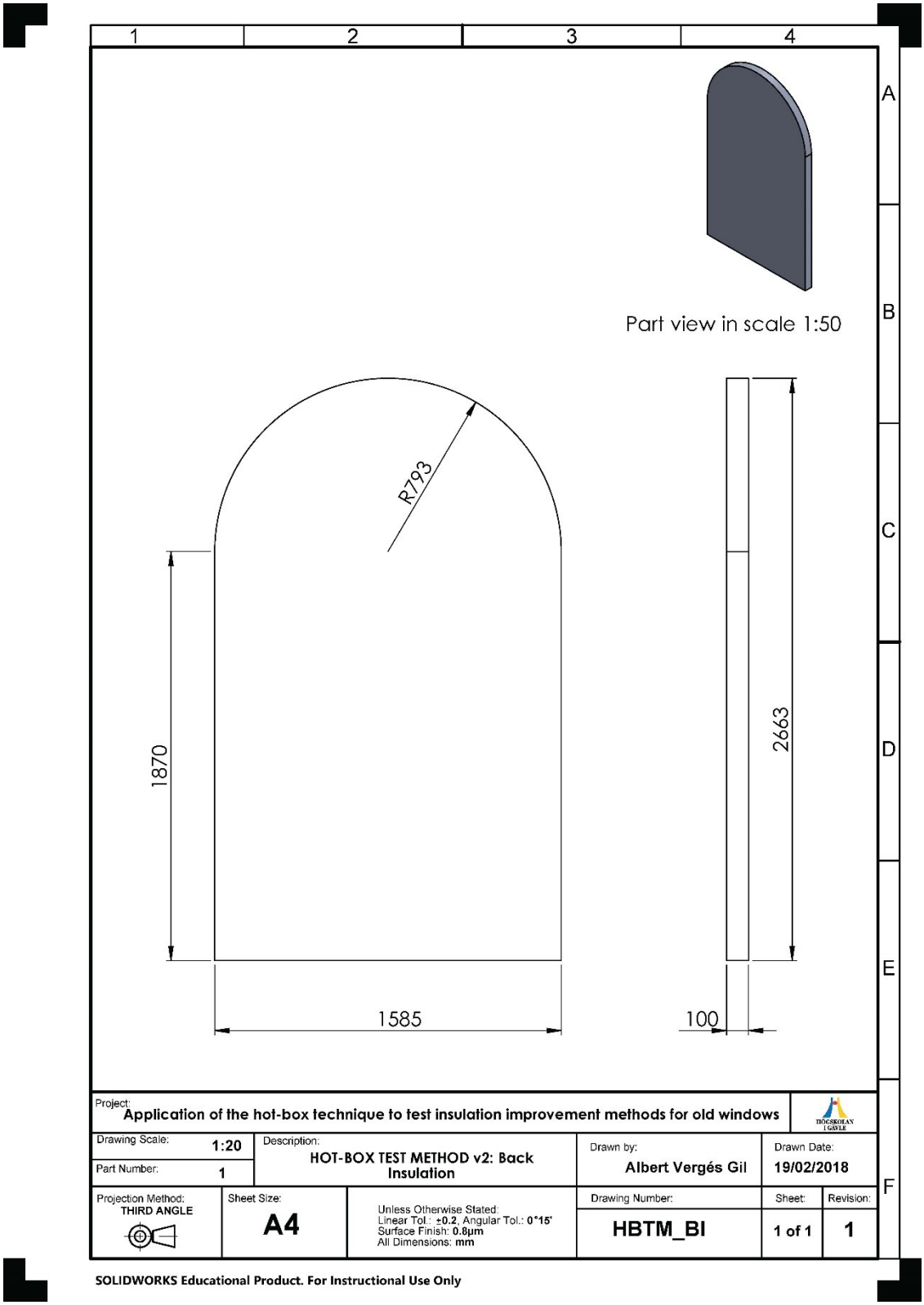

Appendix A 12: Detailed measurements of the back insulation from the final design.

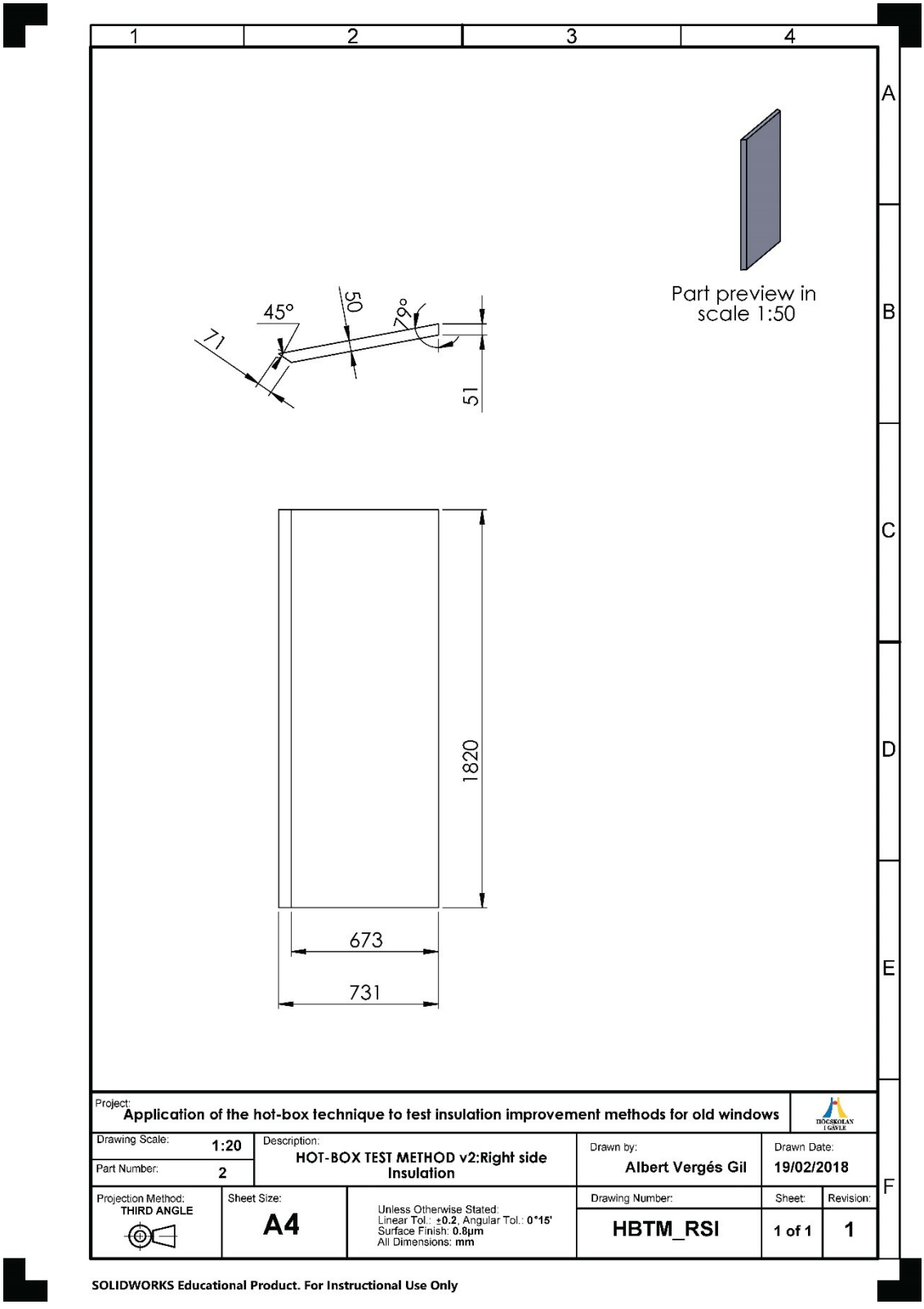

Appendix A 13: : Detailed measurements of the right side insulation from the final design.

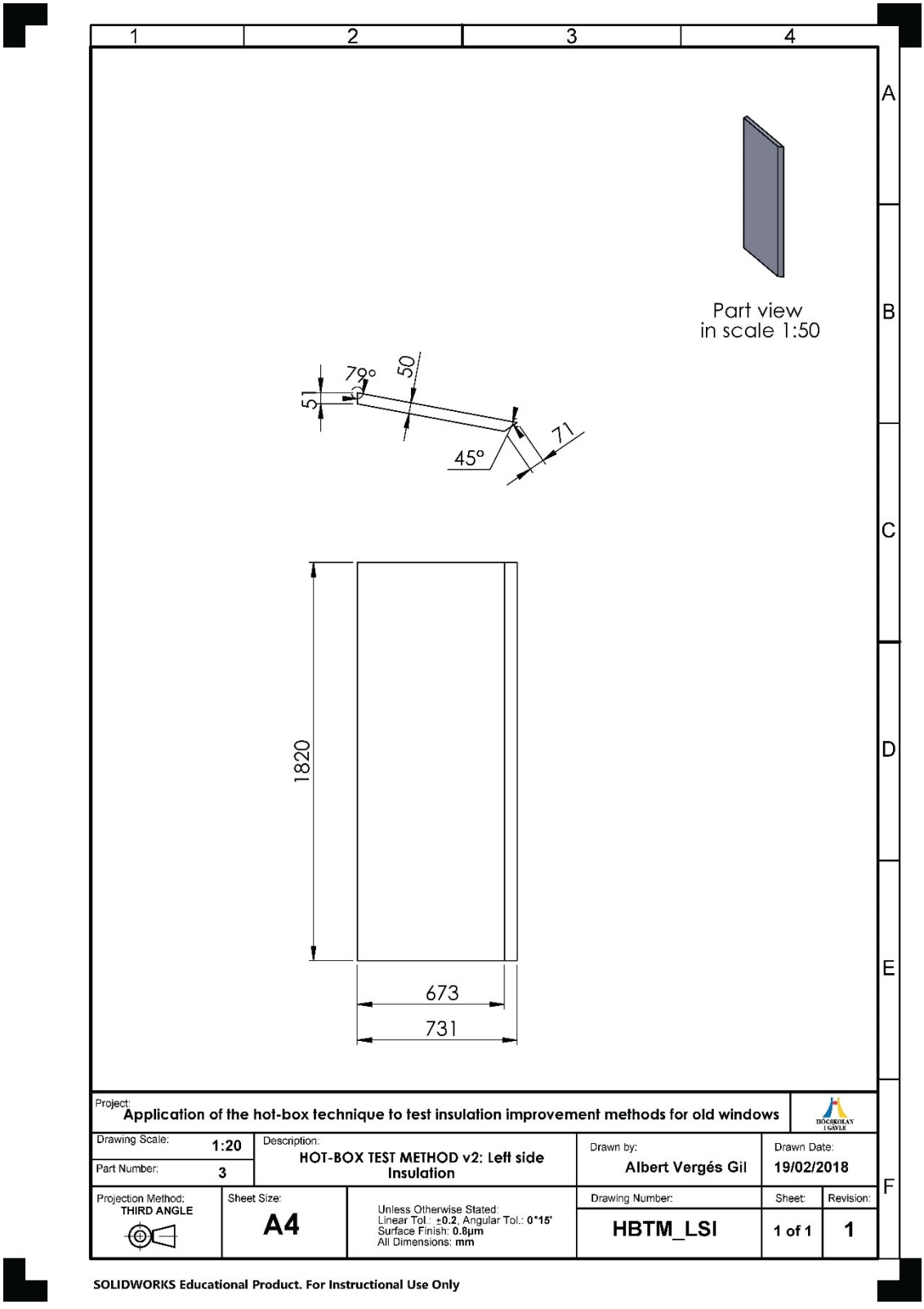

Appendix A 14: Detailed measurements of the left side insulation from the final design.

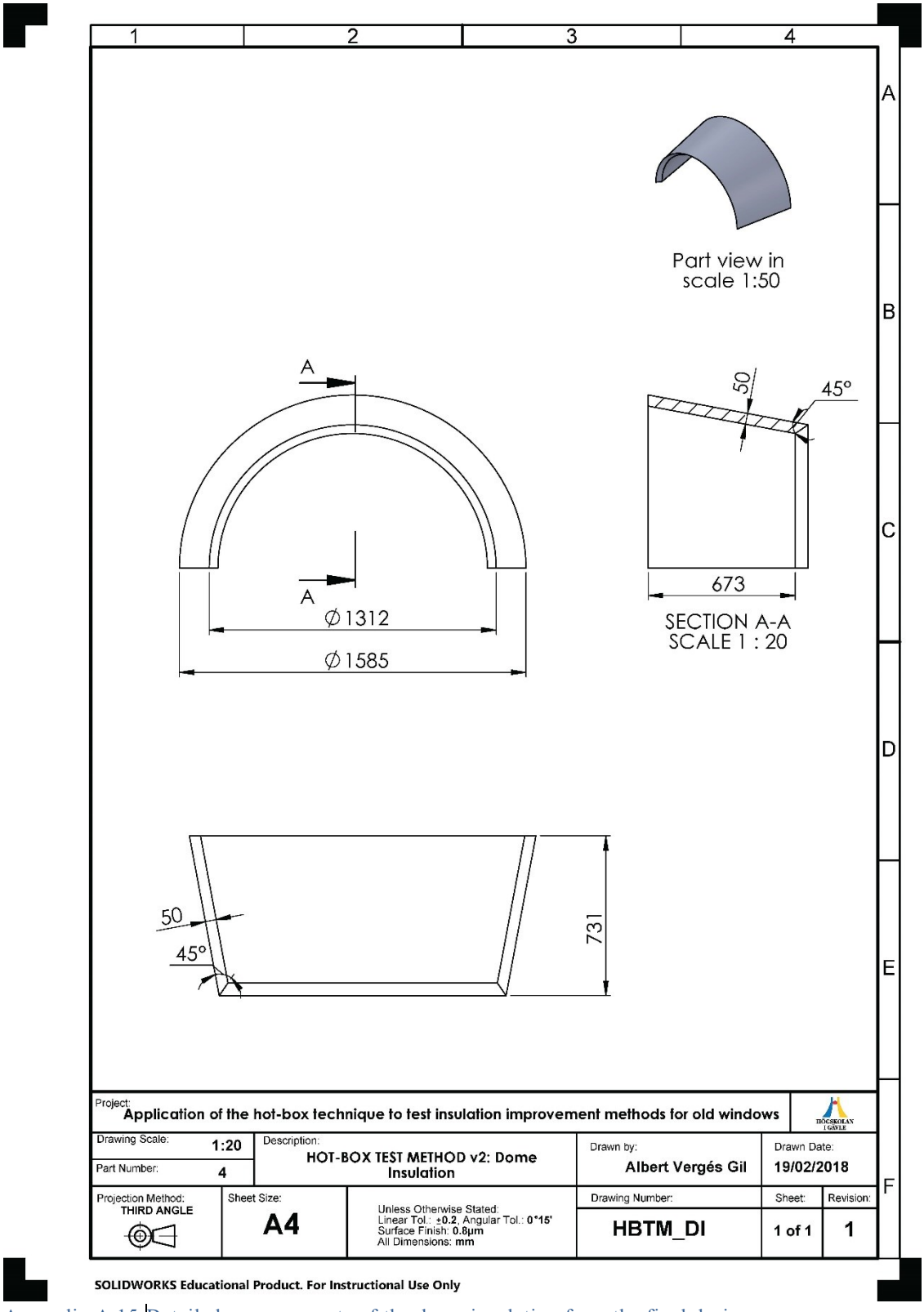

Appendix A 15: Detailed measurements of the dome insulation from the final design.

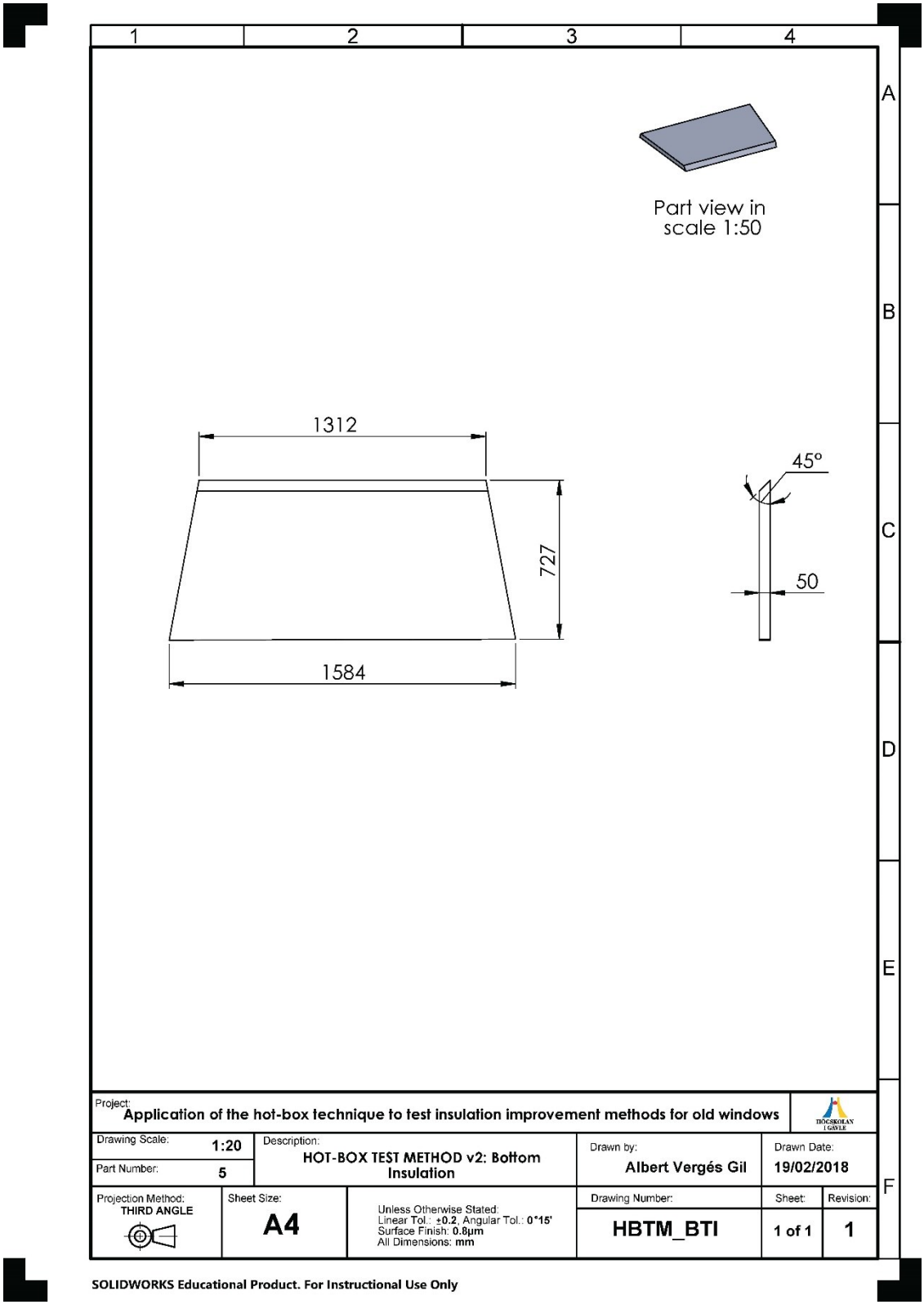

Appendix A 16: Detailed measurements of the bottom insulatiion from the final design.

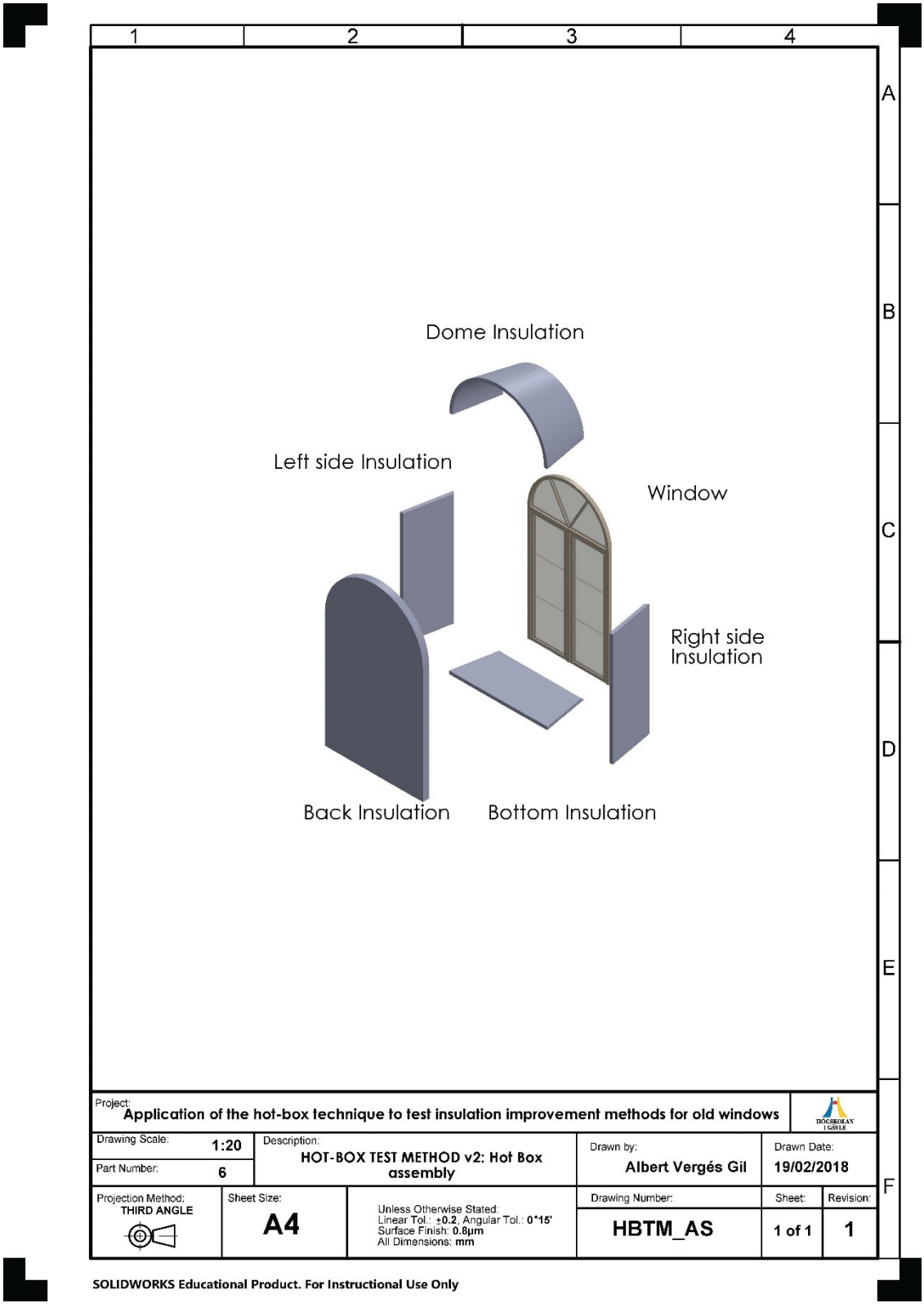

Appendix A 17: Exploited view of the overall hot box assembly.

Appendix B

A. Material selection datasheets: Phenolic foam

CES 2017 EDUPACK

Phenolic foam (closed cell, 0.035)

General information

Designation

Phenol formaldehyde resin closed cell foam, 0.035 specific gravity (based on Koolphen K35)

Tradenames

KOOLPHEN K, CELLOBOND

Typical uses

Thermal insulation, Cores for sandwich structures, Panels, Partitions, Refrigeration, Energy Absorption, Packaging, Buoyancy, floatation.

Composition overview

Compositional summary

((CH2)2-C6H6OH-CH2)n

Form		Foam			
Material family		Plastic (thermoset)			
Base material		PF (Phenol formaldehyde resin)			
Polymer code		PF			

Composition detail (polymers and natural materials)

Polymer		100			%

Price

Price	*	5,92	-	6,71	EUR/kg
Price per unit volume	*	190	-	255	EUR/m^3

Physical properties

Density		32	-	38	kg/m^3
Relative density		0,024	-	0,03	
Cell type		Closed-cell			
Cells/volume	*	1	-	10	/mm^3
Anisotropy ratio		1,4	-	1,6	

Mechanical properties

Young's modulus	*	0,004	-	0,007	GPa
Yield strength (elastic limit)	*	0,09	-	0,11	MPa
Tensile strength		0,15	-	0,21	MPa
Elongation	*	4	-	5	% strain
Compressive modulus	*	0,0191	-	0,0271	GPa
Compressive strength	*	0,084	-	0,172	MPa
Flexural modulus		0,004	-	0,007	GPa
Flexural strength (modulus of rupture)		0,14	-	0,21	MPa
Shear modulus	*	0,0016	-	0,0028	GPa
Shear strength		0,045	-	0,055	MPa
Bulk modulus	*	0,004	-	0,007	GPa
Poisson's ratio	*	0,27	-	0,3	
Shape factor		2,3			
Hardness - Vickers	*	0,0084	-	0,0172	HV

Appendix B 1: Material selection first candidate phenolic foam datasheet, page 1 of 3.

Fatigue strength at 10^7 cycles	*	0,105	-	0,147	MPa
Mechanical loss coefficient (tan delta)	*	0,005	-	0,01	
Densification strain		0,94	-	0,952	

Impact & fracture properties

Fracture toughness	*	0,0041	-	0,0057	MPa.m^0.5

Thermal properties

Glass temperature		140	-	160	°C
Maximum service temperature		120	-	130	°C
Minimum service temperature		-200			°C
Thermal conductivity		0,019	-	0,02	W/m.°C
Specific heat capacity		1,85e3	-	1,91e3	J/kg.°C
Thermal expansion coefficient		40	-	70	µstrain/°C

Electrical properties

Electrical resistivity	*	1e17	-	1e19	µohm.cm
Dielectric constant (relative permittivity)	*	1,17	-	1,21	
Dissipation factor (dielectric loss tangent)	*	0,0019	-	0,0024	
Dielectric strength (dielectric breakdown)	*	5,17	-	5,21	MV/m

Magnetic properties

Magnetic type	Non-magnetic

Optical properties

Transparency	Opaque

Critical materials risk

Contains >5wt% critical elements?	No

Absorption & permeability

Water absorption @ 24 hrs		5	-	6	%

Durability

Water (fresh)	Excellent
Water (salt)	Excellent
Weak acids	Excellent
Strong acids	Limited use
Weak alkalis	Unacceptable
Strong alkalis	Unacceptable
Organic solvents	Excellent
Oxidation at 500C	Unacceptable
UV radiation (sunlight)	Good
Flammability	Non-flammable

Primary production energy, CO2 and water

Embodied energy, primary production	*	82,7	-	91,1	MJ/kg
CO2 footprint, primary production	*	8,06	-	8,89	kg/kg
Water usage	*	148	-	163	l/kg

Appendix B 2: Material selection first candidate phenolic foam datasheet, page 2 of 3.

Processing energy, CO2 footprint & water

Polymer extrusion energy	* 9,93	-	11	MJ/kg
Polymer extrusion CO2	* 0,795	-	0,876	kg/kg
Polymer extrusion water	* 6,53	-	9,8	l/kg
Polymer molding energy	* 25,8	-	28,5	MJ/kg
Polymer molding CO2	* 2,07	-	2,28	kg/kg
Polymer molding water	* 15,6	-	23,3	l/kg
Coarse machining energy (per unit wt removed)	* 0,508	-	0,561	MJ/kg
Coarse machining CO2 (per unit wt removed)	* 0,0381	-	0,0421	kg/kg
Fine machining energy (per unit wt removed)	* 0,802	-	0,887	MJ/kg
Fine machining CO2 (per unit wt removed)	* 0,0602	-	0,0665	kg/kg
Grinding energy (per unit wt removed)	* 1,13	-	1,25	MJ/kg
Grinding CO2 (per unit wt removed)	* 0,0847	-	0,0937	kg/kg

Recycling and end of life

Recycle	✗			
Recycle fraction in current supply	0,1			%
Downcycle	✓			
Combust for energy recovery	✓			
Heat of combustion (net)	* 31,2	-	32,8	MJ/kg
Combustion CO2	* 2,86	-	3,01	kg/kg
Landfill	✓			
Biodegrade	✗			

Links

ProcessUniverse

Producers

Reference

Shape

Appendix B 3: Material selection first candidate phenolic foam datasheet, page 3 of 3.

A. Material selection datasheets: PVC-Cross linked foam

CES 2017 EDUPACK

PVC cross-linked foam (rigid, closed cell, DH 0.030)

General information

Designation

Polyvinylchloride polyurethane cross-linked foam, rigid, closed cell, 0.030 specific gravity (based on Divinycell H30)

Tradenames

Airex C (Herex C), Divinycell, Klegecell, Termino, Plasticell

Typical uses

Sandwich structure cores, Insulation, floatation

Composition overview

Compositional summary

Interpenetrating polymer network (IPN) of (i) PVC (CH2CHCl)n and (ii) polyurethane thermoset (NH-R-NH-CO-O-R'-O-CO)n, R from a diisocyanate, R' from a polyol

Form	Foam
Material family	Plastic (thermoplastic, amorphous)
Base material	PVC+PUR (Polyvinyl chloride + polyurethane blend)
Polymer code	(PVC+PUR)

Composition detail (polymers and natural materials)

Polymer	100			%

Price

Price	* 13,7	-	15,1	EUR/kg
Price per unit volume	* 384	-	483	EUR/m^3

Physical properties

Density	28	-	32	kg/m^3
Relative density	* 0,02	-	0,023	
Cell type	Closed-cell			
Cells/volume	* 1	-	10	/mm^3
Anisotropy ratio	* 1	-	1,5	

Mechanical properties

Young's modulus	0,028	-	0,032	GPa
Yield strength (elastic limit)	* 0,28	-	0,32	MPa
Tensile strength	0,8	-	0,9	MPa
Elongation	* 3	-	5	% strain
Compressive modulus	* 0,0163	-	0,0202	GPa
Compressive strength	* 0,28	-	0,32	MPa
Flexural modulus	0,028	-	0,032	GPa
Flexural strength (modulus of rupture)	* 0,8	-	0,9	MPa
Shear modulus	0,013	-	0,015	GPa
Shear strength	0,14	-	0,16	MPa
Bulk modulus	* 0,028	-	0,032	GPa
Poisson's ratio	0,31	-	0,33	
Shape factor	2,6			

Appendix B 4: Material selection second candidate, PVC-Cross linked foam, foam datasheet, page 1 of 3.

Hardness - Vickers	* 0,028	-	0,032	HV
Fatigue strength at 10^7 cycles	* 0,224	-	0,256	MPa
Mechanical loss coefficient (tan delta)	* 0,05	-	0,15	
Densification strain	* 0,963	-	0,968	

Impact & fracture properties

Fracture toughness	* 0,0014	-	0,0017	MPa.m^0.5

Thermal properties

Glass temperature	74	-	88	°C
Maximum service temperature	67	-	72	°C
Minimum service temperature	-100	-	-93	°C
Thermal conductivity	0,022	-	0,024	W/m.°C
Specific heat capacity	* 1,12e3	-	1,14e3	J/kg.°C
Thermal expansion coefficient	34	-	36	µstrain/°C

Electrical properties

Electrical resistivity	* 1e19	-	1e21	µohm.cm
Dielectric constant (relative permittivity)	1,04	-	1,06	
Dissipation factor (dielectric loss tangent)	5e-4	-	8e-4	
Dielectric strength (dielectric breakdown)	* 5,3	-	5,34	MV/m

Magnetic properties

Magnetic type	Non-magnetic

Optical properties

Transparency	Opaque

Critical materials risk

Contains >5wt% critical elements?	No

Absorption & permeability

Water absorption @ 24 hrs	* 6,45	-	7,34	%

Durability

Water (fresh)	Excellent
Water (salt)	Excellent
Weak acids	Excellent
Strong acids	Excellent
Weak alkalis	Excellent
Strong alkalis	Excellent
Organic solvents	Limited use
Oxidation at 500C	Unacceptable
UV radiation (sunlight)	Good
Flammability	Self-extinguishing

Primary production energy, CO2 and water

Embodied energy, primary production	* 76,5	-	84,4	MJ/kg
CO2 footprint, primary production	* 4,91	-	5,41	kg/kg
Water usage	* 436	-	482	l/kg

Values marked * are estimates.
No warranty is given for the accuracy of this data

Appendix B 5: Material selection second candidate, PVC-Cross linked foam, foam datasheet, page 2 of 3.

Processing energy, CO2 footprint & water

Polymer extrusion energy	* 7,51	-	8,28	MJ/kg
Polymer extrusion CO2	* 0,601	-	0,662	kg/kg
Polymer extrusion water	* 5,52	-	8,29	l/kg
Polymer molding energy	* 19,3	-	21,3	MJ/kg
Polymer molding CO2	* 1,55	-	1,71	kg/kg
Polymer molding water	* 12,9	-	19,3	l/kg
Coarse machining energy (per unit wt removed)	* 0,57	-	0,63	MJ/kg
Coarse machining CO2 (per unit wt removed)	* 0,0428	-	0,0473	kg/kg
Fine machining energy (per unit wt removed)	* 1,43	-	1,58	MJ/kg
Fine machining CO2 (per unit wt removed)	* 0,107	-	0,118	kg/kg
Grinding energy (per unit wt removed)	* 2,38	-	2,63	MJ/kg
Grinding CO2 (per unit wt removed)	* 0,178	-	0,197	kg/kg

Recycling and end of life

Recycle	✗			
Recycle fraction in current supply	0,1			%
Downcycle	✓			
Combust for energy recovery	✓			
Heat of combustion (net)	* 17,1	-	18	MJ/kg
Combustion CO2	* 1,37	-	1,44	kg/kg
Landfill	✓			
Biodegrade	✗			

Links

ProcessUniverse
Producers
Reference
Shape

Appendix B 6: Material selection second candidate, PVC-Cross linked foam, foam datasheet, page 3 of 3.

Appendix C

A. Sensor length calculation

As previously mentioned, the calculation was performed using the approximations of the 3D model previously built as well as assuming them as straight lines, for this reason, 100 cm were added in order to connect the logger to the reference as well as to counteract this simplifications. The length used can be obtained in Table Appendix C 1.

Appendix C 1: Summary table of the length calculated for the sensors that were calibrated.

PART	Surface	Distances needed [cm] Ref Left. Names used in Detailed Calc										Lenght Cable Added	
		S1	S2	S3	S4	S5	S6	S7	S8	S9	S10		
WINDOW	Labelling	F1	F2	F3	F4	F5	F6	F7	F8	F9	F10		
	Inner Window	236,85	294,85	352,84	409,83	454,84	417,05	320,60	322,35	273,35	267,10	100,00	[cm]
	Labelling	F11	F12	F13	F14	F15							
	Outer Window	353,18	297,25	353,18	455,25	323,47						100,00	[cm]
SIDES	Labelling	F16	F17	F18	F19	F20	F71						
	Inner Right	166,71	226,00	282,71	248,59	201,90	300,00					100,00	[cm]
	Labelling	F21	F22	F23	F24	F25							
	Outer Right	172,64	210,07	288,64	207,83	254,82						100,00	[cm]
	Labelling	F26											
	Inner Left	363,04										100,00	[cm]
	Labelling	F27											
	Outer Left	368,97										100,00	[cm]
BACK	Labelling	F28	F29	F30	F31	F32							
	Back Part	274,63	332,63	390,63	433,82	406,88						200,00	[cm]
	Labelling	F33	F34	F35	F36	F37							
	Front Part	279,63	337,63	395,63	439,01	406,88						200,00	[cm]
BOTTOM	Labelling	F38	F39	F40	F41								
	Up Part	141,49	162,46	183,44	223,11							100,00	[cm]
	Labelling	F42	F43	F44	F45								
	Lower Part	190,94	170,00	149,01	241,31							100,00	[cm]
ARCH	Labelling	F46	F47	F48	F49	F50							
	Inner Part	456,29	431,39	406,48	459,15	363,11						100,00	[cm]
	Labelling	F51	F52	F53	F54	F55							
	Outer Part	459,98	435,07	410,16	506,62	361,79						100,00	[cm]
AIR TEMP.	Labelling	F56	F57	F58	F59	F60	F61	F62	F63				
	-	209,43	267,43	325,43	384,37	301,15	293,15	293,15	301,15			100,00	[cm]
ROOM TEMP.	Labelling	F64	F65	F66	F67								
	-	831,61	889,61	947,61	1006,51							100,00	[cm]
WALL	Labelling	F68											
	Outer Wall	343,80										100,00	[cm]
	Labelling	F69											
	Inner Wall	220,50										100,00	[cm]

B. Sensor construction and calibration.

The methodology followed for the construction of the sensors and lately calibration was the following.

Firstly, the thermocouple were cut in the desired length, previously calculated as seen before. After, 5mm was peeled in every direction for the ones related to the surfaces and 25mm for the ones positioned in the air and inserted in the connector.

For improving its mechanical strength, the thermocouple peeled tip was twisted then soaked in pine resin for improving the welding between cooper and constantant and welded.

Once done, the join was verified by microscope, and labelled for further installation as seen in Appendix C 2.

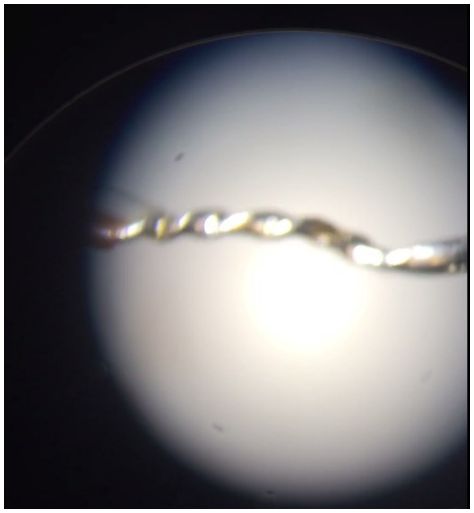

Appendix C 2: microscope picture of the welding done in one of the thermocouples.

As previously mentioned, the calibration was performed following the standard ASTM 220. A picture of the tool used for the calibration is shown in Appendix C 3 and temperatures of 5, 15, 25 and 30ºC.

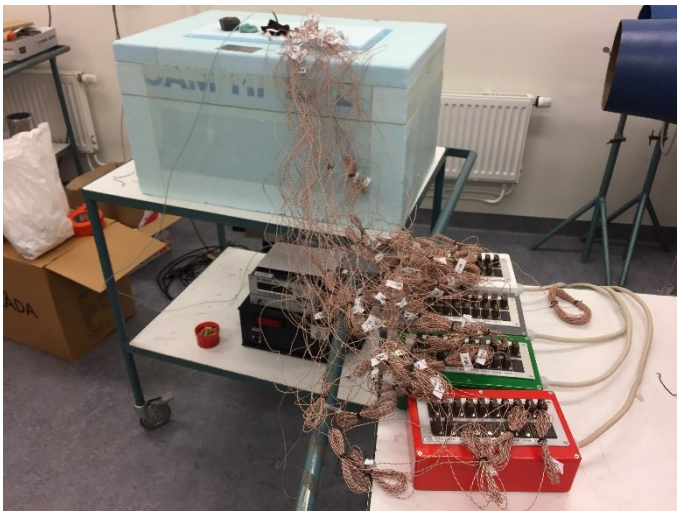

Appendix C 3: Picture of the isolated box used for the calibration.

In table Appendix C 4 a summary of the maximum value found for each surface can be seen and the test temperature where it has been found. Except for the window and walls, the surfaces are expected to work at an approximate temperature of 22ºC, being lower in most of the cases that the maximum difference found.

Appendix C 4: Summary of the maximum differences between opposite surfaces for each part, where the maximum has been obtained for the air sensors, that are not directly correlated at a temperature of 5ºC, that would not be reached by them during the project.

Part	Maximum difference between surface [ºC]	Ref. Temperature Max difference [ºC]
Window	0,054	5
Right Side	0,018	5
Vertical air sensor	0,179	5
Left Side	0,018	5
Back Insulation	0,030	5
Horizontal air sensor	0,026	5
Arch	0,053	5
Wall	0,007	15
Bottom	0,008	5

The results of such calibration can be found in the following pictures sorted by surface.

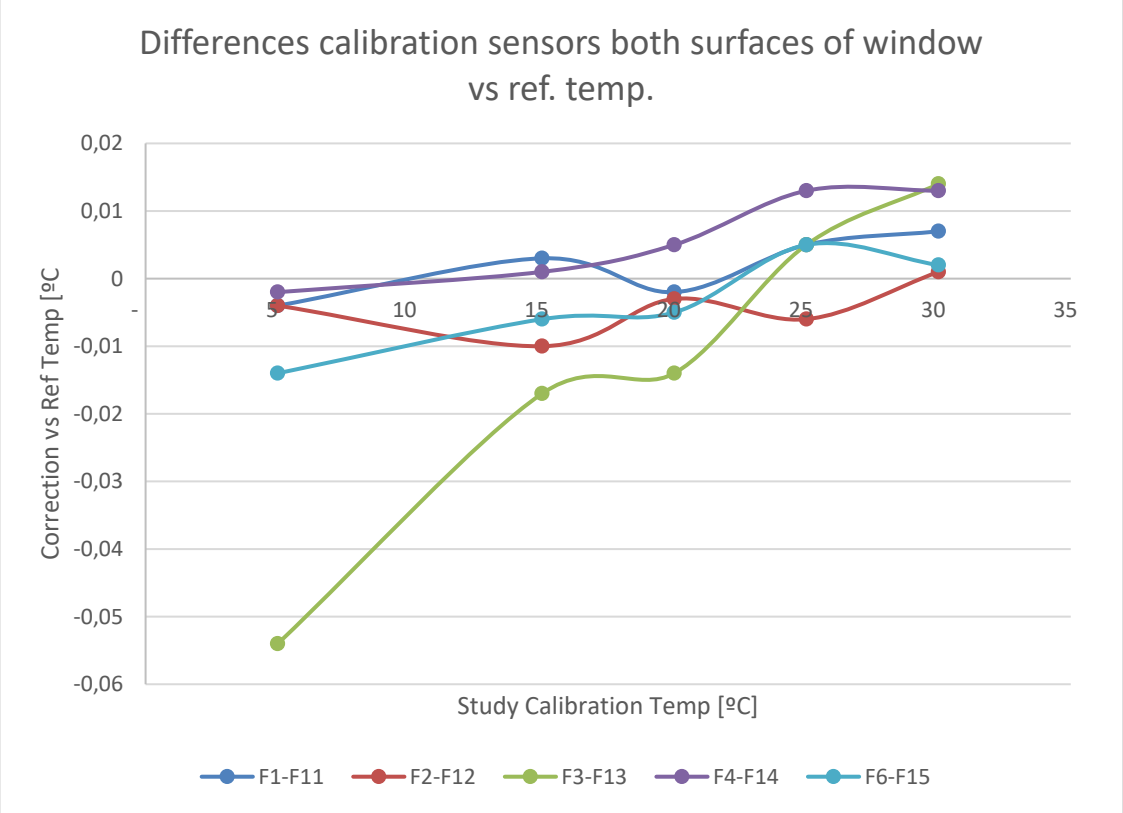

Appendix C 5: Calibration of the opposite sensors that were lately installed in the window.

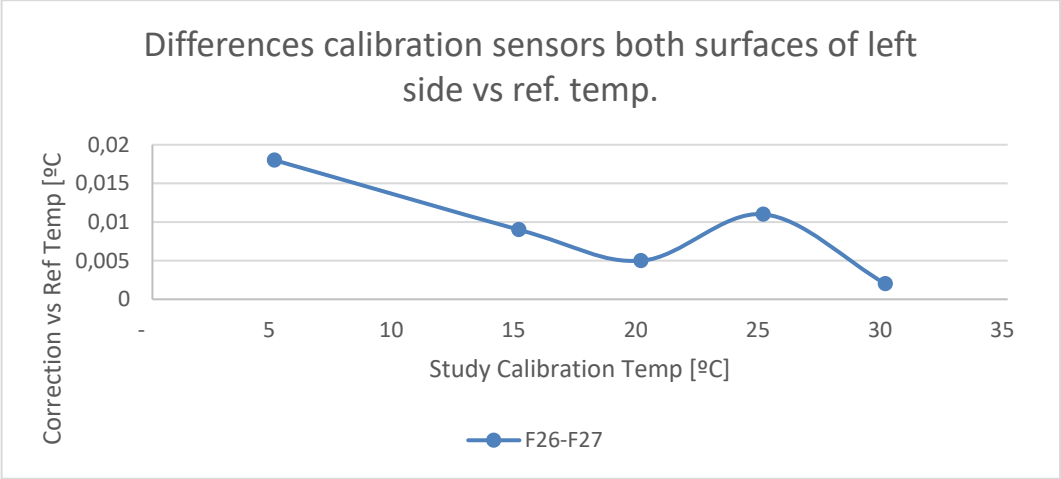

Appendix C 6: Calibration of the opposite sensors that were lately installed in the left side insulation

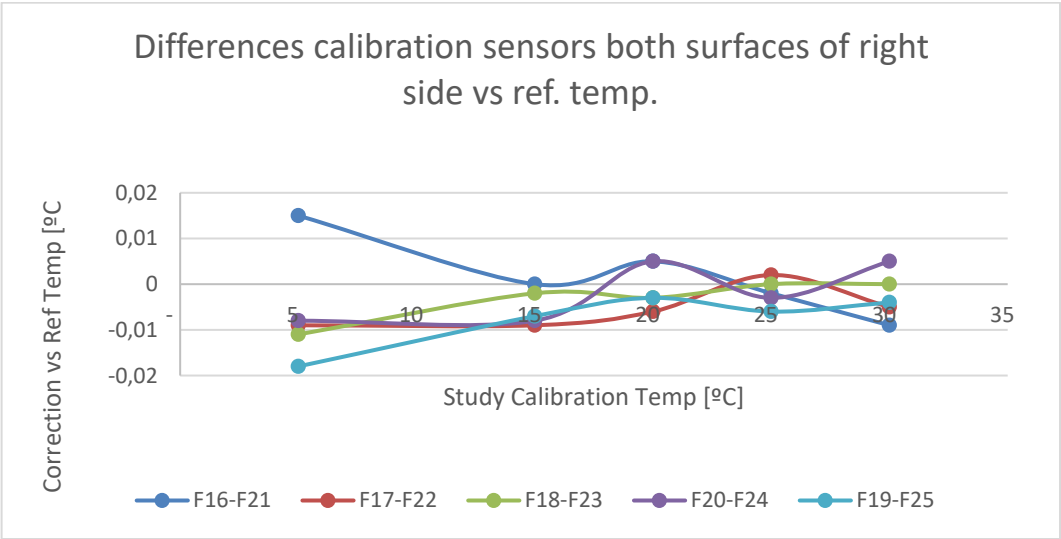

Appendix C 7: Calibration of the opposite sensors that were lately installed in the right side insulation

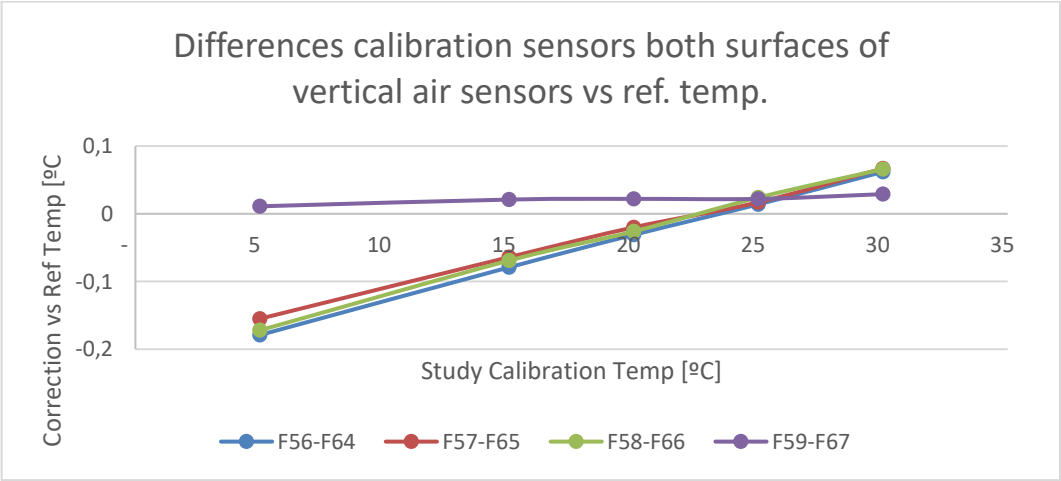

Appendix C 8: Calibration of the opposite sensors that were lately installed in the right side insulation.

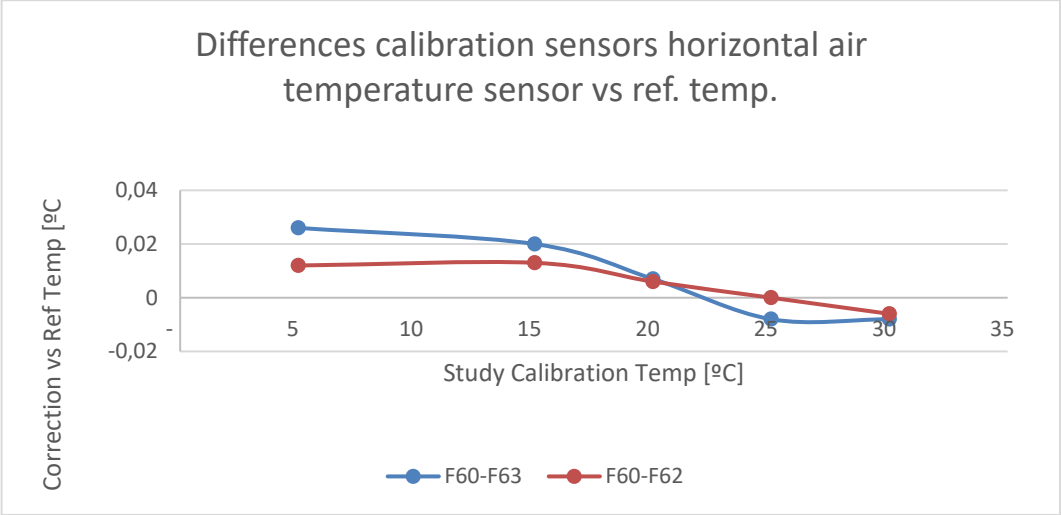

Appendix C 9: Calibration of the opposite air sensors that were lately installed in the inside of the hot box and the room.

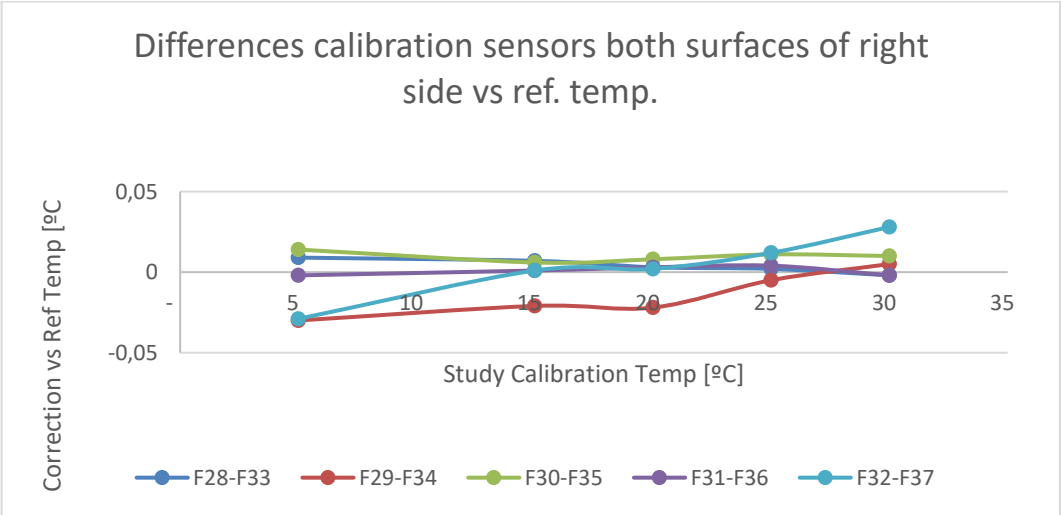

Appendix C 10: Calibration of the opposite sensors that were lately installed in the back part insulation.

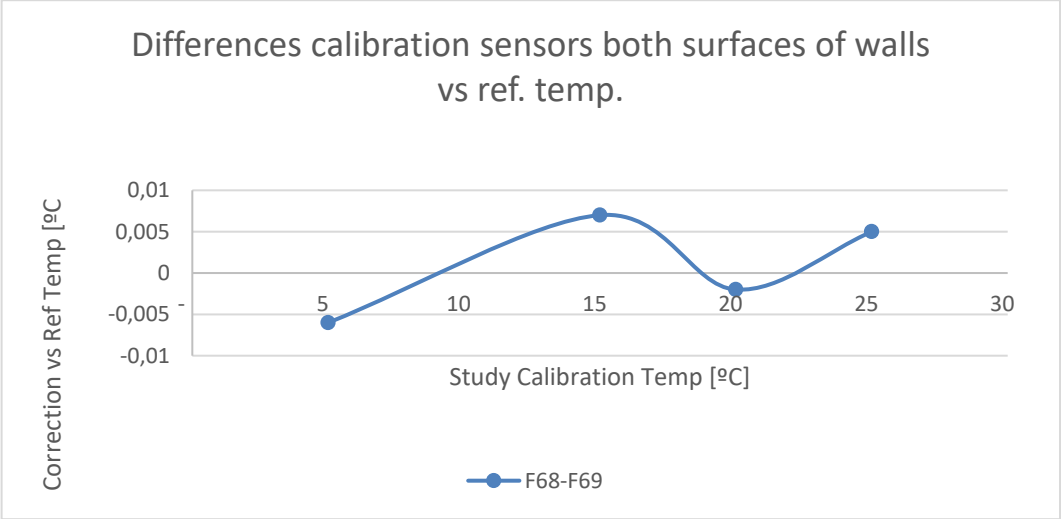

Appendix C 11: Calibration of the opposite air sensors that were lately installed on both sides of the walls.

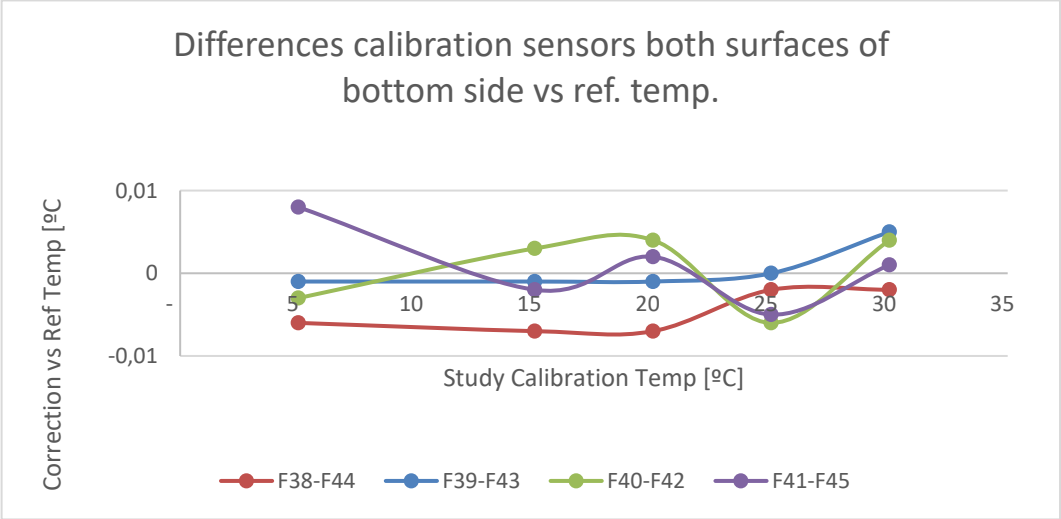

Appendix C 12: Calibration of the opposite sensors that were lately installed in the Bottom insulation.

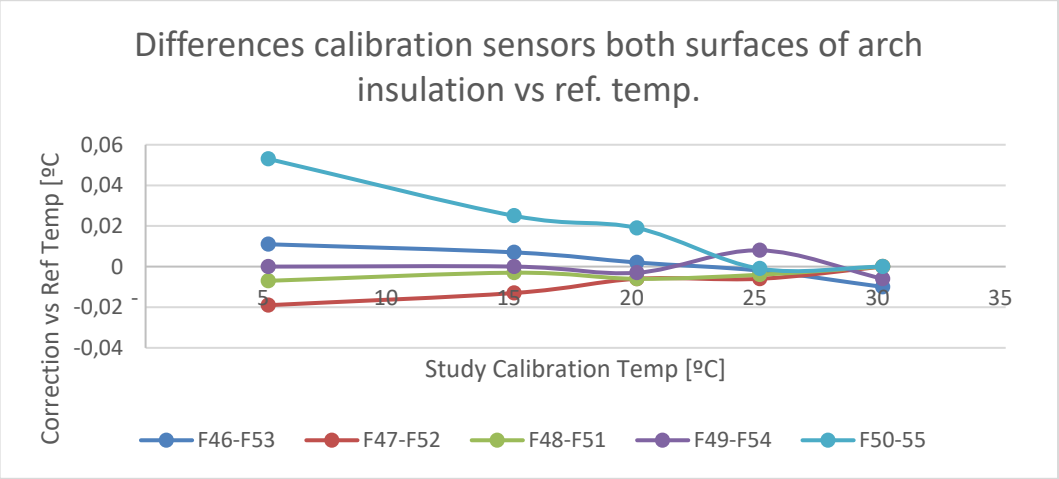

Appendix C 13: Calibration of the opposite sensors that were lately installed in the arch insulation.

Appendix D

A. Statistical results obtained for calculations using ΔTw.

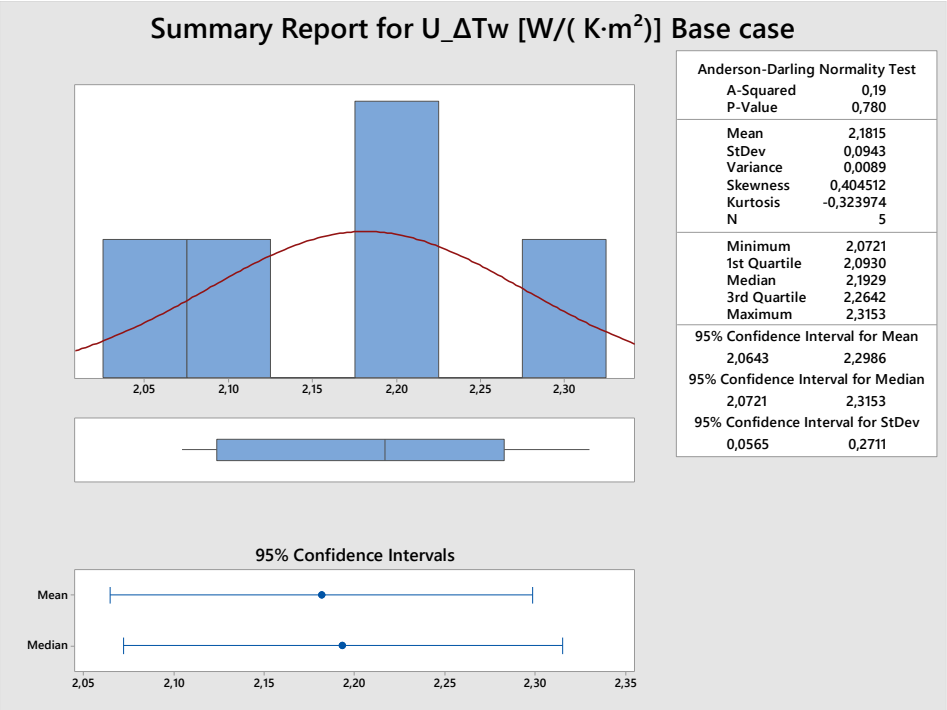

Appendix D 1: Results obtained for the base case using the outdoor window as environment.

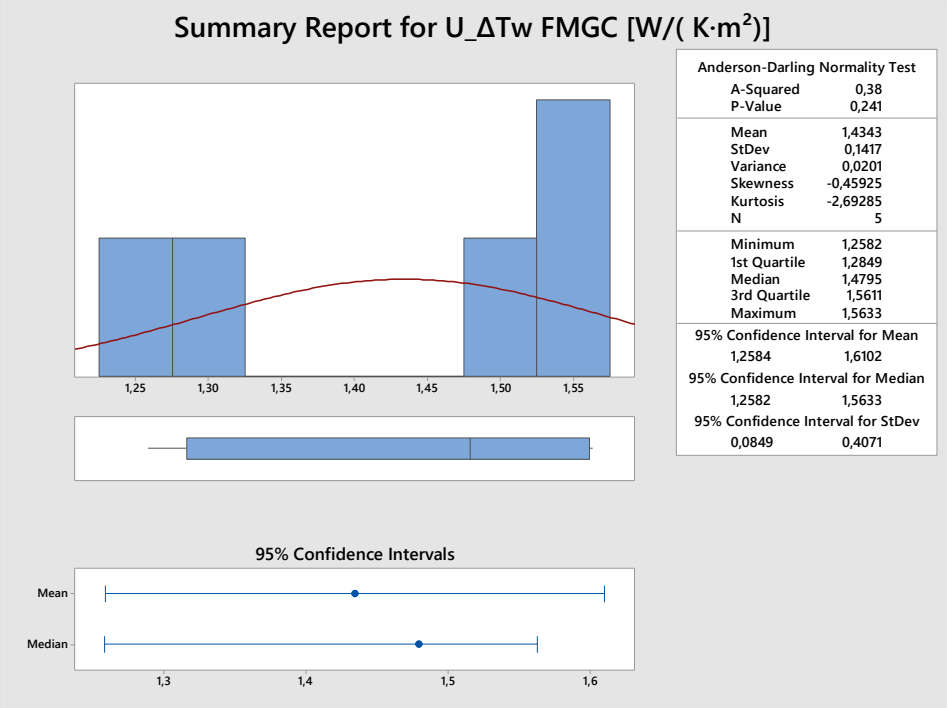

Appendix D 2: Results obtained for the Film middle glass case using the outdoor window as environment.

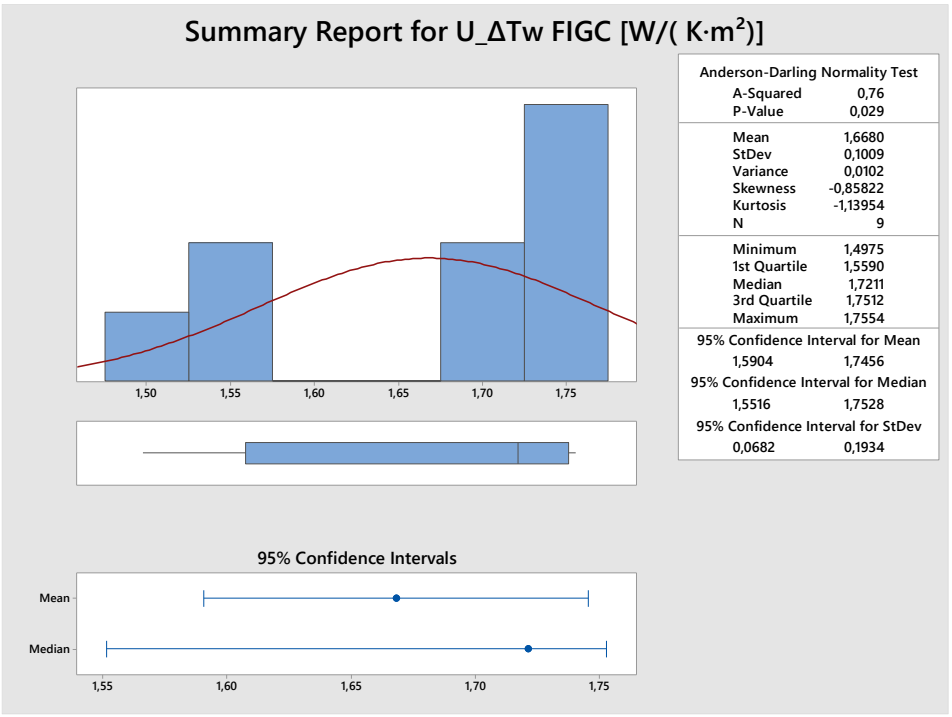

Appendix D 3: Results obtained for the Film inner glass case using the outdoor window as environment.

B. Statistical results obtained for calculations using ΔTa.

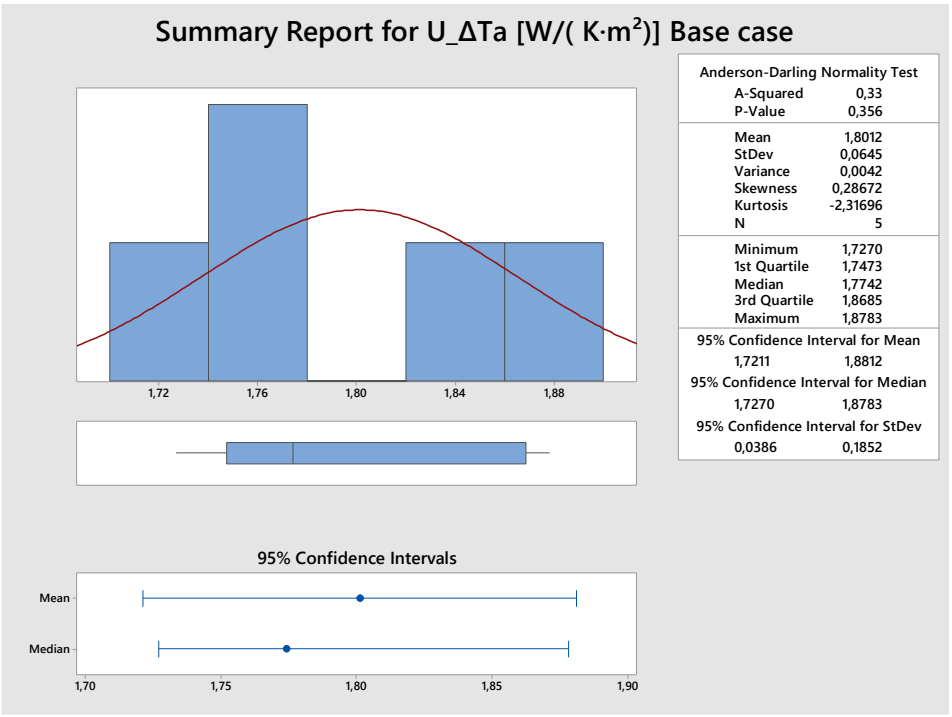

Appendix D 4: Results obtained for the base case using the outdoor air temperature as environment.

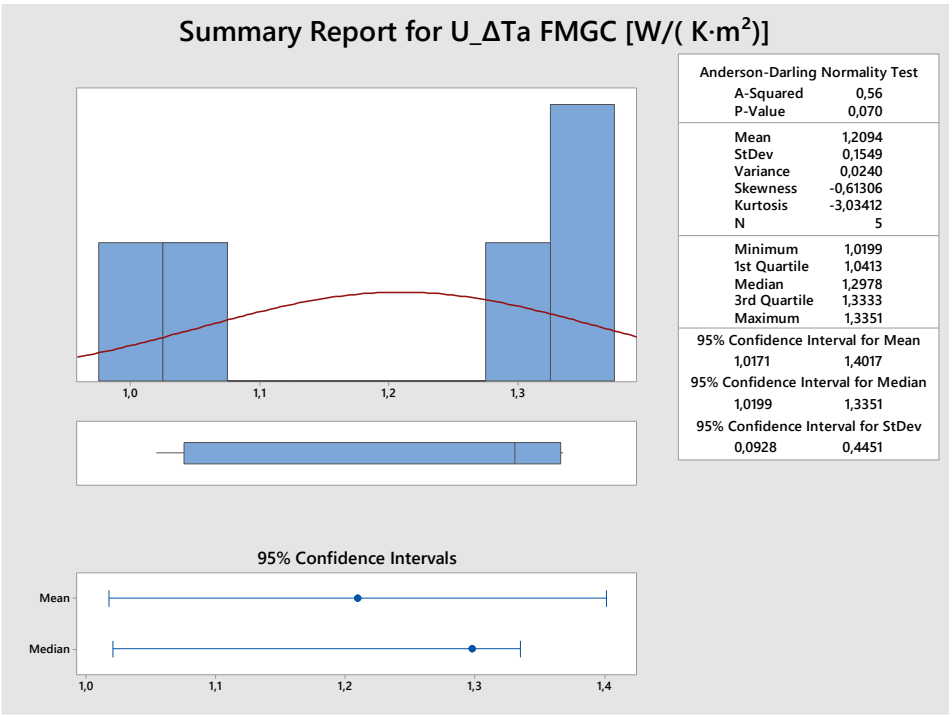

Appendix D 5: Results obtained for the film middle glass case using the outdoor air temperature as environment.

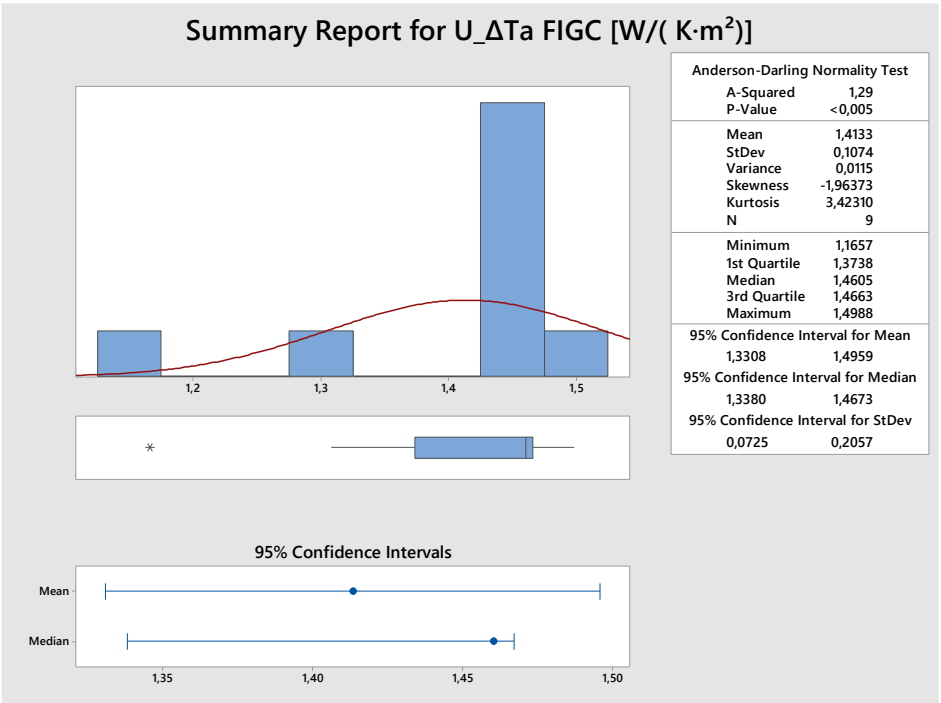

Appendix D 6: Results obtained for the film inner glass case using the outdoor air temperature as environment.

C. Additional plots of the data sets.

For validating, the points used in the calculations as well as to verify the correct behaviour of the hot box additional plots were made.

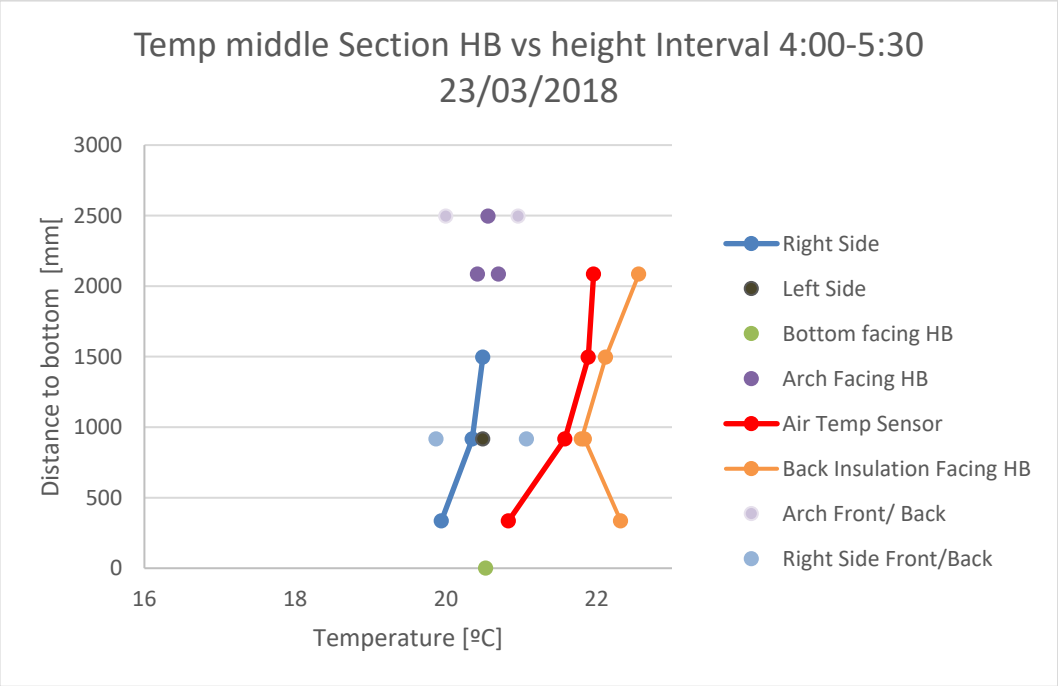

Appendix D 7: Surface temperature by surface by height. The slice had been done at x=327 mm from the inner backplate

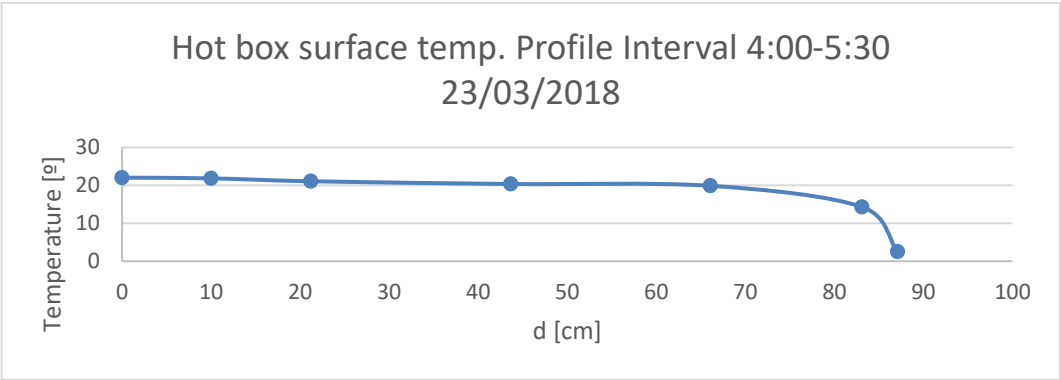

Appendix d 8:Evolution of the surface temperature profile from the back insulation external side. The selected height has been y = 915mm.

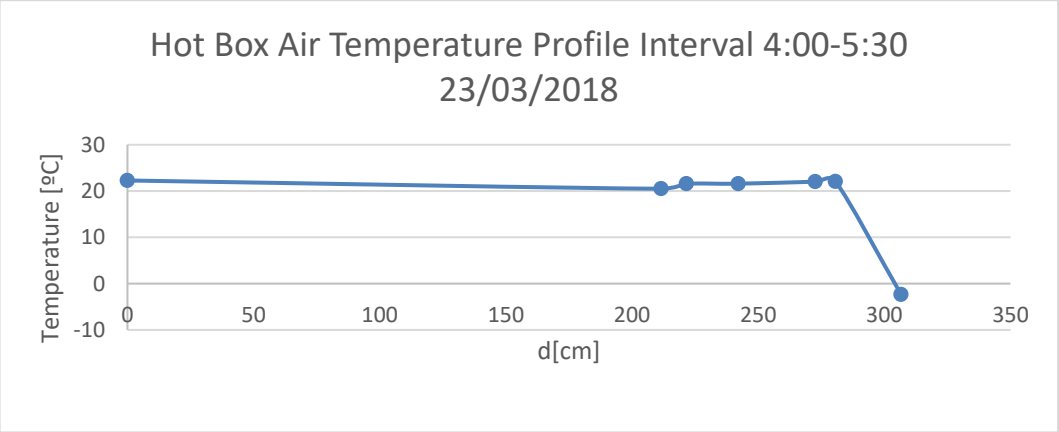

Appendix D 9: Evolution of the air temperature profile taking as origin the location of the room sensors. The selected height has been y = 915mm.

D. Additional plots for humidity

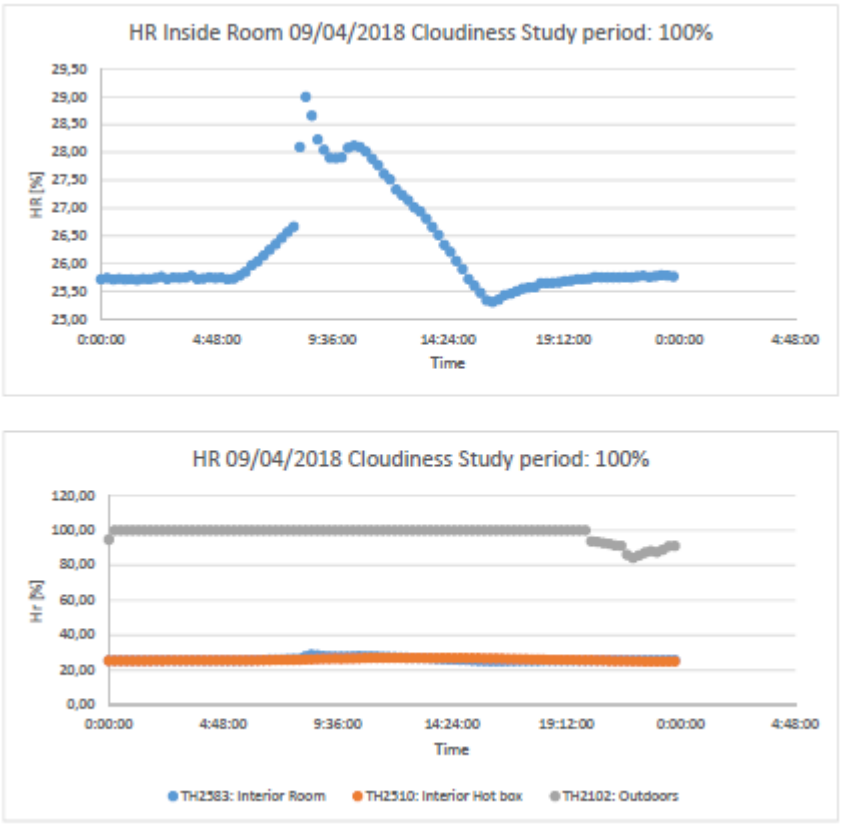

Appendix D 10: Evolution of the relative humidity for a cloudy day.

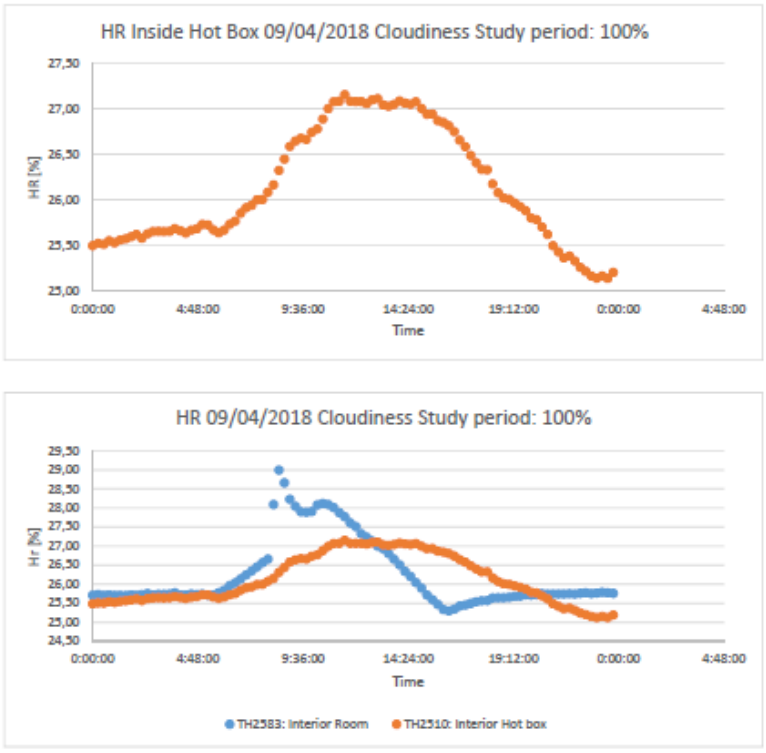

Appendix D 11: Evolution of the relative humidity for a cloudy day.

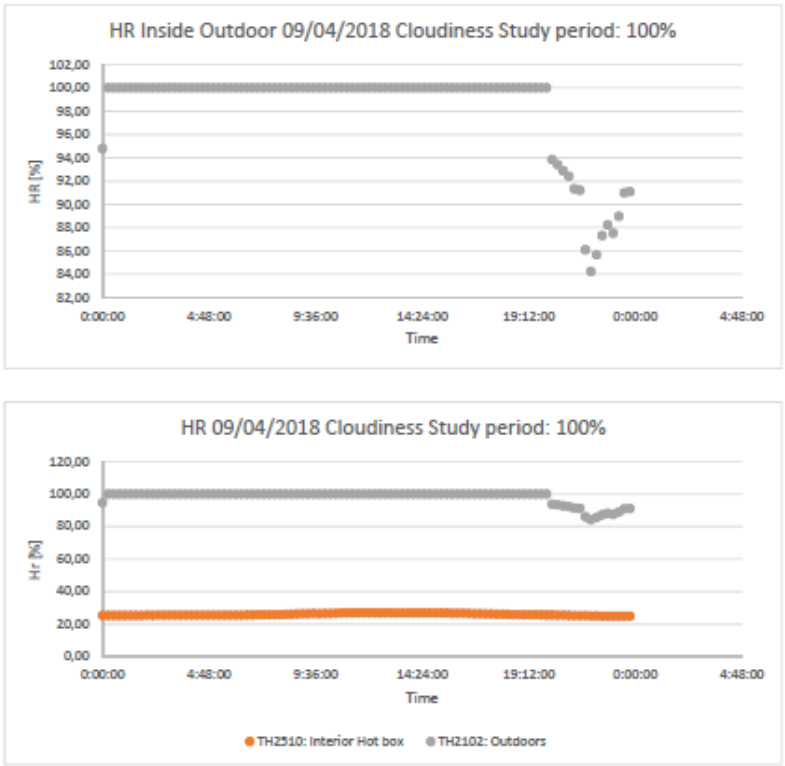

Appendix D 11: Evolution of the relative humidity for a cloudy day.

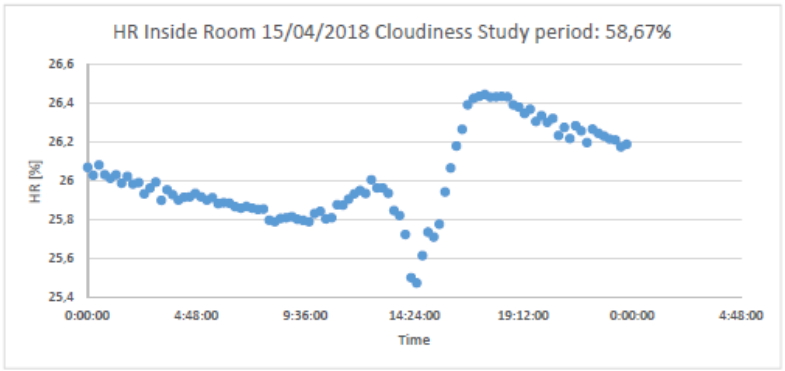

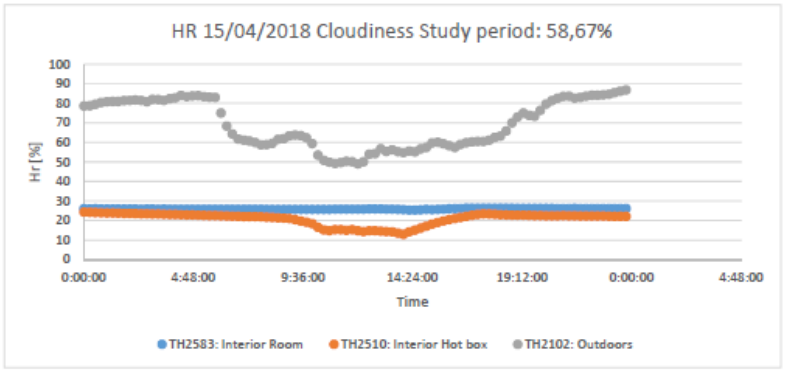

Appendix D 12: Evolution of the relative humidity for a not sunny or cloudy day

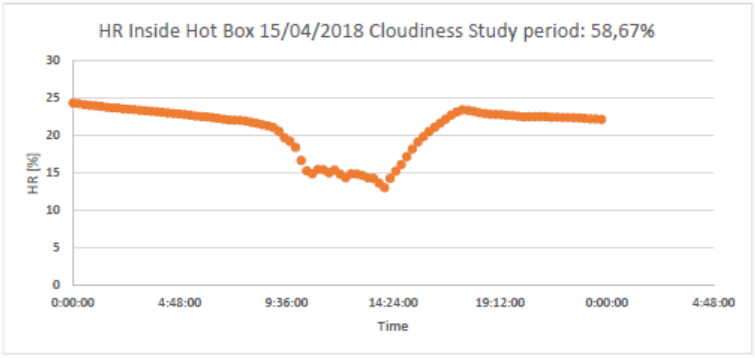

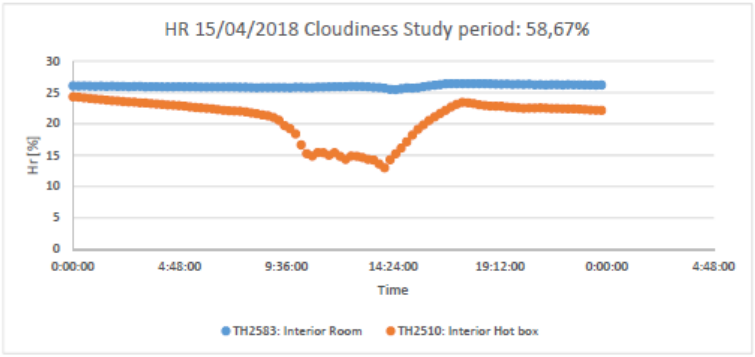

Appendix D 13: Evolution of the relative humidity for a not sunny or cloudy day

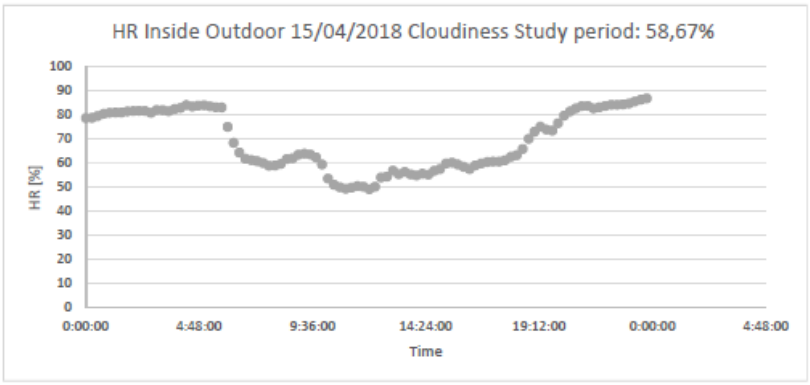

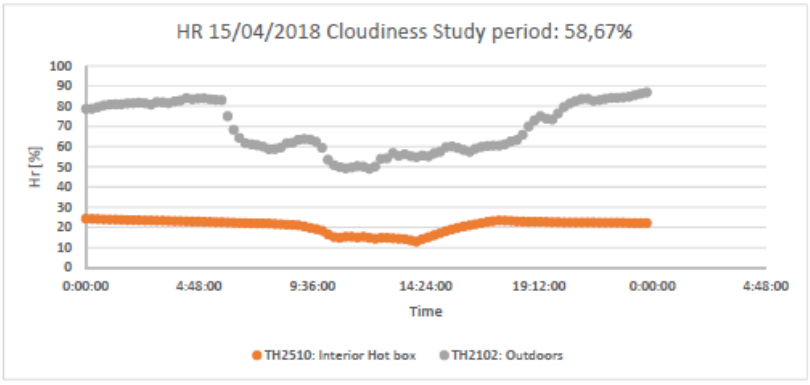

Appendix D 14: Evolution of the relative humidity for a not sunny or cloudy day

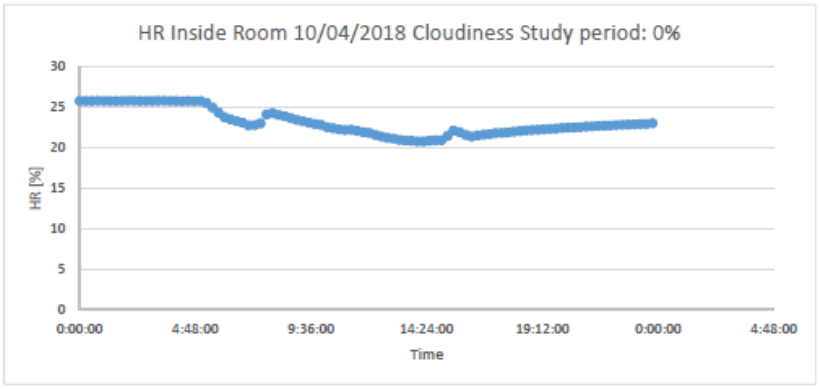

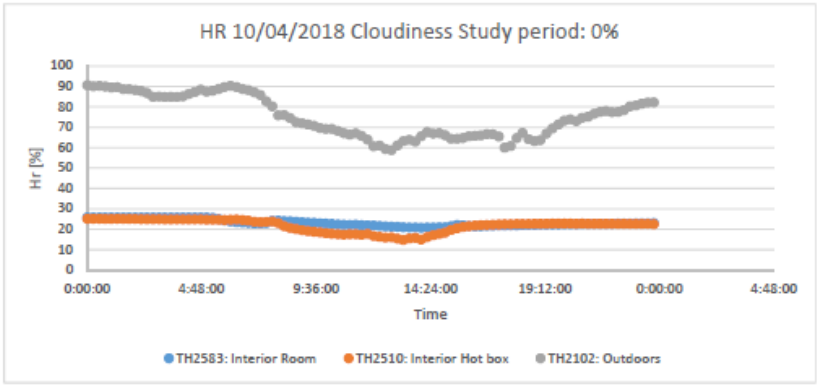

Appendix D 15: Evolution of the relative humidity for a not sunny or sunny

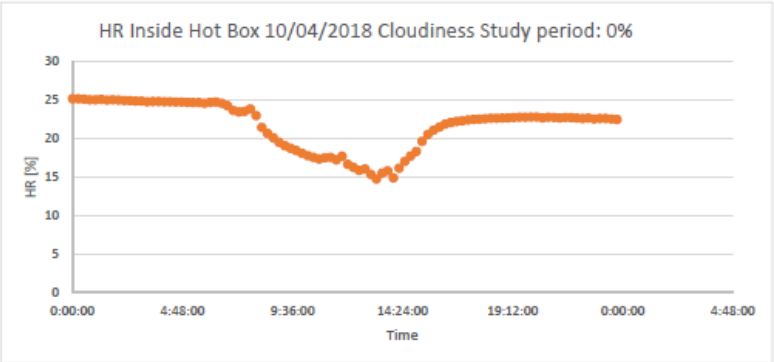

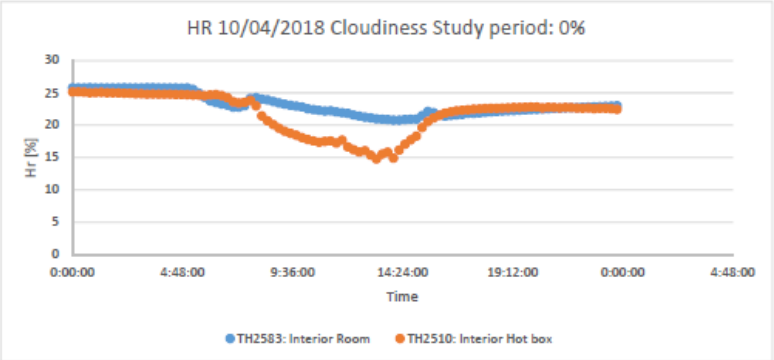

Appendix D 16: Evolution of the relative humidity for a not sunny or sunny day

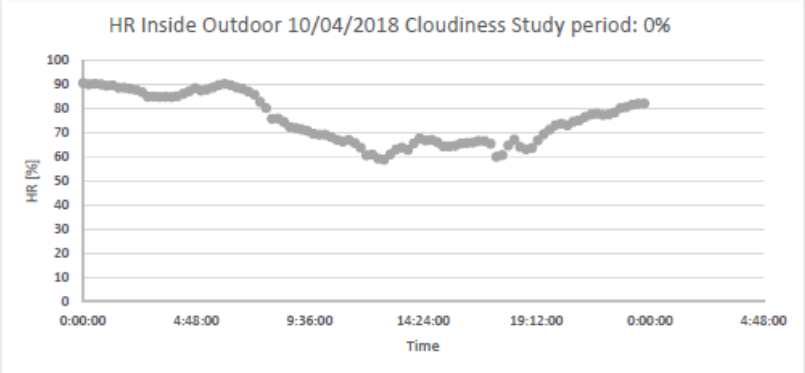

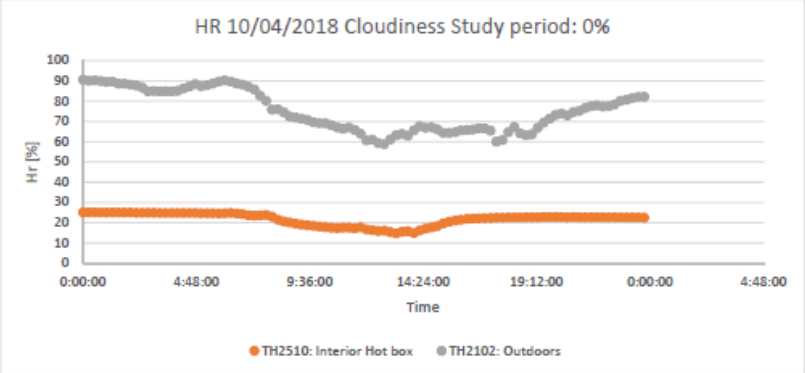

Appendix D 17: Evolution of the relative humidity for a not sunny or cloudy day

E. ANOVA study of the relation between U value and humidity

The following study of the correlation between both variables has a p value lower than 0.05 confirming the dependence between both variables. The study has been done using Minitab 18.

General Linear Model: U_Ta[W/ (K·m²)] versus Abs. ... kgAir; Scenarios

Method

Factor coding (-1; 0; +1)

Factor Information

Factor	Type	Levels	Values
Scenarios	Fixed	3	Base Case; Film Inner Case; Film Middle Case

Analysis of Variance

Source	DF	Adj SS	Adj MS	F-Value	P-Value
Abs. Humidity Outdoor [gw/kgAir	1	0,05845	0,058453	5,99	0,027
Scenarios	2	0,80252	0,401258	41,13	0,000
Error	15	0,14635	0,009757		
Total	18	1,12033			

Model Summary

S	R-sq	R-sq(adj)	R-sq(pred)
0,0987771	86,94%	84,32%	79,95%

Coefficients

Term	Coef	SE Coef	T-Value	P-Value	VIF
Constant	1,6698	0,0832	20,08	0,000	
Abs. Humidity Outdoor [gw/kgAir	-0,0587	0,0240	-2,45	0,027	1,09
Scenarios					
Base Case	0,3056	0,0357	8,55	0,000	1,31
Film Inner Case	-0,0420	0,0313	-1,34	0,199	1,32

Regression Equation

Scenarios			
Base Case	U_Ta[W/ (K·m²)]	=	1,9754 - 0,0587 Abs. Humidity Outdoor [gw/kgAir
Film Inner Case	U_Ta[W/ (K·m²)]	=	1,6278 - 0,0587 Abs. Humidity Outdoor [gw/kgAir
Film Middle Case	U_Ta[W/ (K·m²)]	=	1,4063 - 0,0587 Abs. Humidity Outdoor [gw/kgAir

Fits and Diagnostics for Unusual Observations

Obs	U_Ta[W/ (K·m²)]	Fit	Resid	Std Resid	
11	1,1657	1,3777	-0,2120	-2,31	R

R Large residual

Residual Plots for U_Ta[W/ (K·m²)]

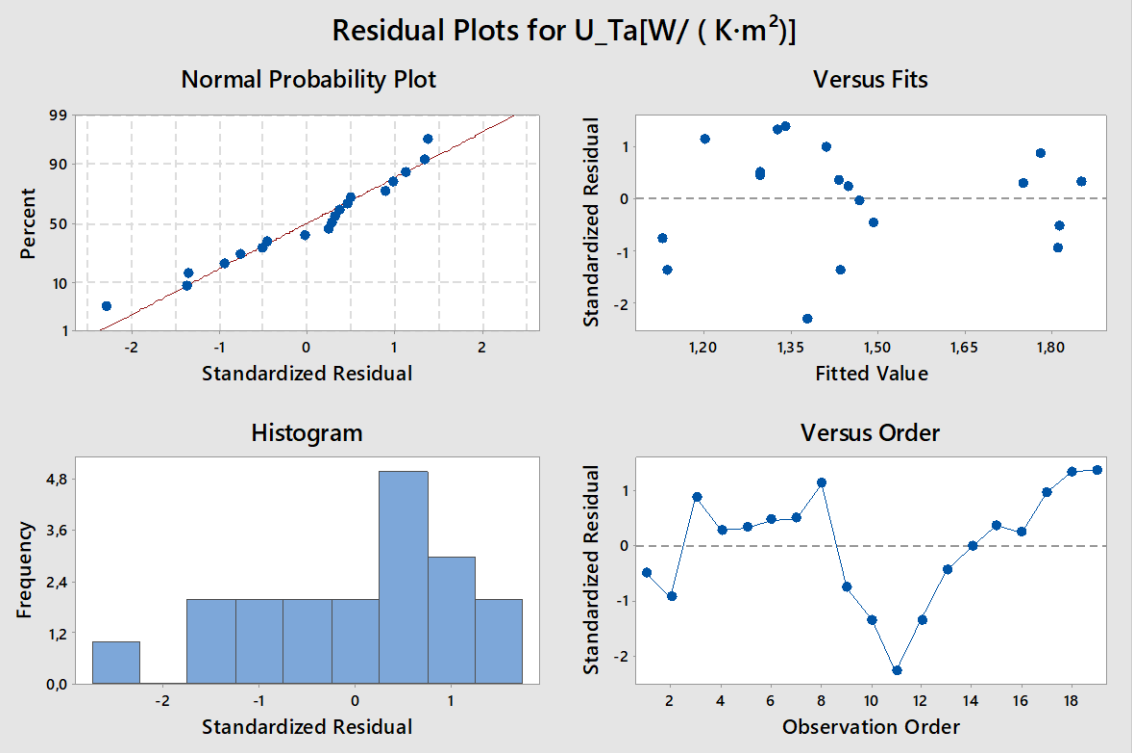

Appendix D 18: Residual plots for comparison between the u value using the outdoor temperature and the absolute humidity

F. Additional plots for temperature variation inside the hot box.

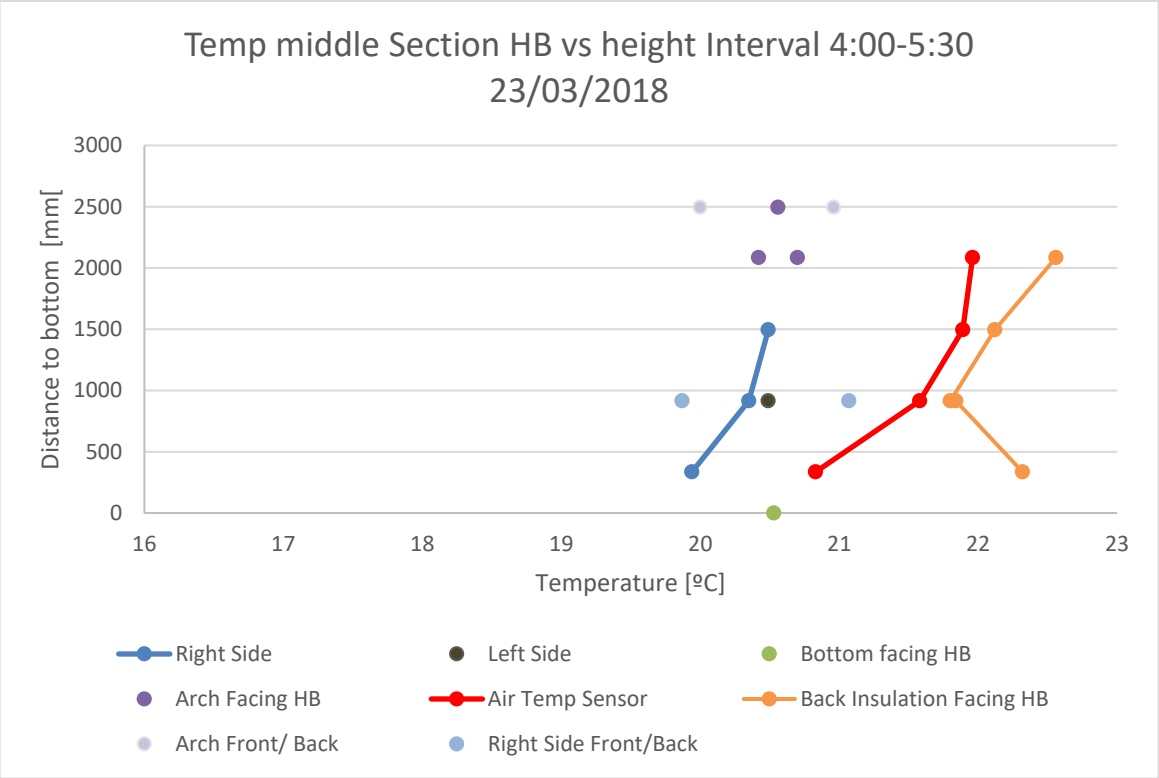

Appendix D 19: Differences of temperatures variation in height for the overall hot box.

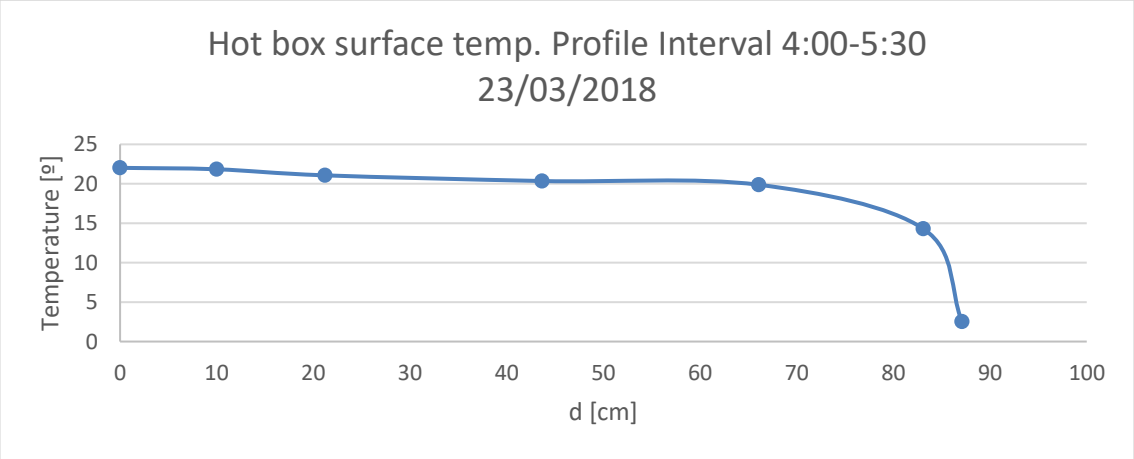

Appendix D 19: Differences of temperatures variation in depth of the hot box method at the height of 915mm,